Alma Mater Studiorum - Università di Bologna

Master Thesis

in

Building Engineering/Architecture

Degree Program: LM-4 - Architecture and Architectural engineering

Water-Harvesting Envelopes

Integration of Sorption-based Atmospheric Water Harvesting in a Façade System

Presented by: John Adel Naseem Fam Tadrous

Thesis Advisor

Alessio Erioli

Co-advisor

Maria Matheou

University of Stuttgart, ILEK

Abstract

Faced with increasing water scarcity each year, regions with arid-hot climates are having a hard time collecting fresh water due to the limited rainfall or the geographic and technological difficulty of desalination of sea water. Atmospheric water harvesting (AWH) technology comes as a renewable water source that has a lot of methodologies, one of which is sorption-based AWH (SAWH). This thesis explores the potential of the integration of SAWH technology on building facades in arid-hot climates. Giving the fact that SAWH depends on low relative humidity and an abundant sorbent material it becomes a sustainable water resource that meets other façade functions like thermal and visual comforts in these regions. Using parametric design tools, the thesis explores the suggested design's potential as architectural envelope for a variety of building uses while maintaining the visual and thermal comfort.

Acknowledgments

I would like to express my gratitude to Professor Maria Matheou for her support and guidance during my four-month stay at the ILEK Institute. Her hospitality, encouragement and expertise played a huge role in shaping my thesis as well as her motivation which made me delve deeper into my research topic.

Additionally, I would like to extend my appreciation for my Professor Alessio Erioli for his contribution to my thesis. His expertise in parametric design helped me develop my thesis to a higher level as well as his guidance to develop and finalize my research project. I am honoured that I had this opportunity to learn from both expertise.

To my family, my deepest gratitude for the continuous support throughout all of my educational journey and the sacrifices they have made for me to get to this place.

Table of Contents

1 Introduction

The word façade (from the Italian *facciata*, from *faccia* meaning 'face', ultimately from post-classical Latin facia) as quoted from the Oxford English dictionary (2011)[1] came to describe the outer building envelope, putting a visual emphasis as it is the first element people see approaching a building which also contains the entrance, as well as a symbolic significance; as the face of a person shows their emotions and character, a façade as well is often used by architects to deliver a certain feeling or a message to the viewer. As for its cultural value the façade is used by architects to reflect and showcase the identity of the location on which the building was built. As for the structure itself it can act as a protector from climate conditions as well as a filter allowing light, heat, sound, and air flow according to the user preference.

The façade went under a lot of changes throughout the decades regarding style, functionality, materials used and technologies. The technologies implemented in a building façade were used to serve under the main roles of a façade to boost its serviceability, functionality and adaptability to exterior conditions. The adaptability of a building façade to conditions like solar radiation advanced as technology did, to become sensor and user controlled making some façade elements kinetic to enhance its overall performance. As a whole, as quoted from (Design for façade adaptability) In order to enhance the overall performance of the building, a kinetic façade can adapt its features, functions, or behaviour over time in response to boundary circumstances and temporary performance requirements.[2] The primary goal of intelligent kinetic systems according to Michael F, Miles K in their book of (Interactive Architecture) should be to act as a moderator responding to changes between human needs and environmental conditions. [3]. In a comparative study made on kinetic facades, in most and nearly all cases of kinetic façades worldwide the conditions dealt with are daylight, thermal conductivity and air flow,[4]. In this research an addition to the functions of kinetic facades is being explored, that deals with water production.

Despite the inevitable significance of water in human life and a wide range of industrial processes, increasing global demand and shortage of water resources have rendered the water situation critical, as quoted from the UNESCO report for the water development (2015).[5] Some architects made contributions to water production using water collection methods like fog harvesters as seen in the project of Warka tower designed by Atruio Vittori & Andreas Vogler that allows fog, humidity and precipitation to collect on surfaces and then be collected in containers, yet the conventional water production methods primarily use seawater. Both of these methods are geographically limited as they need high relative humidity levels and a seaside respectively, which leaves other less fortunate areas vulnerable to water scarcity so another method of water production should be used as a replacement instead.

The abundant amount of water in the atmosphere is gaining attention and there is a growing body of literature that recognizes the importance of atmospheric water harvesting (AWH).AWH is divided into three major categories: fog collection, dew collection and sorption-based atmospheric water harvesting (SAWH), the first two require high relative

humidity (∼RH > 60%), where the third one (SAWH) can work with as low as 20% of RH.as mentioned in a paper (Awareness of Atmospheric Water Harvesting Technology) [6] This RH working level makes it a good choice for water production in arid-hot climates, which in parallel has a very high level of water stress and scarcity.

The research problem addressed in this thesis is the possibility of integrating the SAWH technology onto the building façades not only to act as a typical building envelope but to contribute to the pool of solutions to the problem of water scarcity in arid-hot climates. This technology aims to be implemented with different building usage scenarios. The parametric design tools are used to design a system that can be implemented on different building uses, building shapes and locations. These design scenarios are asessed using programs like Climate Studio which gives me a simulation for glare and point-in-time illuminance to be able to asses the thermal and visual comforts for building occupants and Grasshopper which has plugins like (Lady bug) that allows me to simulate the irradiance on my façade. These tools allow a comparison to be made between different design scenarios which is beneficial for choosing the best design according to the criteria that chosen, in this case it is water production, thermal and visual comforts.

For the used programs to be accurate, a location must be given to them on which the calculations for radiance, glare and in-time-illuminance to be made on accurately. In this research the location chosen was Egypt. Egypt is under the list of high level of water scarcity, and with a freshwater withdrawal rate that exceeds 100% as cited in (The world's road to water scarcity) [7]. With its arid-hot climate Egypt was a good candidate for which it can give an accurate general idea of the quantitative values of such technologies in such climates. This research will dive into a comparative analysis of different design solutions and its effect on the water production values, comparing different sorbent materials and geometries of sorbent beds, elements of thermal comfort such as point-in-time-illuminance and glare, as well as visual comfort elements as the ability for a user interaction without affecting the water production values. The comparative analysis of sorbent materials will depend on experiments done and mentioned in papers regarding SAWH, with a focus on experiments done in Egypt or climate similar locations. Unfortunately, no product is found to be made using SAWH that can used as a technical reference as the technology is relatively new and still needs further experimentation.

2 Literature Review

As the danger of water scarcity increases every year, with an increasing demand and decreasing of non-renewable water resources especially in arid hot climates where the water resources are naturally scarce, along with the non-sustainable use of water, the demand for a water source increases. In arid hot climates water sources like rivers, lakes and underground water are being exploited rapidly in a way that would create serious water shortage problems for the next generations.

To solve this crisis different water generating technologies have been studied by researchers to create a renewable water supply. One of these technologies, Atmospheric Water Harvesting (AWH) was studied as a promising renewable water resource, which transfers atmospheric moisture into potable water. AWH condenses the water vapor in the air into liquid form that can be stored and then used for various purposes like drinking, agriculture and industrial uses.

Within the AWH technology, Sorption-based AWH (SAWH) stands out as a suitable solution for arid-hot climates, as it uses the solar energy for the water vapor condensation which increases the water production rate, even with minimal relative humidity values. With a fully sustainable water production cycle, depending on renewable solar energy without integrating fossil fuels or CO_2 emissions, SAWH stands out as a suitable alternative for water production instead of methods like sea water desalination, minimizing environmental impacts.

As a tool for urban water sustainability SAWH can be a good candidate to be integrated within architecture, more specifically within building envelopes. This literature review shows the key functions that a building envelope is responsible for maintaining to try to bridge the gap between SAWH and Architecture without sabotaging the traditional building envelope's functions, like thermal and visual comforts.

Using parametric design tools, a system was realized that carries out the functions of a traditional building envelope as well as the water production capacity of a SAWH technology. Finalizing with a theoretical concept and climate tests done using parametric software, a huge part remains for an actual experiment using this element to touch upon its water production capacities.

2-1-Water Scarcity

In many places of the world, the overuse of freshwater resources poses a threat to global food security and human welfare. To get an idea about the numbers worldwide, four billion people which is almost two thirds of the world's population experience severe water scarcity for at least one month each year. Half of the world's population could be living in areas facing water scarcity by as early as 2025. 700 million people could be misplaced by intense water scarcity by 2030. By 2040, roughly 1 in 4 children worldwide will be living in areas of extremely high-water stress, these numbers come from the official UNICEF website.[8]. Moreover, according to a paper about "Atmospheric Water Generator Technologies" in the near future, it is expected to be much harder to maintain water use at sustainable levels due to factors like climate change, changing water consumption trends, and growing population.[9]

The two factors affecting water scarcity is either water shortage or water stress or both together as cited from "The world's road to water scarcity" paper shown in Fig 1, which highlights the high water scarcity levels in the middle east and north Africa which therefor justifies the needing for a renewable water source.
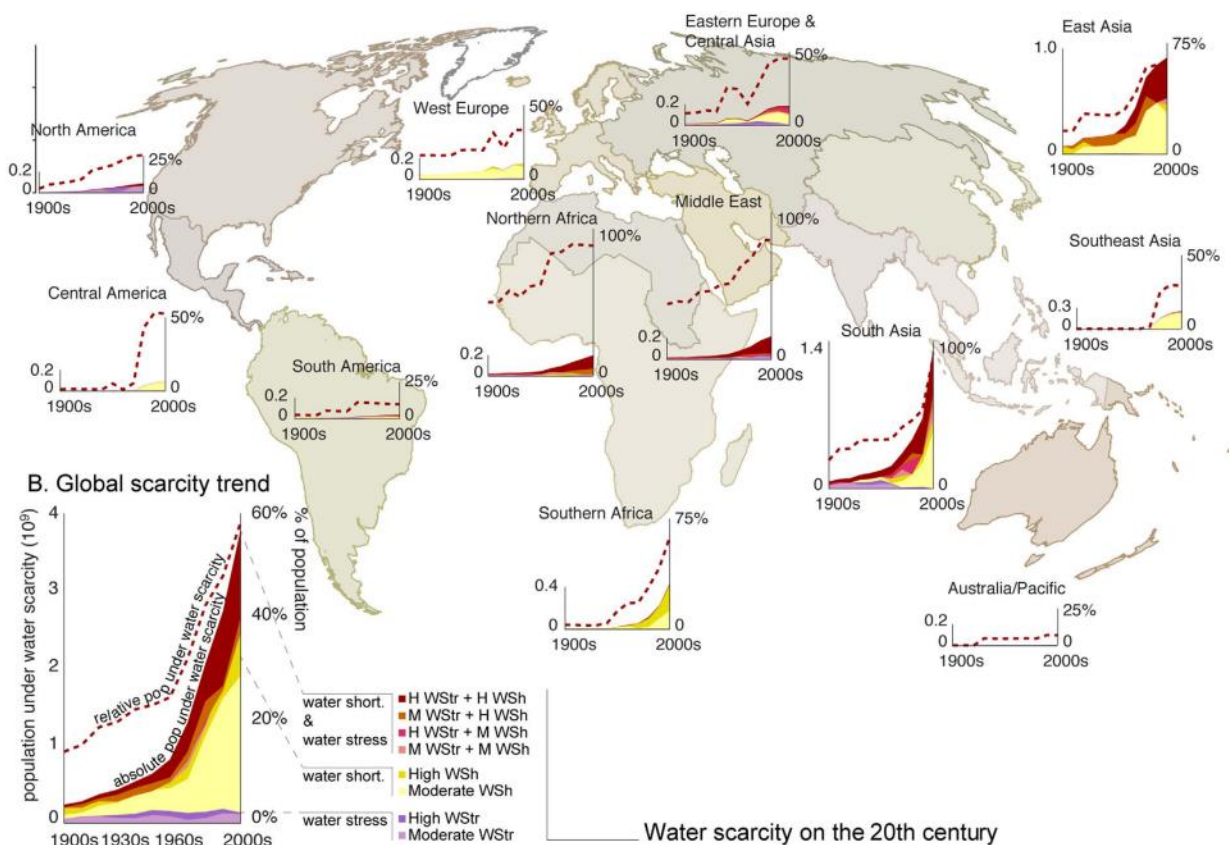
WStr: Water Stress, WSh: Water Shortage

Fig 1 [7] - Water scarcity and shortage map

2-2- Atmospheric Water Harvesting (AWH)

There is a variety of methods to collect water worldwide such as filtration of water in rivers and lakes, desalination of sea water, collection of rainwater or digging and bumping of underground water. Such methods are geographically dependant, and it requires for water to be in its liquid form. For places lacking the technology to harvest or the availability of such water, due to a geographical position or a climate condition that does not allow the falling of large quantities of rain, another method for water harvesting can be introduced which is independent from both geography or complex technologies. In other words, a passive or a semi passive system must be put into place to make up for the shortage of liquid water. The atmosphere contains about 12,900 cubic kilometers of water, enough to meet part of the water needs for domestic, agricultural, and industrial purposes according to (Progress and Expectation of Atmospheric Water Harvesting paper) [10] With its non-liquid form the atmospheric water needs to be harvested through a number of ways which all fall under the umbrella of Atmospheric water harvesting (AWH). Divided into two main categories as shown in Fig 2, cited from (Review of sustainable methods for atmospheric water harvesting) [11] fog water collection and dew water collection.
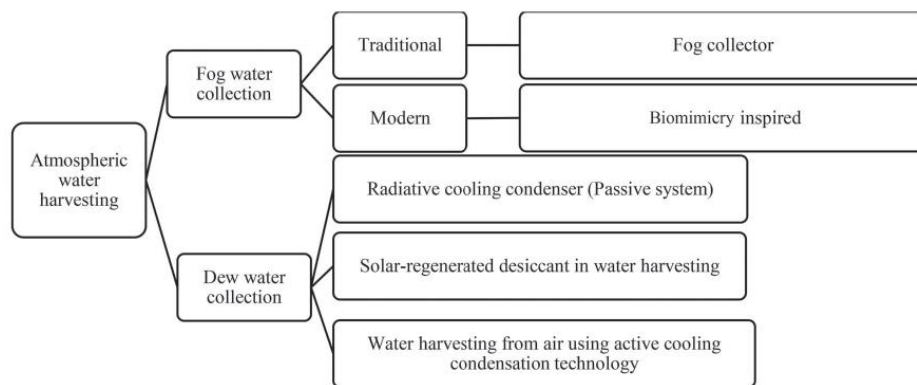
Fig 2 [11] – Categories of atmospheric water harvesting

In this thesis, the locations targeted are with hot-arid climates such as north Africa and the middle east, parts in which they have low relative humidity and a low level of yearly rainfall, which is essential for the first method of (Fog water collection) or the traditional rain collecting systems. This leaves us to the second method of (Dew water collection), which is divided into three main categories: Radiative cooling condenser, Solar-regenrated desiccant and water harvesting using active cooling condensation technology. The first and last methods require large spaces as well as a large energy consumption. As for solar-regenerated desiccant in water harvesting, it is a passive system that depends on solar energy to evaporate the collected water vapor on desiccant bed which is later condensed on a surface and goes down to tubes and collected later on under the effect of gravity. This passive technique is highly efficient in areas with relatively low humidity levels, yet its main problem is the low water yield. This method is also called (Sorption-based AWH) as its water yielding mainly depends on sorbent material and sorbent bed area as main factors and on other factors like wind speed and topographic cover.

2-3- Sorption-based Atmospheric Water Harvesting (SAWH)

i - Working Principle

The main working principle of SAWH is based on a cyclic process that is mainly divided between sorption and desorption. First, the sorbent is exposed to the air in an open system for a certain period, after which it starts to sorb and trap air moisture. The system is then closed, and the sorbent is heated directly or indirectly to release the sorbed water as in Fig 3. As cited from (Sorption-Based Atmospheric Water Harvesting) [12]. A lot of sorbent materials are being developed in the mean while that increases the water uptake with relatively lower temperature and low relative humidity. The main parameters affecting the amount of water produced using SAWH over a certain period of time is the surface area of the sorbent bed, air humidity and temperature difference between the open and closed systems to allow water condensation.
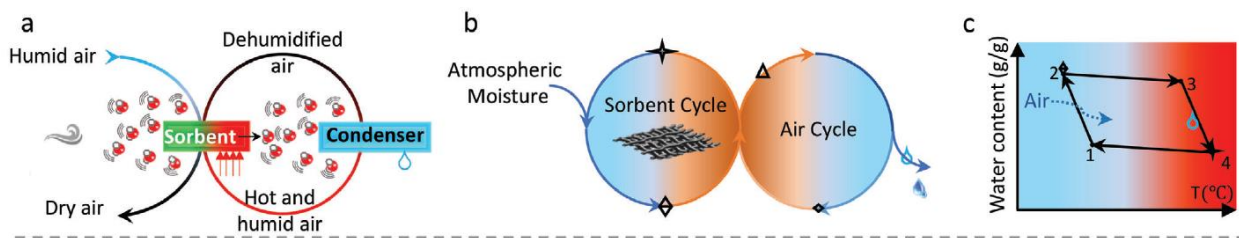
Fig 3 [12] – Working principle of sorption based AWH

ii- Experiments done with different SAWH systems

To get an idea of the morphology of the SAWH technology research was done about the experiments conducted using different sorbent materials and different system morphologies, allowing to compare different water production rates due to sorbent materials per square meter. In Fig 4, it is shown the most common system morphologies in experiments that used salt solutions as main sorbent material with sorbent beds that differ between saw wood, cloths or sand. All of these materials are economically efficient materials with long life cycles and easy maintenance as cited from (Performance Evaluation of Solar-Powered Atmospheric Water Harvesting) [13]. Most of the experiments were done in Egypt which gave a clearer idea for the water yielding ratios in the location that was intended to do the thermal comfort tests on. In Table 1. a comparison is done between sorbent bed materials, water production values and their location of experiments cited from (Performance Evaluation of Solar-Powered Atmospheric Water Harvesting) [13].
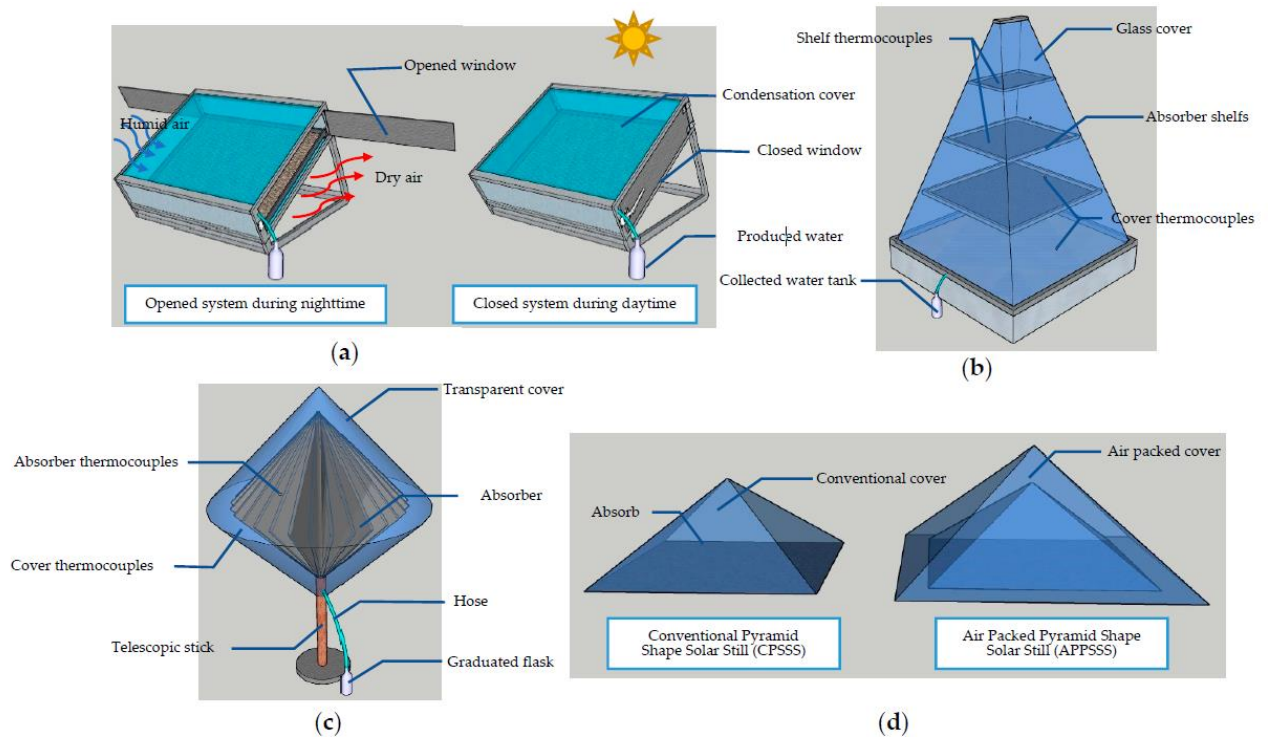
Fig 4 [13] – Different morphologies of apparatuses used in experiments for SAWH

(**a**) Solar glass desiccant box type system (SGDBS), adopted from [13 a]; (**b**) Trapezoidal prismsolar collector, adopted from [13 b]; (**c**) Double-faced conical finned absorber, adopted from [13 c] and (**d**) traditional pyramid-shaped solar still and air-filled pyramid-shaped solar still, adopted from [13 d].

Location	Procedure	Desiccant	Water Production	Efficiency (%)
Egypt	Experimental and theoretical	$CaCl_2$/sand	1.2 L/m^2/day	-
Egypt	Experimental	$CaCl_2$/saw wood and cloth	2.5 L/m^2/day	90–95%
China	Experimental	$CaCl_2$/MCM-41	1.2 kg/m^2/day	-
Saudi Arabia	Experimental	$CaCl_2$/sand	1.0 L/m^2/day	-
India	Experimental	Silica gel	200 mL/kg/day	-
India	Experimental	$CaCl_2$/saw wood	180 mL/kg/day	-
India	Experimental	$CaCl_2$/vermiculite/saw wood	195 mL/kg/day	-
Egypt	Experimental	$CaCl_2$/cloth	Cloth = 2320 gm/m^2 Sand = 1235 gm/m^2	Cloth = 29.3% Sand = 17.76%
China	Experimental	LiCl/consolidated active carbon	14.5 kg/40.8 dry sorbent/day	-
India	Experimental	LiCl, $CaCl_2$ and LiBr	LiCl = 90 mL/1.54 m^2/day $CaCl_2$ = 115 mL/1.54 m^2/day LiBr = 73 mL/1.54 m^2/day	-
Egypt	Experimental and theoretical	$CaCl_2$/cloth	0.33–0.63 kg/m^2/day	22.56%
Egypt	Experimental and mathematical	$CaCl_2$/cloth	1.5 L/m^2/day	17%
Saudi Arabia	Experimental and theoretical	$CaCl_2$/Cotton cloth	0.51 L/kg (dry sorbent)/day	24.61%

Table 1 [13] – Comparison between sorbent materials and their water production values

These values leave us with an average of 1.5 litres of water per a square meter of desiccant bed per cycle or day. Generally, there are other materials that perform better for water production, yet it is costly like metal organic frame works which can give up to 25 litres/m2/day. As for this paper no interest was put in costly materials for water production and more dependence was put on other water production factors like desiccant bed area. This was one of the main reasons to choose façades as an implementation area for this system.

iii- Main SAWH system components

To be able to integrate the SAWH on an architectural level, there has to be an understanding of the main components responsible for water production, which are shown in Fig 5. cited from (Application of a solar desiccant/collector system for water recovery from atmospheric air) [14] shows us the main elements that should be put in design for it to function properly. The elements highlighted in red are disposable in the case of designing an element that would not use a separate condenser. The dimensions of this apparatus are 1.42m x 1.42m x 0.3m.

1- Flat plate collector.
2- Glass cover.
3- Fans openings.
4- Collected water channel.
5- Foam (Insulation).
6- Aluminum sheets.
7- Steel sheets.
8- Metallic frame.
9- Collected water tube of condenser.
10- Collected water tube of collector.
11- Graduated Flask.
12- Flat plate condenser.
13- Connected channel.
14- Condenser support.
15- Condenser opening.
16- Collector support.
17- Glass cover support.
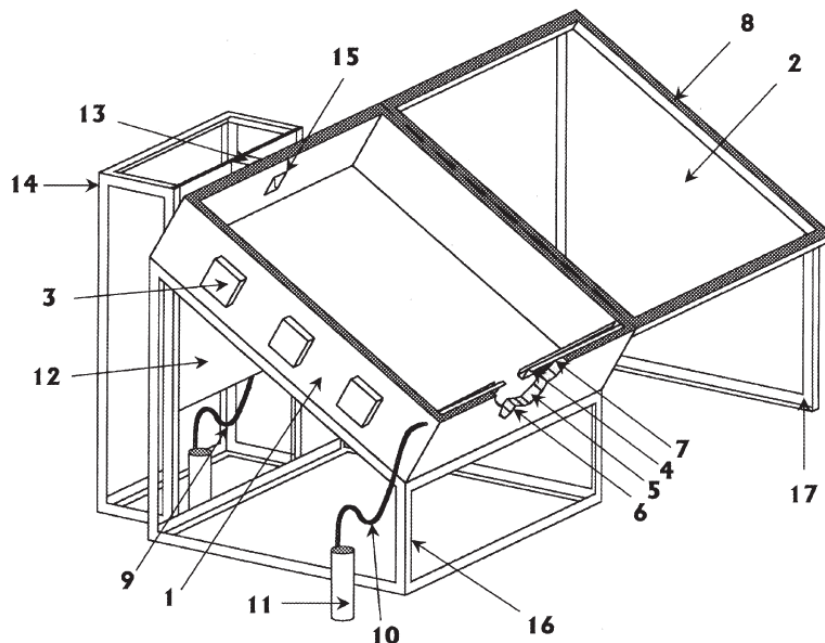
Fig 5 [14] – Main componentsof sorption-atmospheric water harvesting unit

6

2-4- Kinetic Façades

In terms of introducing cutting edge technologies into the architectural realm, façade design is one of the most prominent fields. Kinetic façades are examples of that approach as the façade benefits in terms of aesthetic appeal and functionality. The moveable components of the façade interact with the environmental conditions resulting in a change of position, orientation and even colour of these components. These environmental conditions can be sunlight, temperature or wind, conditions in which traditional static façades don't deal with such efficiency in terms of visual and thermal comforts of the occupants.

Kinetic facades can manage the amount heat, sunlight and wind that enters the space enhancing energy efficiency which will lead to a lower use of artificial heating or cooling and therefore a lower energy consumption building. Temperature and sunlight management is essential in places with extreme weather conditions like Dubai, in which we can see an example of kinetic façades: Al Bahar Towers in Abu Dhabi Fig 6. [15 x] The hexagonal screens of the tower open and close in response to the sunlight, which reduces the solar gain of the building.

Fig 6 [15] – Al Bahar Tower

Other than energy efficiency, kinetic façades can be designed to optimize lighting conditions without the need for interior artificial lighting to improve user comfort by reducing glare and excessive heat which are common issues that can affect occupants.

The aesthetic advantage that the kinetic façades also give can not be overseen as when the building change and adapt over time, it becomes a living entity that creates constantly changing visual experience.

A comparative study on responsive façade systems was done by Ecenur Kızılörenli and Feray Maden , shown in Table 2[16] the table sums up some of the buildings worldwide that include kinetic facades and the function these kinetic facades deliver.
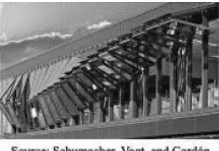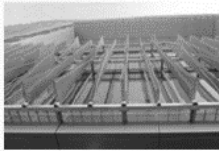
Project	Project Location/ Year	Image of The Facade	Type of System		Type of Movement							Type of Control System		Control Type of Elements		Function of the Facade			Response Time			Visibility		
			Passive	Active	Full Rotation	Oscillatory Motion	Deforming	Folding	Sliding	Hybrid	Hand-Operated Control	Central Control	Individually	Total Movement	Daylight Control	Thermal Control	Air Flow	Seconds	Minutes	Hours	Low	Medium	High
Kiefer Technic Showroom	AT / 2007	Source: Matin, Eydgahi, and Shyu 2017		X				X				X	X		X	X		X					X
Al-Bahr Towers	UAE / 2012	Source: Schumacher, Vogt, and Cordón Krumme 2019		X				X				X	X		X	X		X				X	
OPEN Café-Restaurant	NLD / 2008	Source: Schumacher, Vogt, and Cordón Krumme 2019		X				X				X	X				X	X					X
Mokyeoari Wood Culture Museum	KR / 2017	Source: Schumacher, Vogt, and Cordón Krumme 2019		X				X				X		X	X			X			X		
ThyssenKrupp Headquarters	DE / 2010	Source: Spiegelhalter 2017		X	X							X	X		X	X	X		X			X	
Sebrae Headquarters	BR / 2010	Source: Singhal 2011		X	X							X	X		X	X			X			X	
Mpavilion 2014	AUS / 2014	Source: Schumacher, Vogt, and Cordón Krumme 2019		X	X							X	X				X		X				X

Table 2 [16] – Comparison between different kinetic facades

The functions as seen in the table are primarily: Daylight control, Thermal control and Airflow control, which then gave the idea of introducing another function which in this case is atmospheric water harvesting.

3 Methodology

The primary goal of this study is to test the availability of integrating the SAWH within the building façade system, without compromising other façade roles like thermal comfort and visual comfort, as well as testing the suggested system's possibilities to cover the different building uses or dimensions. As mentioned in the previous chapter, the SAWH contains some main elements that are necessary for the water production cycle, such as: desiccant beds, glass covers, openable shutters and water collection tubes. These elements were the main components on which the design was made upon. At first different morphologies were studied in accordance with the shape, inclination angle or the number of desiccant beds inside of one system. The next step was the choice of materials to lay on the desiccant bed, in accordance with availability of the materials, the water collection rate and the overall economic potential. A design combining the chosen morphology and desiccant bed type was approached with visual comfort in mind. Later on, thermal comfort was tested by using a plug-in in Rhino 3D to calculate the illuminance and glare of different alterations of the design that were made by parametric design tools in the Rhino 3D's plug-in Grasshopper.

SAWH Element Design

3-i General Morphology

According to experiments done with different morphological shapes of SAWH elements, two main morphologies are found to be used. First one, a cuboid box with an inclination angle with an average of 30 degrees, to allow maximum solar energy on the surface of the desiccant bed, which causes the evaporation of the collected humidity during the day, through a glass surface. The surface opposite the glass surface held the desiccant bed and the two surfaces on the side had openable shutters to allow humidity to enter the system during the night. An example of this first morphology is shown in Fig 7 [14] cited from (Application of a solar desiccant/collector system for water recovery from atmospheric air) which was an experimental apparatus made by researchers in the (Mechanical Power Engineering Department) at Mansoura university, Egypt.

Fig 7 [14] – Experimental apparatus for SAWH (Mansoura University, Egypt)

In their experiment, H.E. Gad, A.M. Hamed and I.I. El-Sharkawy used a corrugated desiccant bed of blackened cloths (to increase the surface area of the bed) with a liquid desiccant of calcium chloride solution. The water production of their experiment was around 1.5L/m2/day.

The same morphology can be seen in Fig 8,9 which show the apparatus during the night and day cycles respectively as cited from (Composite desiccant material "CaCl2 /Vermiculite / Saw wood) [17]. In this experiment Manoj Kumar and Avadhesh Yadav also used Calcium Chloride as a desiccant material but with Vermiculite and Saw wood as desiccant bed base. The water production for their experiment was 0.5L/m2/day.
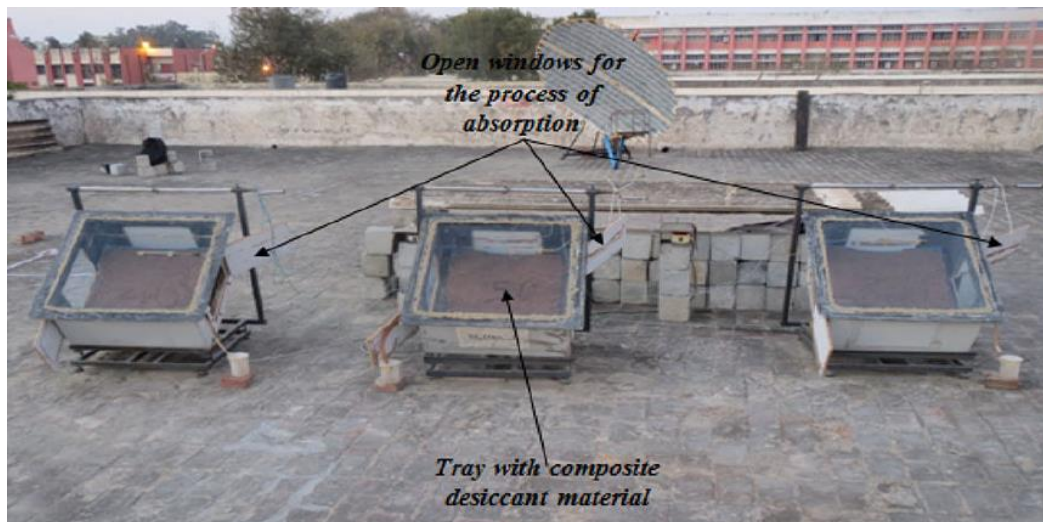
Fig 8[17] – Experimental apparatus for SAWH (open shutters- night phase)
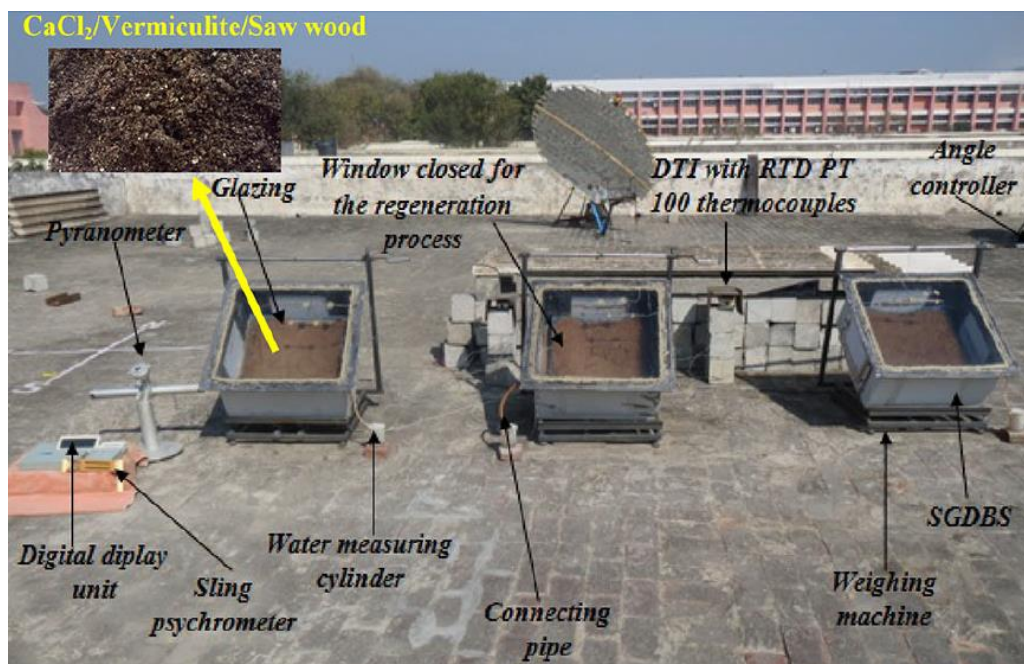
Fig 9 [17] – Experimental apparatus for SAWH (closed shutters- morning phase)

The second morphology is a pyramid shaped glass cover with desiccant beds staggered on top of each other like shelves, with a space between each of them in the vertical and horizontal directions to allow the solar energy to reach each shelf without compromising the water production values.

An example of this second morphology is shown in Fig 10,11 cited from (Desiccant system for water production from humid air using solar energy). An Experiment apparatus done by researchers in (Mechanical Power Engineering Department) at Helwan University, Egypt. In their experiment, G.E. William, M.H. Mohamed and M. Fatouh used two materials to host the desiccant material which were sand and cloths. The desiccant material staying constant as calcium chloride, this gave them a maximum water production rate of 2.3L/m2/day and an average of 1.2L/m2/day for cloths beds. As for sand beds, the maximum water production rate was 1.2L/m2/day and the average rate was 0.3L/m2/day.

Fig 10,11 [18] – Experimental apparatus for SAWH (Helwan University, Egypt)

Another example is shown in Fig 12,13 as cited from (Outdoor Testing of Double Slope Condensation Surface for Extraction of WaterfromAir) [18] an experiment apparatus done by the (Mechanical Power Engineering Department), Mansoura University, Egypt. In their experiment, K. H. Awad, M. M. Awad and A. M. Hamed used sand as a desiccant absorber and Calcium Chloride as a desiccant material, which gave a maximum water production value of 0.7L/m2/day.
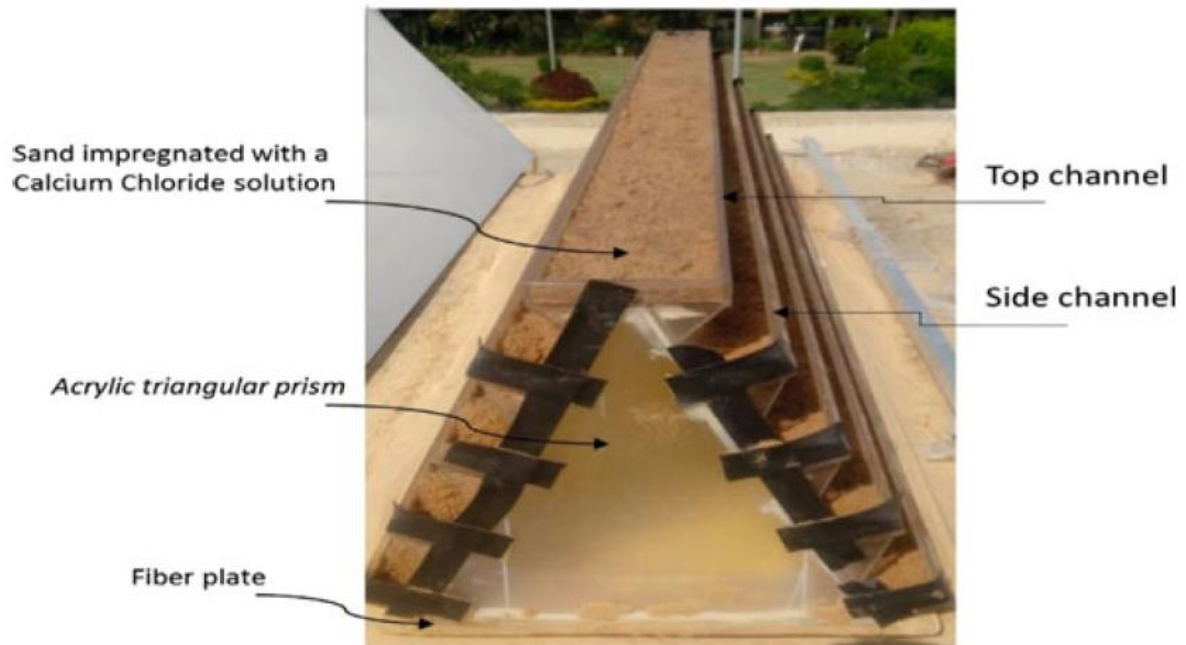
Fig 12,13 [19] – Experimental apparatus for SAWH (Mansoura University, Egypt)

Comparing the two morphologies, both were designed to allow maximum exposure of the desiccant bed to solar energy. The desiccant material played a main role affecting water production values and not the morphology itself if maximum exposure to solar energy was maintained.

Choosing a morphology then to be applied on an architectural façade level would depend on how the desiccant bed would be oriented towards solar rays maximizing the area of effect and exposure. Designing a SAWH element that would be placed on the façade then meant that it also had to maintain the other façade purposes like thermal and visual comforts.

3-ii Desiccant Beds Morphology

The first design question was how it would be possible to apply an opaque material to the façade (desiccant bed) without troubling the view). Abstracting the former two morphologies we can see the relation between sun rays and desiccant bed to get an answer to that question, as follows in Fig 14.

(a)   (b)
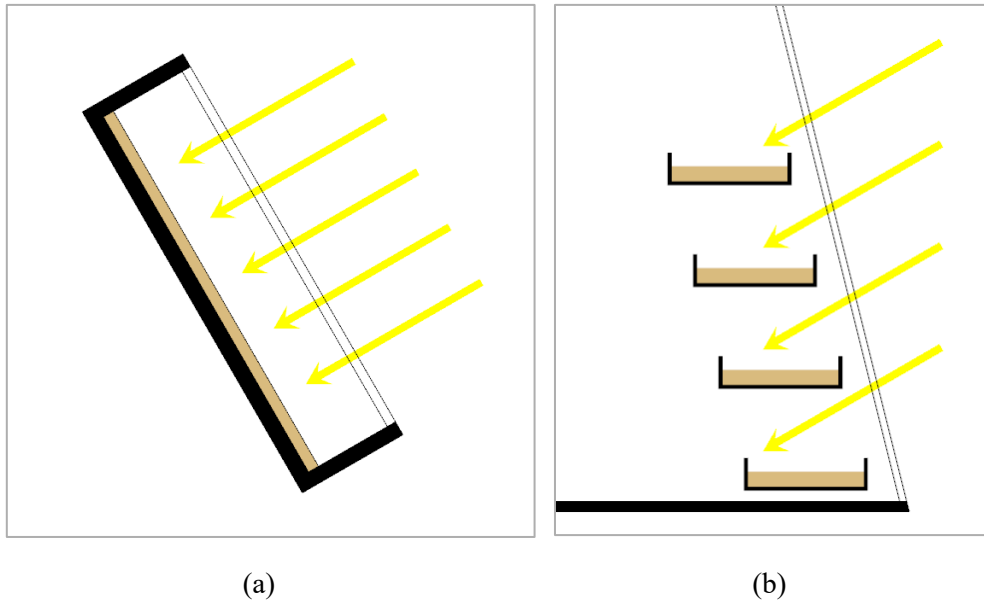
Fig 14 – Abstraction of relation between desiccant beds and sun rays .

a-Rectangular apparatus morphology b-Pyramid apparatus morphology

Fig 14-a describes the morphology of cuboid type, and Fig 14-b describes the morphology of the pyramid type, both in the relation between sun rays and desiccant bed. This abstraction helped to realize the connection between the two morphologies, which is that (b) is divided into segments with rotation of each segment, and that (a) is the connection of the segments of (b) if they rotated around their central, as shown in Fig 15.
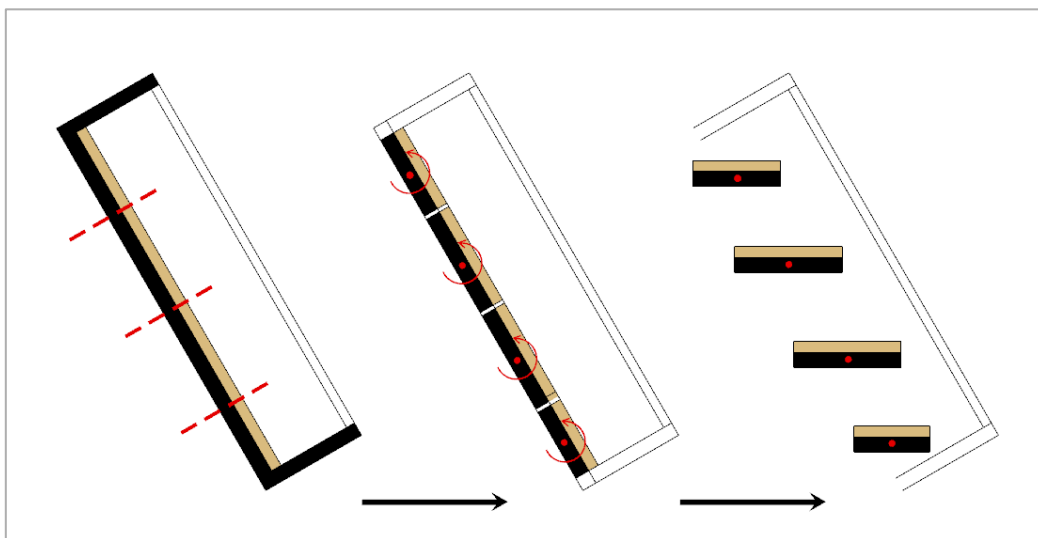
Fig 15 – Abstraction of sorbent beds' morphology and rotation around its axis

This transition became the key element for user-controlled design, as it allows the user to control the percentage of view according to their preferences without sabotaging the water production values, working basically with the same concept as venetian blinds Fig 16.
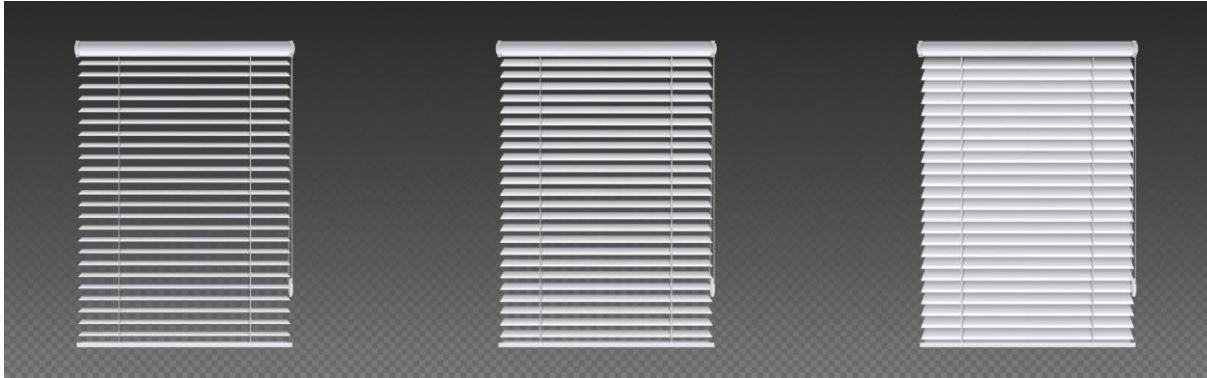
Fig 16 – Venetian blinds with different rotations

From these abstractions we got the general shape of the cross section of the SAWH which is shown in Fig 17. Four main points a,b,c and d were concluded and guided the entire design process. Since the SAWH would be placed directly on the façade, the surface between points (ad) was removed, which transformed the cross section from a rectangular to triangular shape.

The surface between points (ab) would act for both collecting the condensed water droplets on its surface which then will flow towards point (b) due to the force of gravity. The surface between points (cb) would then act as a medium to move the water droplets to the collecting channel at point c due to the force of gravity.

(a)   (b)
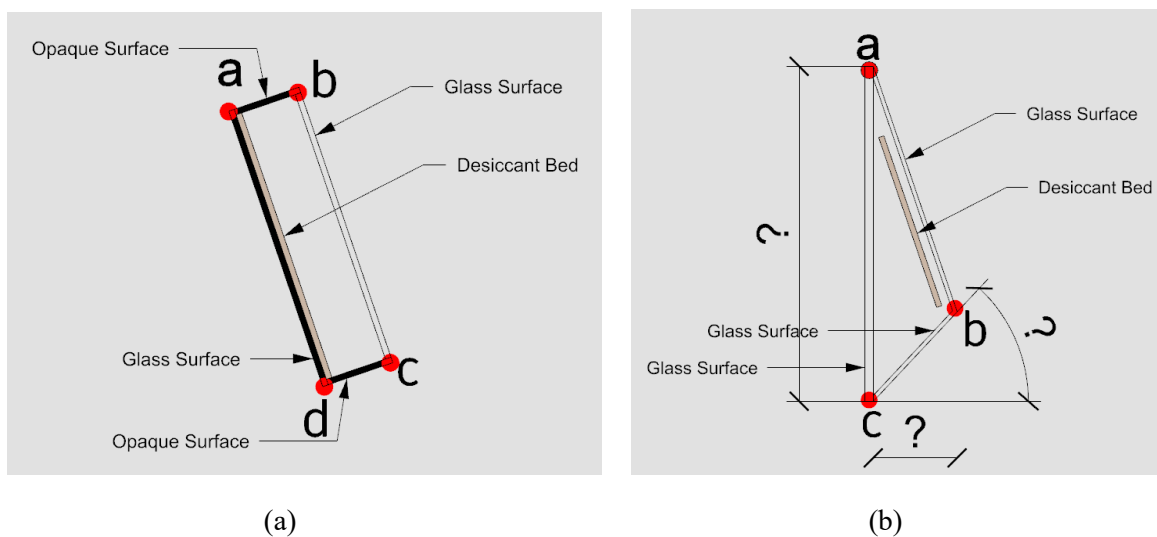
Fig 17 – SAWH element cross-section

a- Rectangular cross-section for experimental apparatus b-Triangular cross-section for façade implementation

3-iii Cross Section Dimensions

A -Inclination Angle

The design questions resulting from this cross section were the angle of inclination, the height of the element and the depth of the element. The angle of inclination of the element should be found so that it would allow maximum exposure to solar radiation on the desiccant bed and therefore block the unwanted light when the element is in full closure state (rotation angle= 0). To get the angle of inclination, a test was made on a surface (resembling a façade) facing absolute south at 9 AM, 12 PM and 3 PM during the Vernal Equinox (20.March), Winter Solstice (21. December), Autumnal Equinox (22.September) and Summer Solstice (21.June) to get the solar energy values and their corresponding altitudes. The altitude for the maximum solar energy value was then used as the inclination angle.

Fig 18-a Vernal Equinox

(All units in kWh/m2)

Fig 18-b Winter Solstice

Fig 18-c Autumnal Equinox

Fig 18-d Summer Solstice
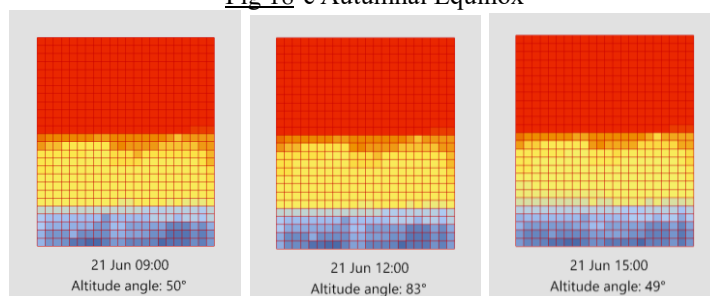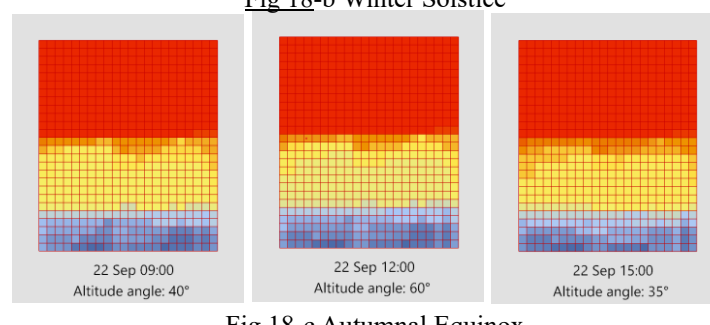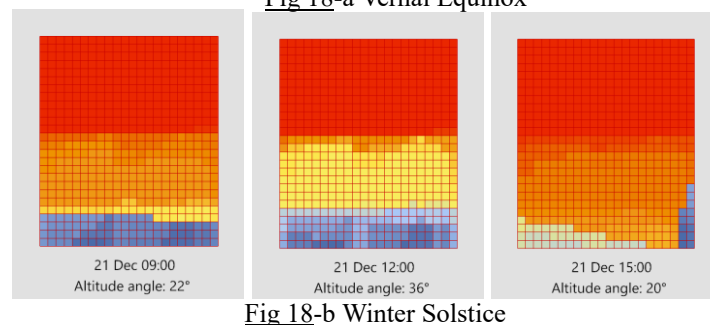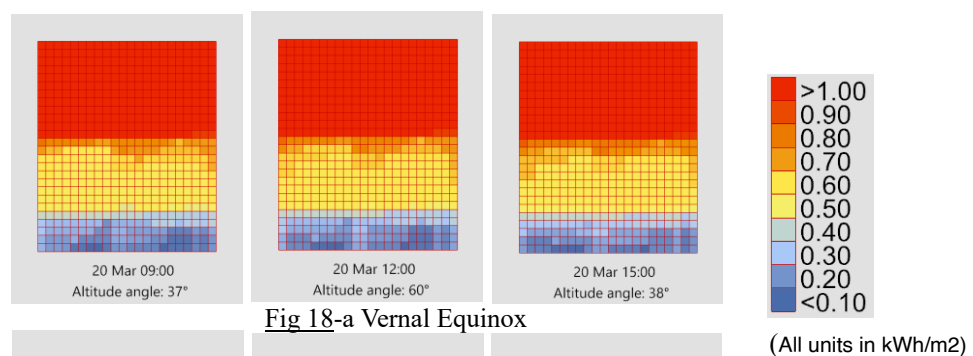
Fig 18- Incident radiation on rectangular facade

15

The solar energy on the surface and the corresponding sun altitude angles were calculated by a plugin in Grasshopper-Rhino called Ladybug for which the location provided to the program to do the tests was Cairo, Egypt. The results were that at 12 PM the solar energy was maximum in all seasons. The maximum solar energy was at the Winter Solstice with a value of 0.71 kWh/m2 and Autumnal Equinox of value 0.57 kWh/m2 as shown in the Fig 18-a-b-c-d. The Autumnal Equinox altitude of the sun was then used for the design as the heat in that season is the maximum which was needed for the condensation of collected vapor later. The Autumnal Equinox altitude is approximately equal to 60°.

The hatched area shown in Fig 22. shows the potential area that the surface allowing the solar energy on the desiccant bed would be placed, and the grey lines connecting point (a) with line (bc) at point (b') show the possibilities of the final cross section depending on the depth of the SAWH element.

According to previously mentioned experiments, surface area of desiccant beds plays a main role for water production values, the larger the area the higher the water production rate. For this reason, the length of line (ab') should be maximized as much as possible as it is equivalent to the length of the glass surface, thus the length of the corresponding desiccant bed.

B - Height, Width and Depth

In this case two assumptions were made regarding the SAWH element. First, its overall height which will be covering the whole floor height of at 3m. Therefore, the depth of the SAWH (Xm) would have a value ranging from (0m < Xm ≤ 1.73m) as shown in Fig 22. Second, its overall width which was assumed to be 1.5m
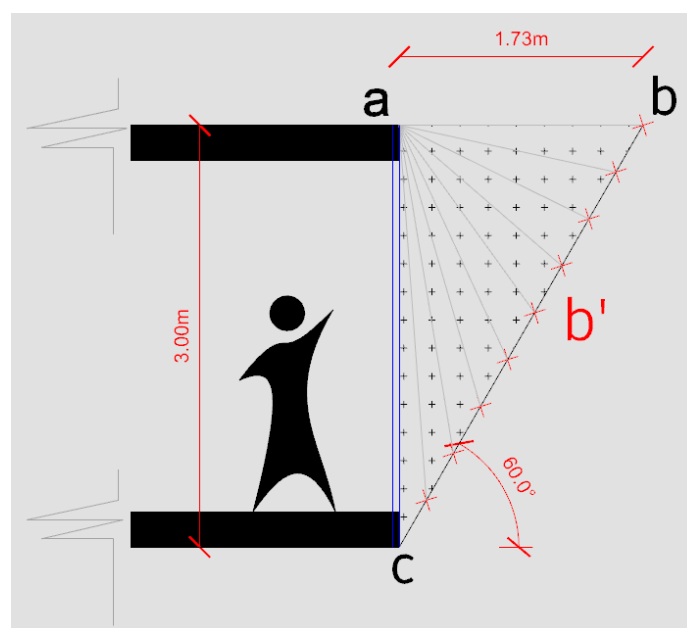
Fig 22 - Depth and inclination angle of the SAWH element on façade

A maximum allowed length of line (ab') then must allow the full rotation of the desiccant beds around their axes, according to the user preferences for maintaining visual comfort as mentioned before.

To get the thickness of the desiccant bed, the desiccant material had to be chosen. As seen earlier in (chapter 2-3) in table 1 there was a comparison between sorbent materials and their water production values in which nearly all sorbent materials consisted of Calcium Chloride on a bed of sand, cloths or wood.

In this case, sand beds would not be convenient as sand would fall off the shelves in case of rotation (no binding materials were mentioned in the previously done experiments, therefore there was no clue about their chemical properties or its effect on the water production process). For the remaining two materials: wood and cloths, a preference was given to the lighter material. First, for the ease of the mechanical rotation due to the lighter weight. Second, for the effectiveness of its water production process and third, for the cheaper price of cloths in comparison to wood, which makes it the more economic option.

According to their experiment G.E.William, M.H. Mohamed and M. Fatouh [18] also mentioned that liquid desiccants seem to have many advantages over solid desiccants as their moisture holding capacity is generally greater than that of solid desiccants. The cloths thickness according to their experiment was (1mm) and as quoted from (Sorption-Based Atmospheric Water Harvesting) [12] In order to reduce the thermal resistance of sorbent beds, thin (1–5 mm) sorbent layers can be directly deposited on metal substrates or fins. Therefor, the thickness of the desiccant bed would consist of 1mm + the thickness of the holding subtrate or fin.

To get the width of the holding fin, a reference was taken from the traditional window venetian blinds which can vary from 60mm to 100mm, as seen in (External venetian blinds Technical data sheet) of a company called Werema.[20]

In this stage tests were made to check the length of the glass surface that would allow maximum count for fins carrying desiccant beds. Line (bc) was divided into a number of points (n b') to check which point of them would be the connection point with point (a) providing maximum surface area for desiccant beds. As shown in Fig 23 line (bc) was divided into 15 points for accuracy of calculations and each point was then connected to point (a).
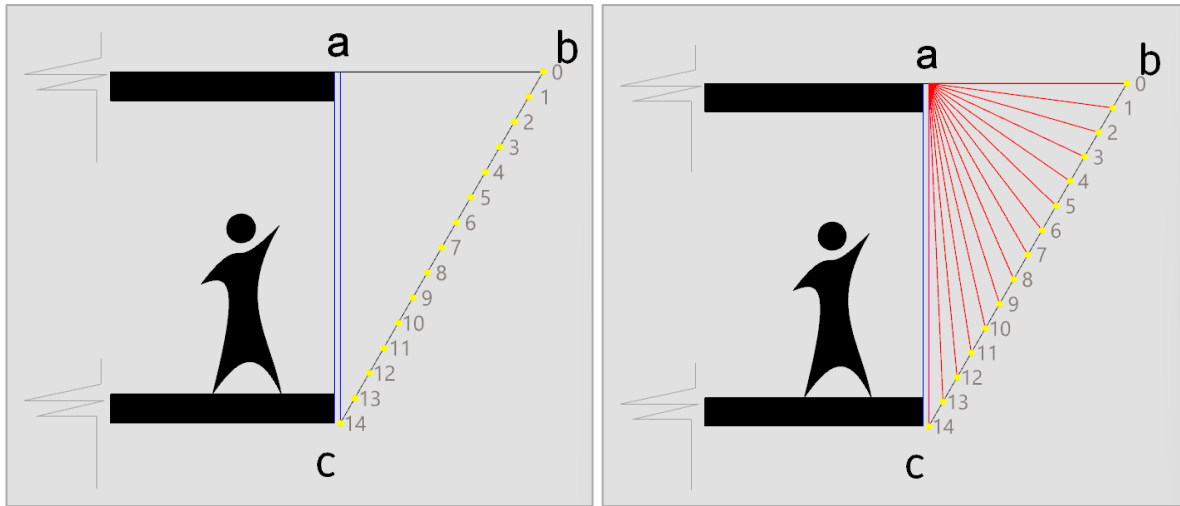
Fig 23 – Different possibilities of the cross section based on depth of the SAWH element

Next step was to draw a parallel line for each of the lines drawn to simulate the desiccant bed that should have a space between itself and the glass surface for at least 20 cm for the condensation process as mentioned in earlier experiments [18] and to allow the rotation of the desiccant beds. Every part of the parallel line that penetrated the façade into the building was then removed to get the actual length of the desiccant bed, as shown in Fig 24.
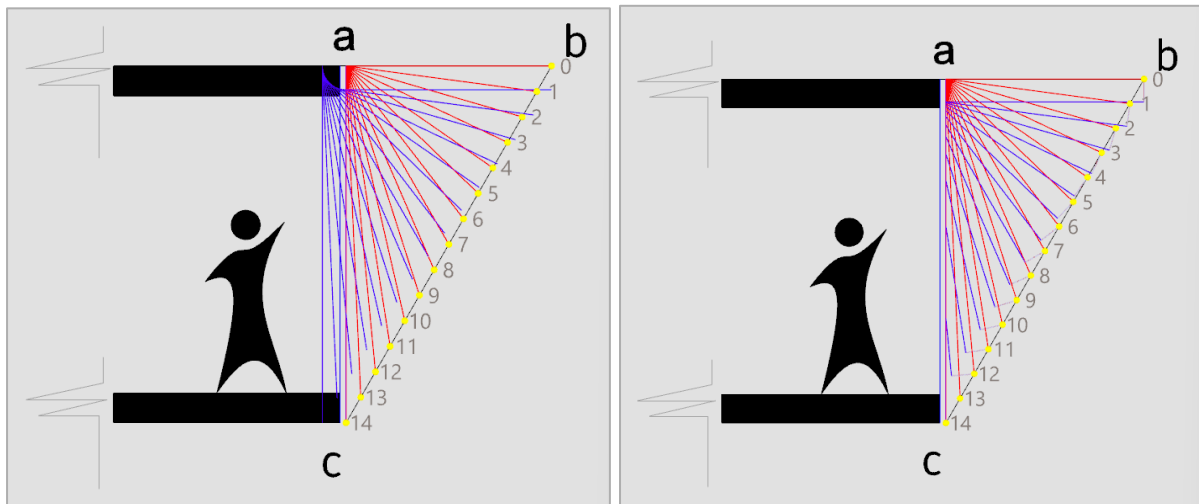
Fig 24 – Testing desiccant bed length with offset from surface (ab)

What remains of the points after excluding the parallel lines that are inside the building was points (0-12), calculating the length of each line, it was ranged between 1.7m and 0.5m as shows in Fig 25.
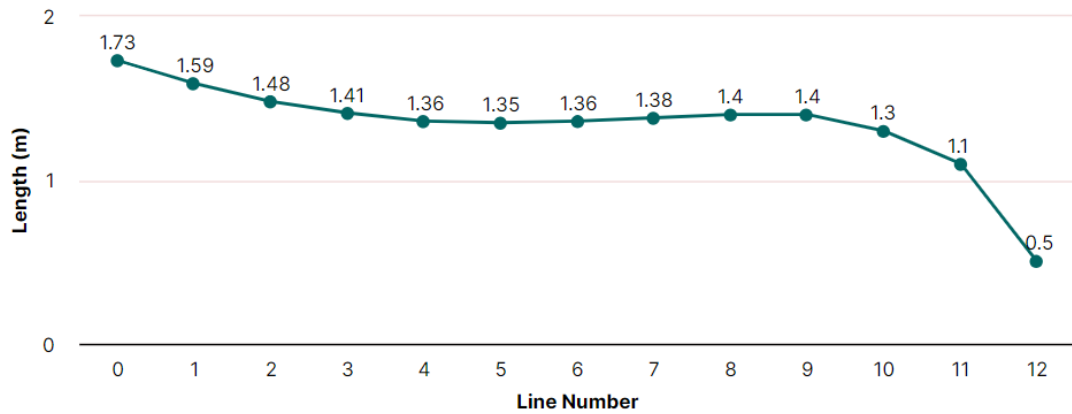
Fig 25 – Different lengths of desiccant beds based on depth of SAWH element

From point 0 to point 5 the length is decreasing, increasing again till point 9 and decreased again till the last point 12. The obvious choice was one from the first 5 numbers, but they were not considered as in winter they would allow sun rays that have an altitude of approximately 36° which will highly increase the glare, as seen previously in Fig 18. Sun rays with an altitude of 36°. As for points 8 and 9 , they would block more sun rays during the winter thus preventing glare as shown in Fig 26.
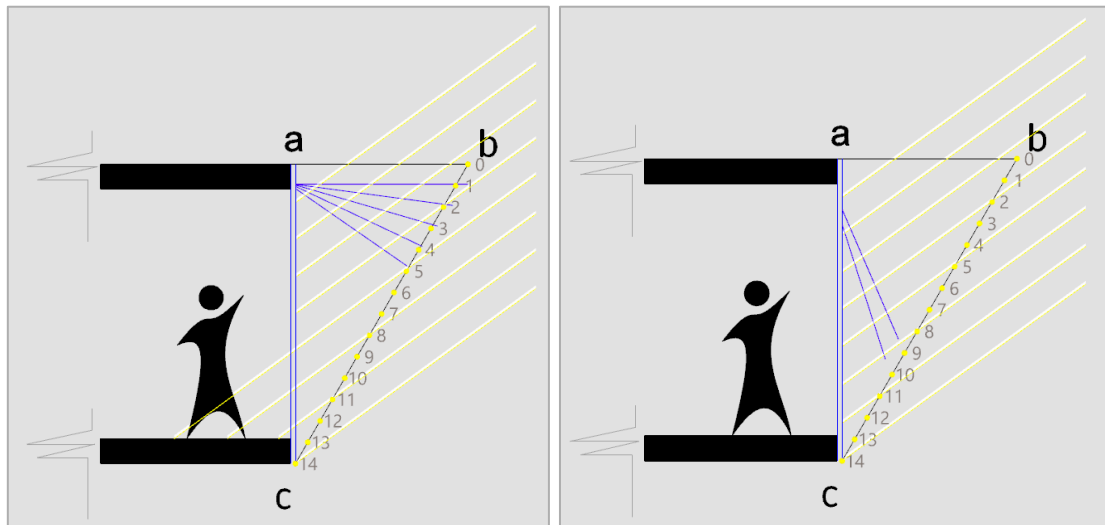
Fig 26 – Comparison of different cross sections and their relation with blocking sun rays

As mentioned earlier, the struts that would contain the desiccant beds can have a width that varies between 60mm and 100mm. Dividing the two lines (ab'8) and (ab'9) which both have an approximate length of 1400mm by 100 mm (the length of a single desiccant bed), the maximum number of fins would be 14.

The depth of the SAWH element that would give a total length of desiccant beds equals to 1.4m divided by 14 fins of width 100mm each would then be between 0.62m and 0.74m as shown in Fig 27.
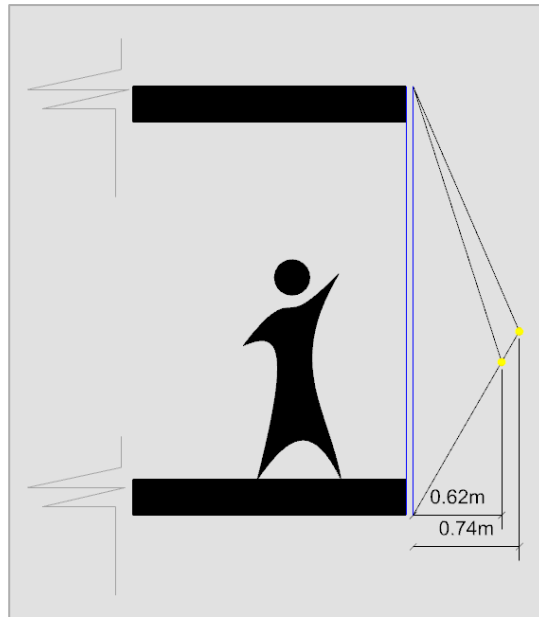
Fig 27 – The outcome depth of the SAWH element

Assuming that the width of the SAWH element is 1.5m, the height is 3m and the depth is around 0.7m, the element would have a morphology with the dimensions shown in Fig 28.
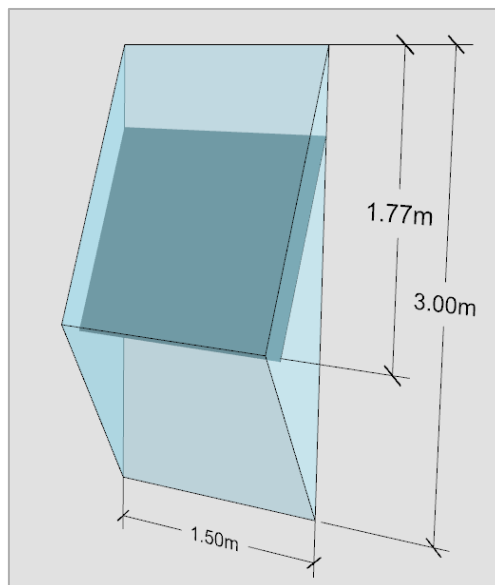
Fig 28 – First outcome of SAWH element Morphology

3-iv Night Phase Shutters

As mentioned earlier, the water production cycle is divided into two phases, a morning phase and a night phase. During the night phase, the system must be in contact with the atmospheric air for the desiccant beds to absorb the humidity, which will be desorbed on the glass surface as water droplets in the morning phase, due to evaporation. Therefor the next

design question was how to integrate an openable door in the SAWH element to allow the air flow inside the element during the night.

To reduce human error, and because the door should close and open at certain hours for the morning and the night phases respectively. A mechanical door should be designed to open automatically at (18:00) for the night phase and close automatically at (6:00) for the morning phase. Fig 29 gives us an idea for what the horizontal arrangement of the element would look like if they are stacked in contact with each other, leaving us with possibility of the openable shutters on either surface (A) or (B). In this case surfaces (A) a freedom of rotation around its upper edge and (B) have a freedom of rotation around its lower edge as shown in Fig 30. With areas of approx. 2.9 m^2 and 2.1 m^2 for Surface (A) and (B) respectively, with the heavy weight of glass material to would be mechanically complex to move them around these axes.
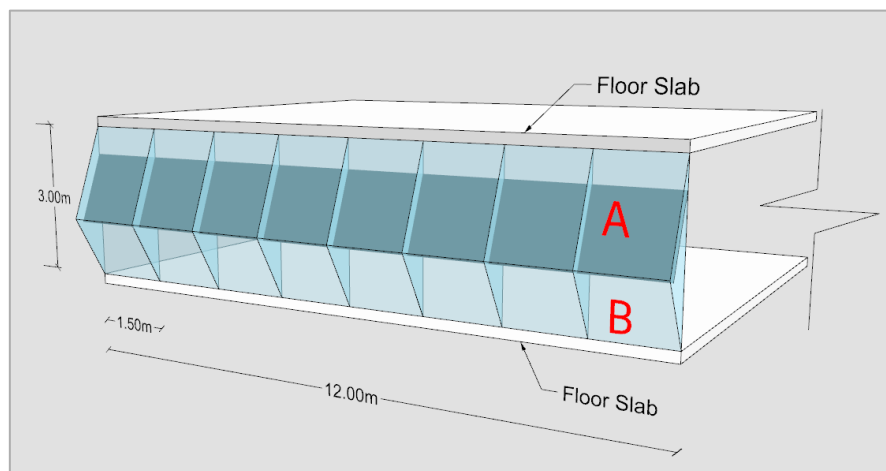
Fig 29 – SAWH element on façade with no openings
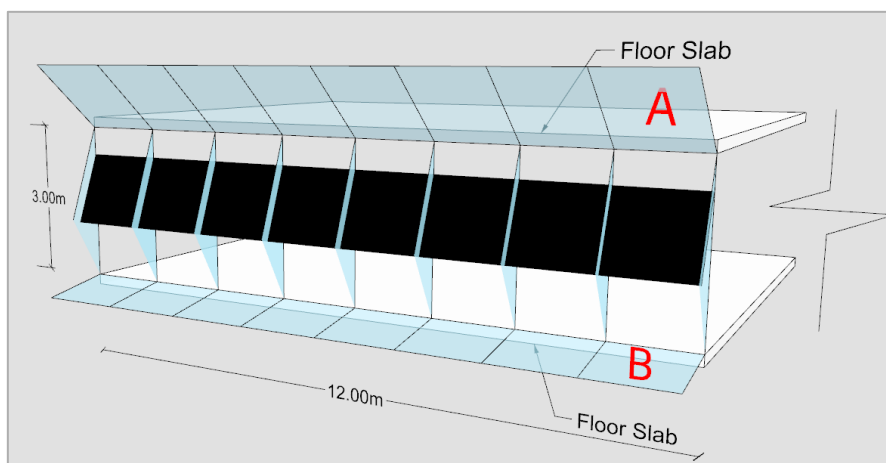
Fig 30 – Possible rotation of SAWH element surfaces

To solve this problem, an intrusion was introduced to the element inwards with the value of 40cm from each side at points (1) and (2) shown as shown in Fig 31.
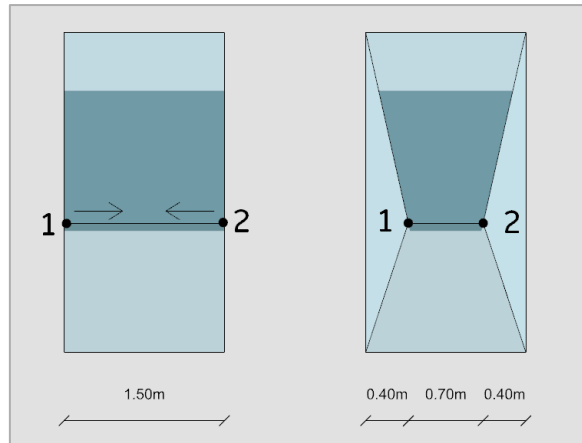
Fig 31 – Introducing of intrusions in SAWH element design proposal to allow rotation

This intrusion would give a space between the SAWH elements, if they were to be horizontally aligned as shown in Fig 31. Surfaces (C) and (D) would then act the shutters for the SAWH element, that would rotate around their axis based on the original glass surface as shown in Fig 33,34.
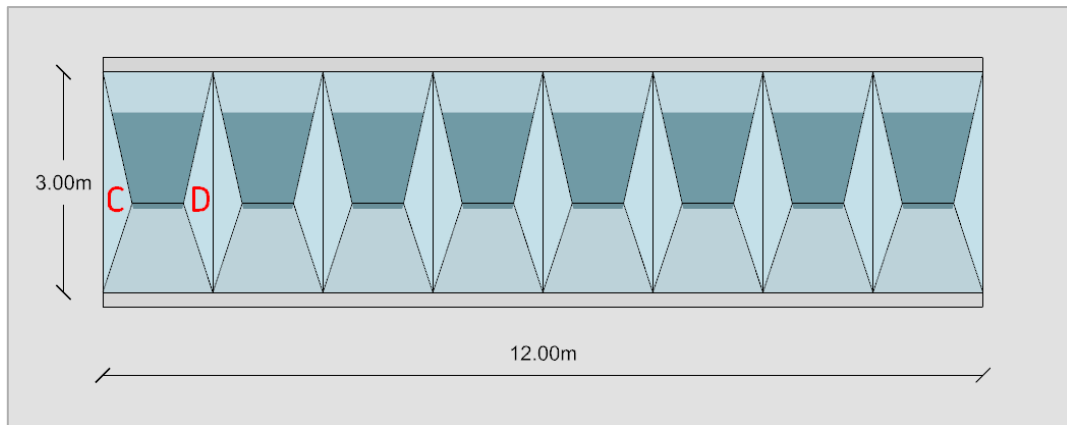
Fig 32 – Surfaces C-D to work as openable shutters
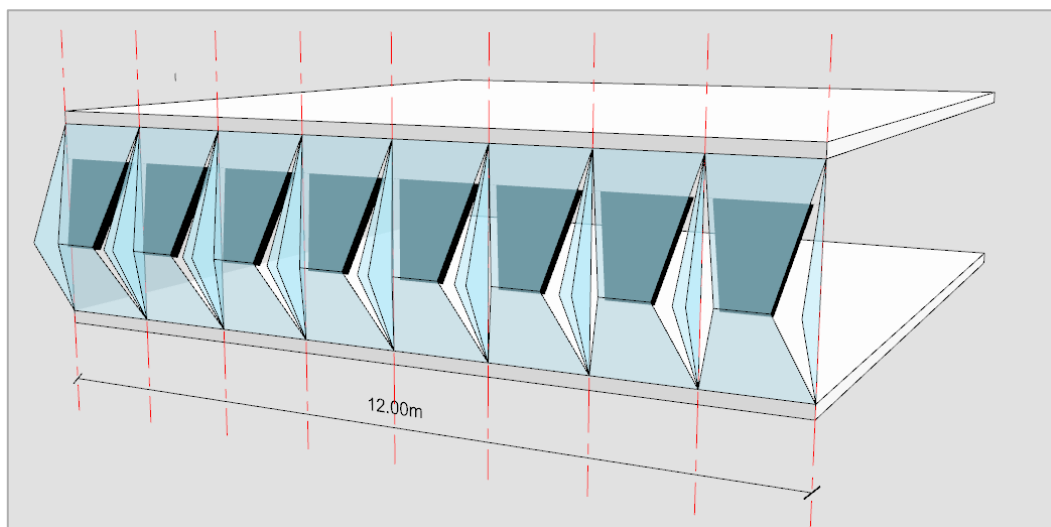
Fig 33 – Axis of rotation for shutters

Fig 34 shows the transition between morning phase and night phase from the left to right respectively.
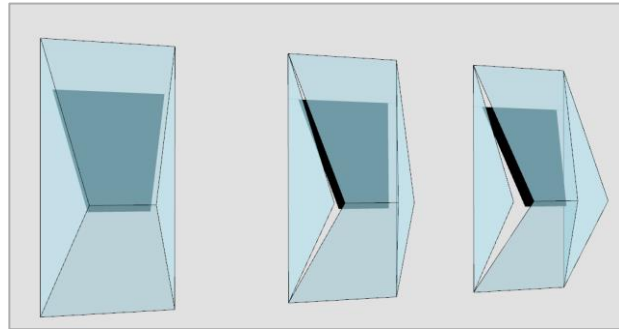
Fig 34- Opening transition of shutters

3-v Materials

The SAWH system in this case as shown in Fig 35 consists of 2 non-moveable glass surfaces (a,b), 2 rotating shutters (c,d) and the desiccant beds (14 beds of 100mm length for each) (e), installed on glass façade. For the glass surfaces and shutters, the right type of material should be chosen to maintain a good level of thermal comfort inside the building as well as keeping a high visibility value for the visual comfort.
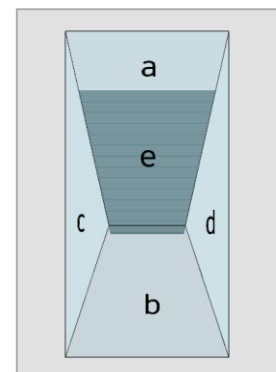
Fig 35 –SAWH element Surfaces

A -Desiccant Beds

As mentioned earlier desiccant beds are going to have cloths saturated with Calcium Chloride, therefore the desiccant beds will be completely opaque.

B -Outer Surfaces

For the outer surfaces, experiments were done to compare different materials and their effect on the (Lux) and (Glare) values inside of the building using (Climate Studio-Rhino)[25].To do these experiments, a test room was designed with dimensions (W=12m, L=10m and H=3.4m) shown in Fig 36. The values of lux and glare were calculated in (Cairo, Egypt) at 9 AM, 12 PM and 3 PM during the Vernal Equinox (20.March), and Summer Solstice (21.June), Autumnal Equinox (22.September) and Winter Solstice (21. December) using different glass materials.
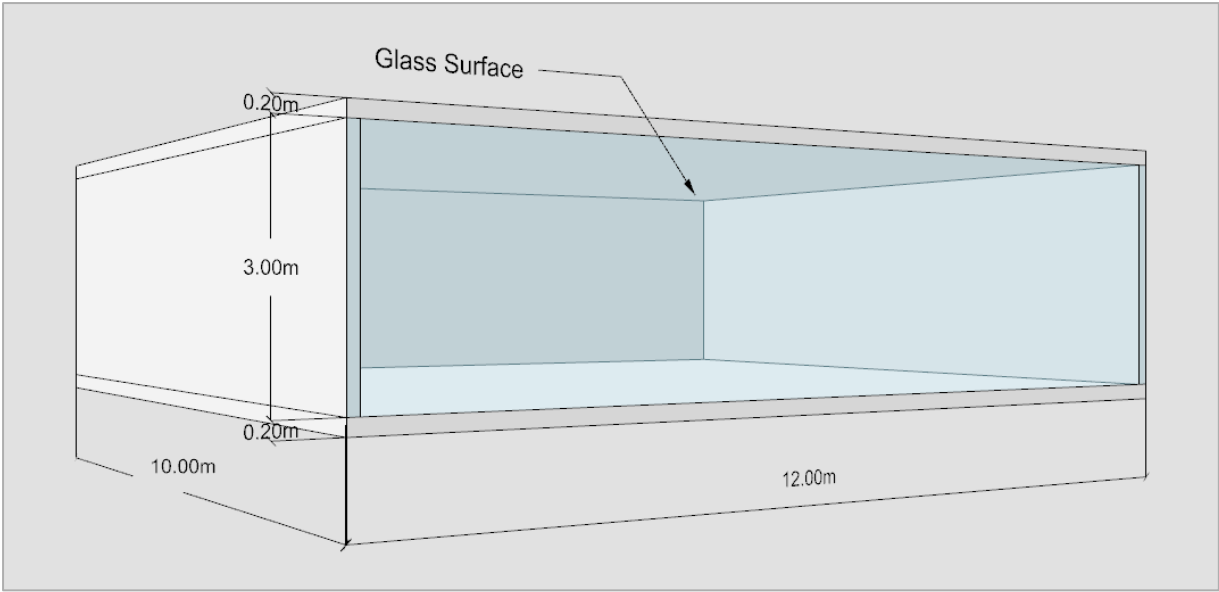
Fig 36 – Test Room Dimensions

Illuminance Threshold values:

The first step was to make a test with just the glass façade without the SAWH element to get the threshold values to know the exact effect on lux and glare when it is added. As for the material of the façade, Climate Studio has a library of materials with their specifications that you can assign for each surface, for this test the material used was "*Atlantica*" as shown in Fig 37. The location of the tests was Cairo, Egypt.
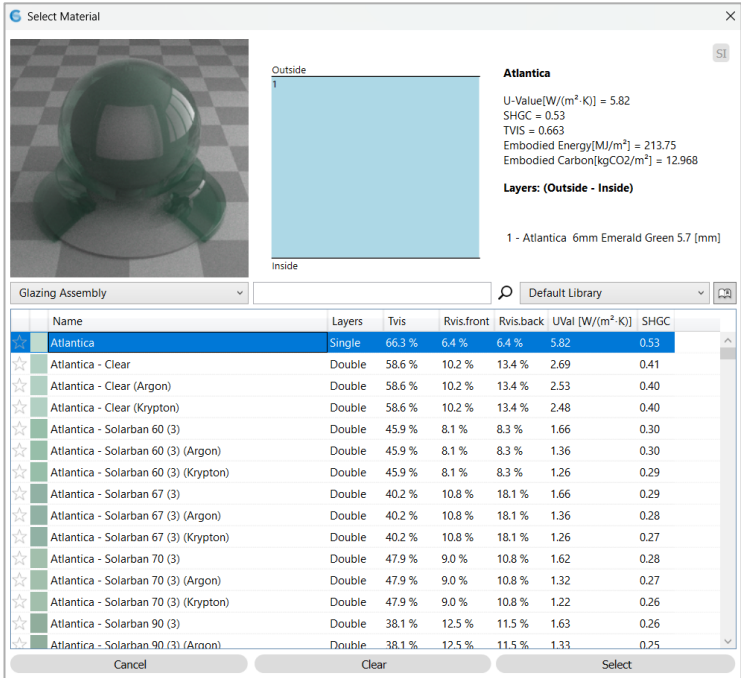
Fig 37 – Glass Materials in Climate-Studio Plug-in

The results are shown in the plan view as in Table 3 for Spring, Summer, Autumn and Winter respectively for (09:00AM, 12:00PM and 15:00PM) with a color gradient shown in Fig 38.
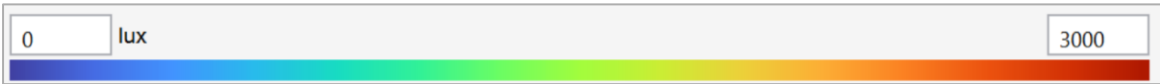
Fig 38 – Legend for Illuminance tests (Units are in LUX)

	09:00	*12:00*	*15:00*
Vernal Equinox	20 Mar 09:00 Mean Illuminance [lux]:3839.8479 Median Illuminance [lux]:852.2289	20 Mar 12:00 Mean Illuminance [lux]:6785.2905 Median Illuminance [lux]:1159.1593	20 Mar 15:00 Mean Illuminance [lux]:3927.2212 Median Illuminance [lux]:847.8906
Summer Solstice	21 Jun 09:00 Mean Illuminance [lux]:1006.7247 Median Illuminance [lux]:545.8939	21 Jun 12:00 Mean Illuminance [lux]:1690.6547 Median Illuminance [lux]:903.7462	21 Jun 15:00 Mean Illuminance [lux]:983.547 Median Illuminance [lux]:547.3862
Autumnal Equinox	22 Sep 09:00 Mean Illuminance [lux]:4189.9326 Median Illuminance [lux]:883.5814	22 Sep 12:00 Mean Illuminance [lux]:6771.4697 Median Illuminance [lux]:1163.223	22 Sep 15:00 Mean Illuminance [lux]:3553.5085 Median Illuminance [lux]:796.1342
Winter Solstice	21 Dec 09:00 Mean Illuminance [lux]:6921.5093 Median Illuminance [lux]:1469.3363	21 Dec 12:00 Mean Illuminance [lux]:10888.8105 Median Illuminance [lux]:1907.8647	21 Dec 15:00 Mean Illuminance [lux]:6302.022 Median Illuminance [lux]:1348.3318

<u>Table 3</u> – Illuminance tests base results for the test room without applying SAWH element

Table 4 shows a comparison of mean values of Illuminance between the seasons according to the chosen material.

TIME/SEASON	VERNAL EQUINOX	WINTER SOLSTICE	AUTOMNAL EQUINOX	SUMMER SOLSTICE
09:00	3840	6921	4190	1006
12:00	6785	10889	6771	1690
15:00	3927	6302	3553	984

Table 4 - Mean base values for Illuminance of the test room (all values are in LUX)

The highest illuminance value was at the Winter Solstice while the lowest illuminance was at the Summer Solstice, with a nearly equal values for Autumnal and Vernal Equinoxes. As heat is not affected by illuminance, the goal for the winter period will be decreasing the glare.

Annual Glare Threshold values:

With the same glass material of the previous test "*Atlantica*" an Annual Glare Threshold was calculated resulting in the values shown in Fig 39 with the highest ratio of intolerable glare was during the winter season and lowest was in summer season.
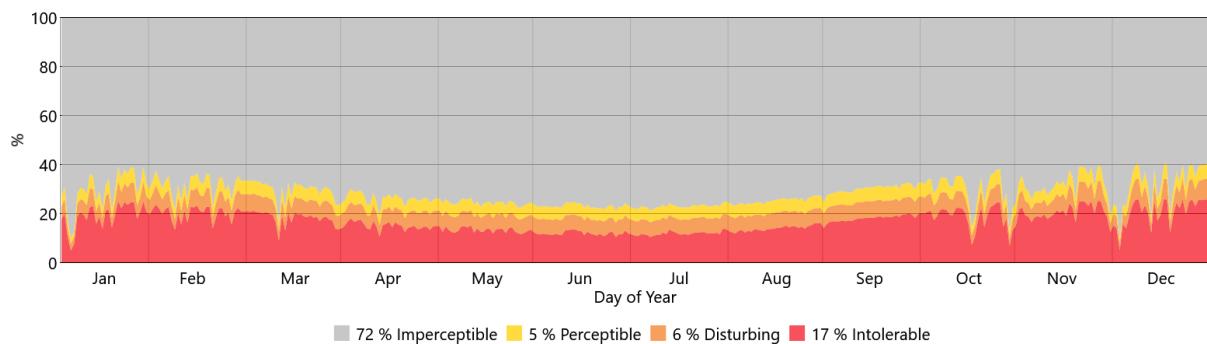
Fig 39 – Annual Glare base percentages for the test room

The distribution of these values is then shown in Table 5, showing the results in a plan view of the test room. The glare during the winter season reached the whole length of the room (10m) , while in the summer season it reached approximately half the span.

26

	09:30	*12:30*	*15:30*
Vernal Equinox			
Summer Solstice			
Autumnal Equinox			
Winter Solstice			
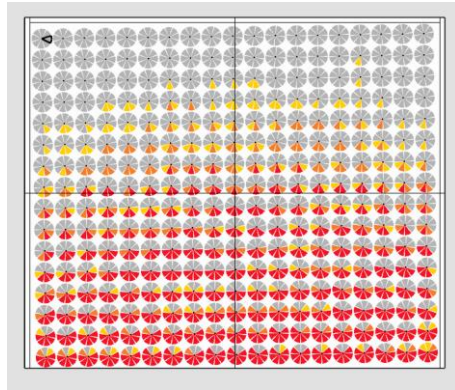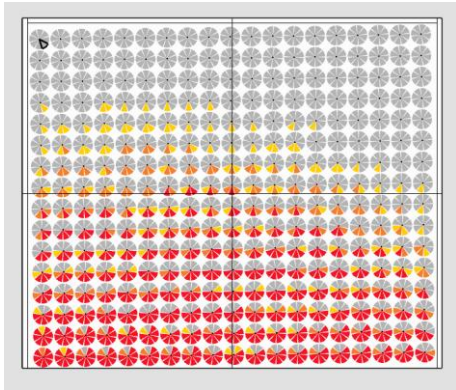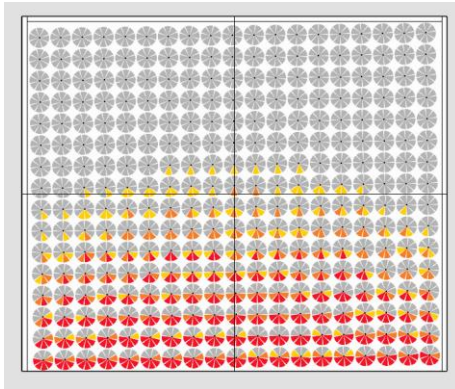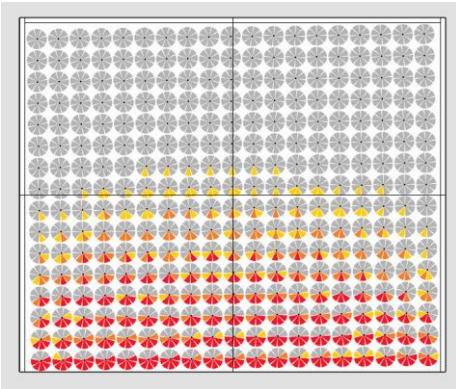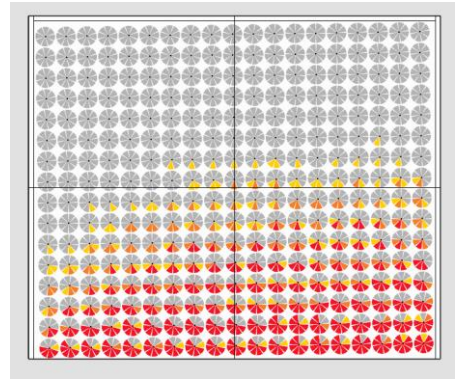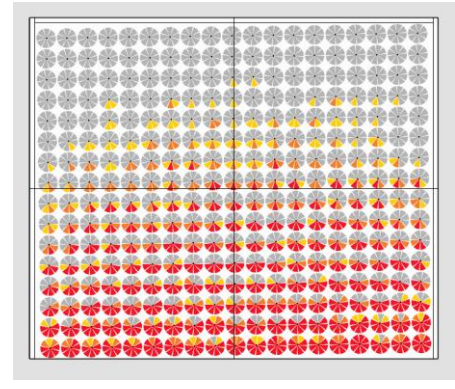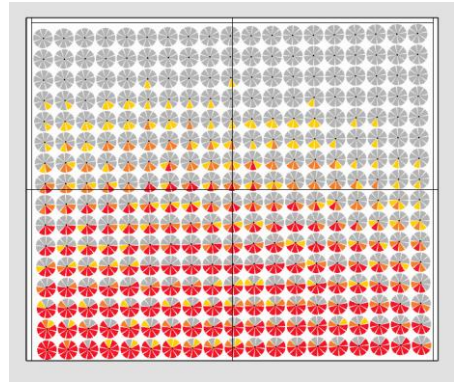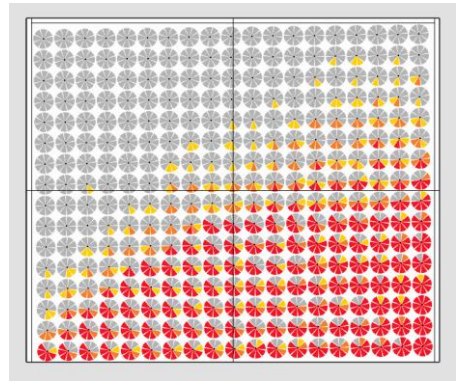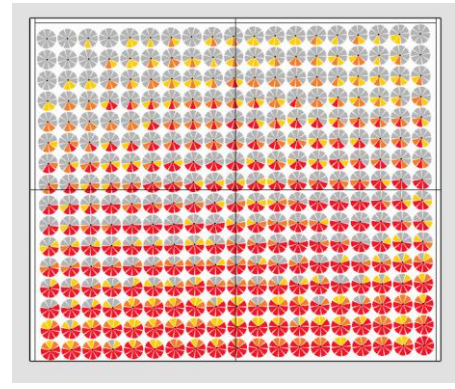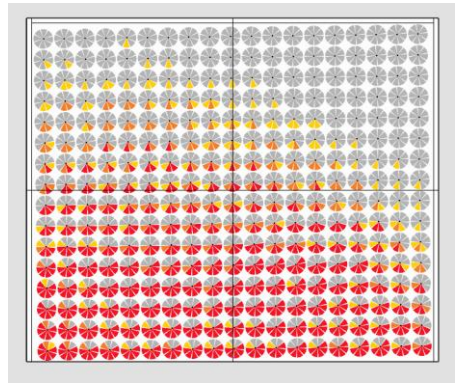
Table 5 – Annual glare distribution for the test room

Illuminance and Glare Tests (Test Room)

Previous values of Illuminance and Glare became the threshold of the tests that will determine what glass material should be used in the SAWH element. For the goal value, the "European Standards" [21] for lighting of workplaces as well as the International Organization for Standardization (ISO) [22] which Egypt usually takes as a standerd stated that the average illuminance in office spaces is 500 lux.

As mentioned earlier Illuminance values will target the Summer, Spring and Autumn seasons, and since the values for Spring and Autumn are very similar, only Autumn values will be calculated. Tests will be done by adding the SAWH element on the glass façade as shown in Fig 40 with 3 variations of the rotation angle for the desiccant beds to get a closed, semi-closed and an open system with (0°,45° and 90°) of rotation respectively, as seen in Fig 41, with the desiccant beds being completely opaque.
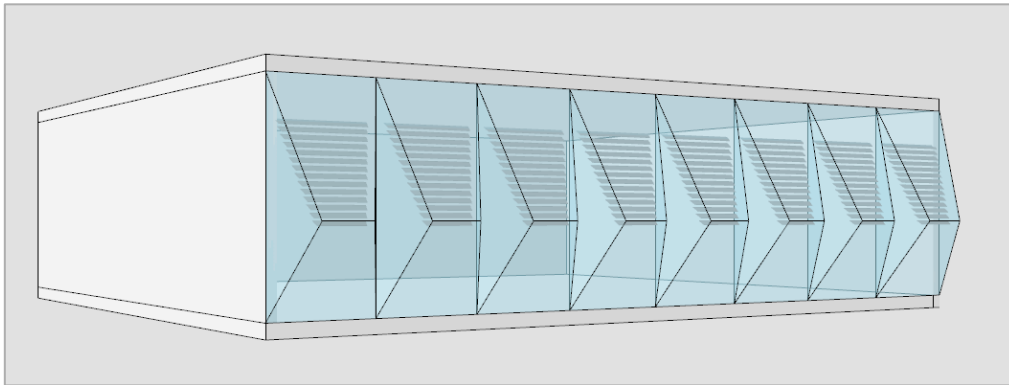
Fig 40 – Positioned SAWH elements on the test room's façade
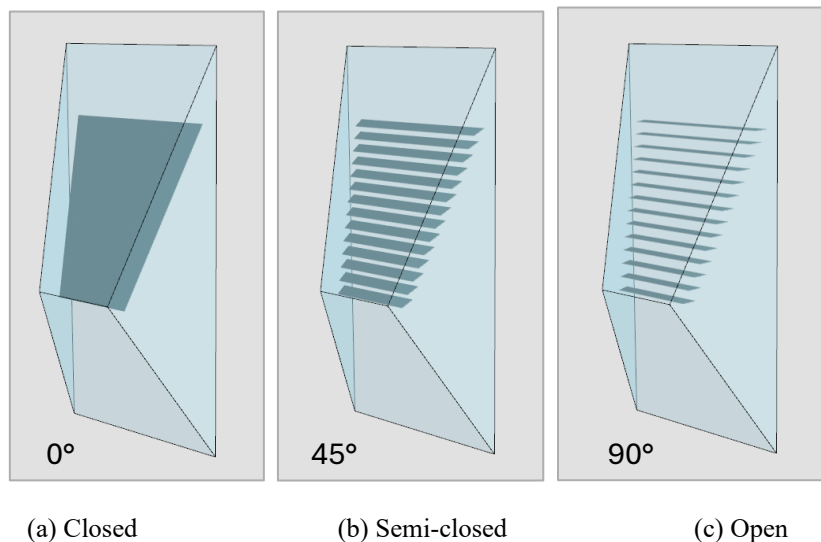
0°	45°	90°
(a) Closed	(b) Semi-closed	(c) Open

Fig 41 – Transition between closed, semi closed and open desiccant bed blinds

Test 1:   Test 1: Glass material: "Atlantica" with specifications shown in Fig 42.

Name	Layers	Tvis	Rvis.front	Rvis.back	UVal [W/(m²·K)]	SHGC
Atlantica	Single	66.3 %	6.4 %	6.4 %	5.82	0.53

Fig 42 – Atlantica material specifications

28

Test 1-1: (Illuminance)

1-1-a (Summer Solstice)
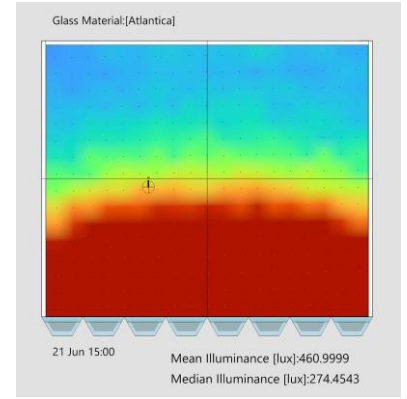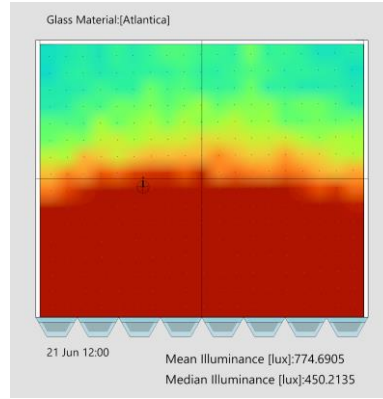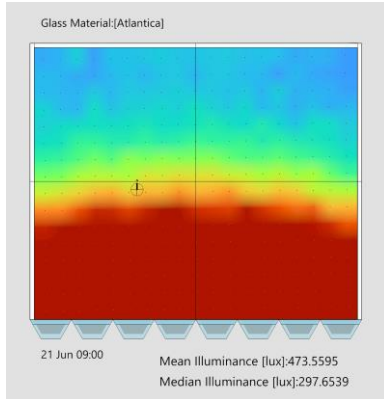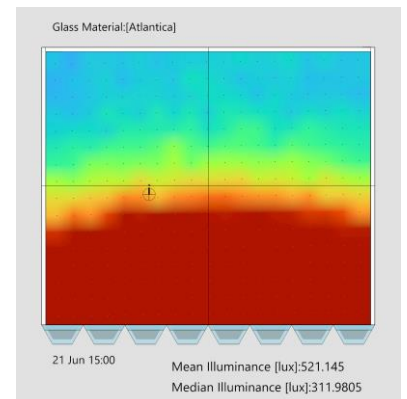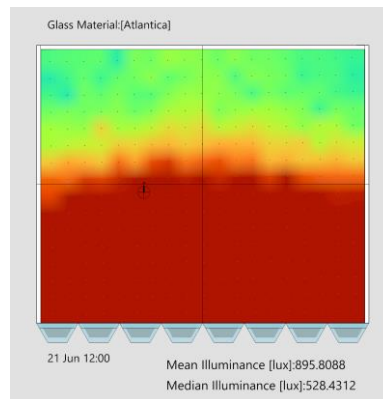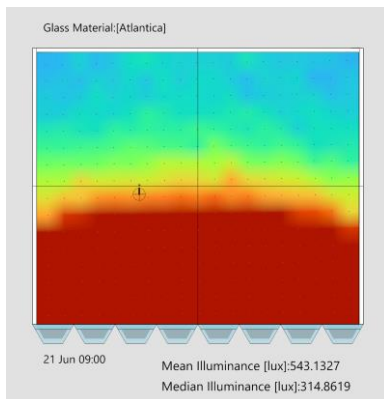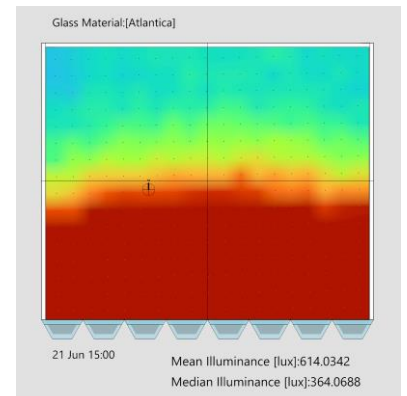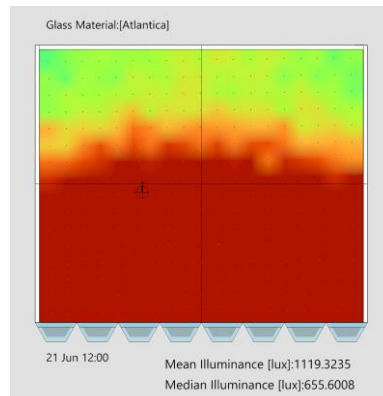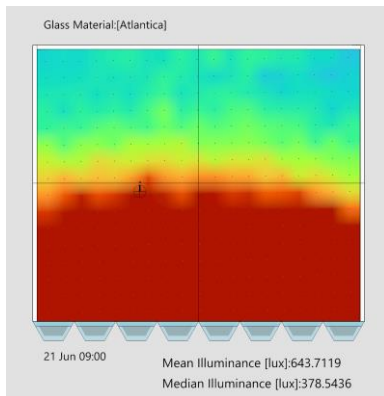
Table 6 – Illuminance distribution for test number 1 under different rotation of blinds in Summer Solstice

Rotation/Time	09:00	12:00	15:00
0°	474	775	461
45°	543	896	521
90°	643	1119	614

Table 7 – Mean values of Illuminance for the Summer Solstice (Test 1) *all values are in LUX

1-1-b (Autumnal Equinox)
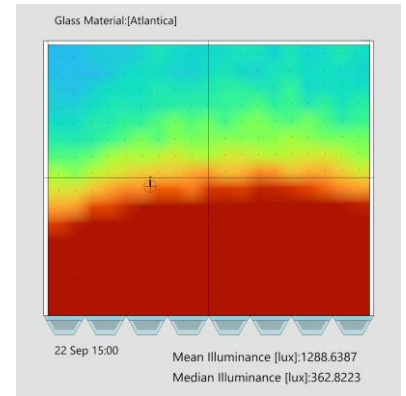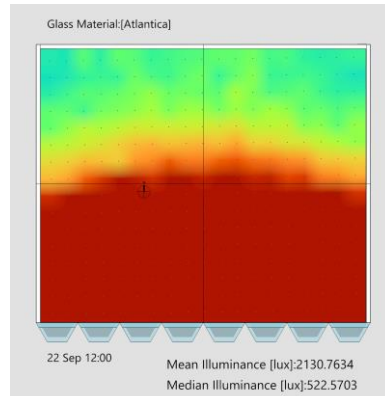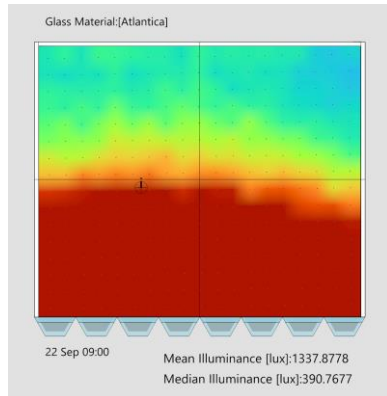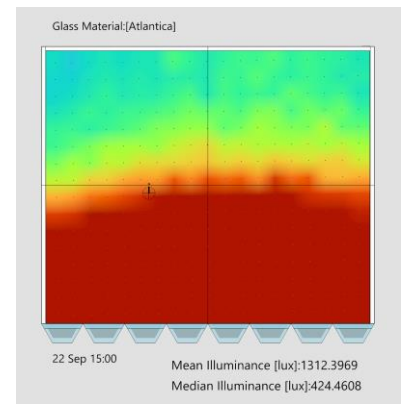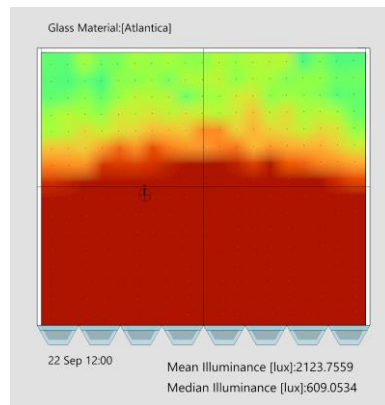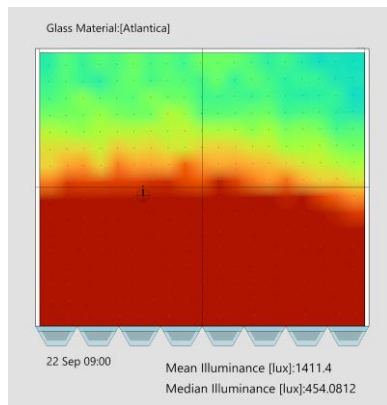
	09:00	*12:00*	*15:00*
0° Rotation			
45° Rotation			
90° Rotation			
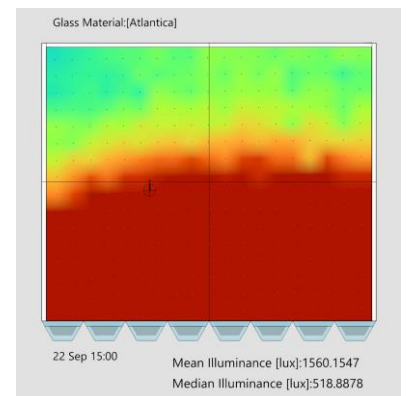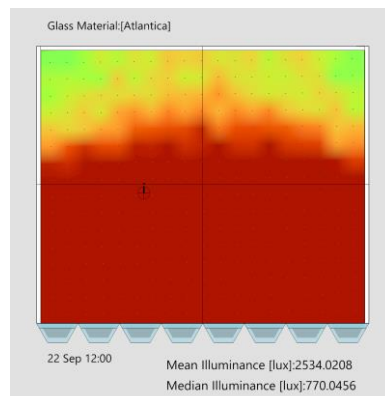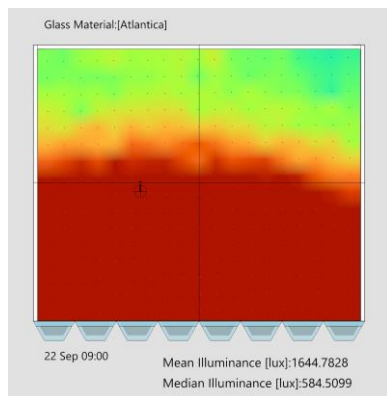
Table 8– Illuminance distribution for test number 1 under different rotation of blinds in Autumnal Equinox

Rotation/Time	09:00	12:00	15:00
0°	1338	2130	1286
45°	1411	2124	1312
90°	1645	2534	1560

Table 9– Mean values of Illuminance for the Autumnal Equinox (Test 1) *all values are in LUX

Test 1-2: (Glare)

For the glare the following annual values were as follows in <u>Fig 42,43 and 44</u>, there was a decrease for the percentage of the intolerable glare that ranges between 9% and 13% from the previous threshold of 17%.

Closed system (0° Rotation):
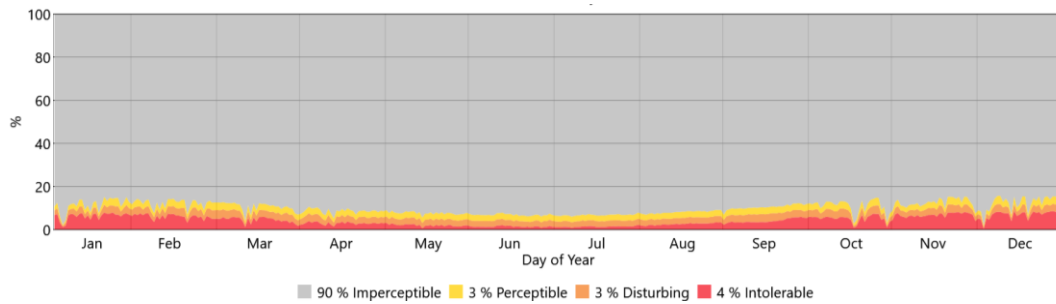
Fig 42 – Annual glare values at 0° rotation of blinds (Test 1)

Semi-closed system (45° Rotation):
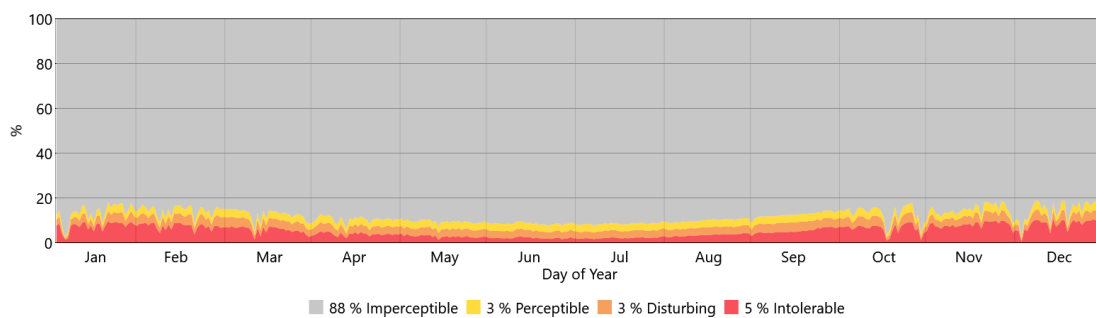
Fig 43– Annual glare values at 45° rotation of blinds (Test 1)

Semi-closed system (90° Rotation):
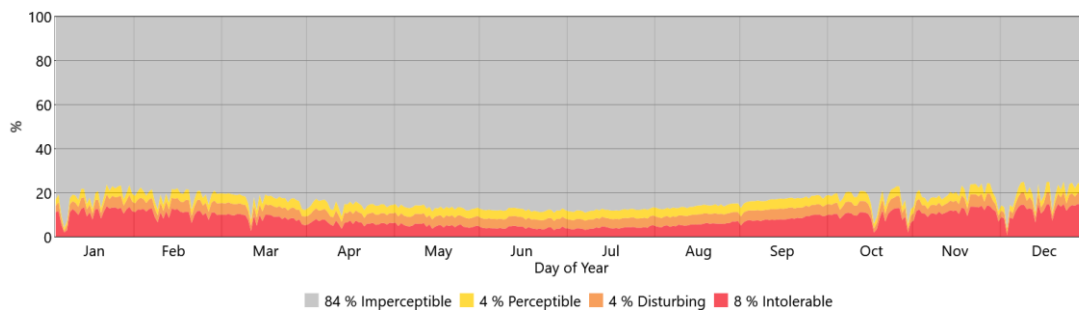
Fig 44– Annual glare values at 90° rotation of blinds (Test 1)

Test 2:

For the second test, a low transparency material was added to the SAWH element in the place where there was no space to add desiccant beds, the space is highlighted in red in Fig 45.

This part can be used for semi-transparent PVC panels, to generate energy for the mechanically openable shutter making the design more sustainable. Companies like OnyxSolar [23] manufacture such panels with a transparency that can reach 38%.
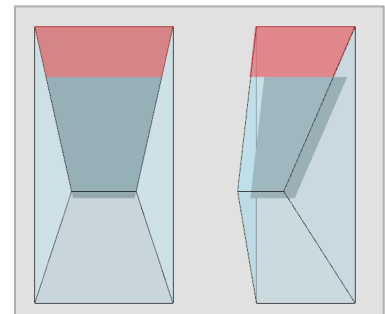
Fig 45 – SAWH element with changing in the material from the original one at the highlighted surface

For starting off, a PVC material was chosen from OnyxSolar website, with transparency of 30% and specifications as shown in Fig 46.[23-a]

THICKNESS CONFIGURATION (mm)**	SHGC	U value m²	U value ft²	External Light Reflection	Transparency	Peak Power
	%	**W/m²K	Btu/h ft² F	%	%	(Wp/m²
3.2+4	41%	5,7	1.00	7,6%	30,0%	28

Fig 46 – PVC panel specifications

For ClimateStudio, since solar panels are not in the program library, a material was chosen to act as the previously mentioned solar panel for the program to understand and to be able to do the illuminance and glare tests with similar specifications for transparency and reflection, shown in Fig 47.

	Name	Layers	Tvis	Rvis.front	Rvis.back	UVal [W/(m²·K)]	SHGC
☆	Solarban 90 (2) on Solarbronze - Clear	Double	30.3 %	7.1 %	18.1 %	1.63	0.18

Fig 47 – Glass material specifications to be used in place of PVC panel during tests

The Glass Material for the rest of the SAWH will remain to be "Atlantica" with transparency of approximately 66%.

Test 2-1: (Illuminance)

2-1-a (Summer Solstice)
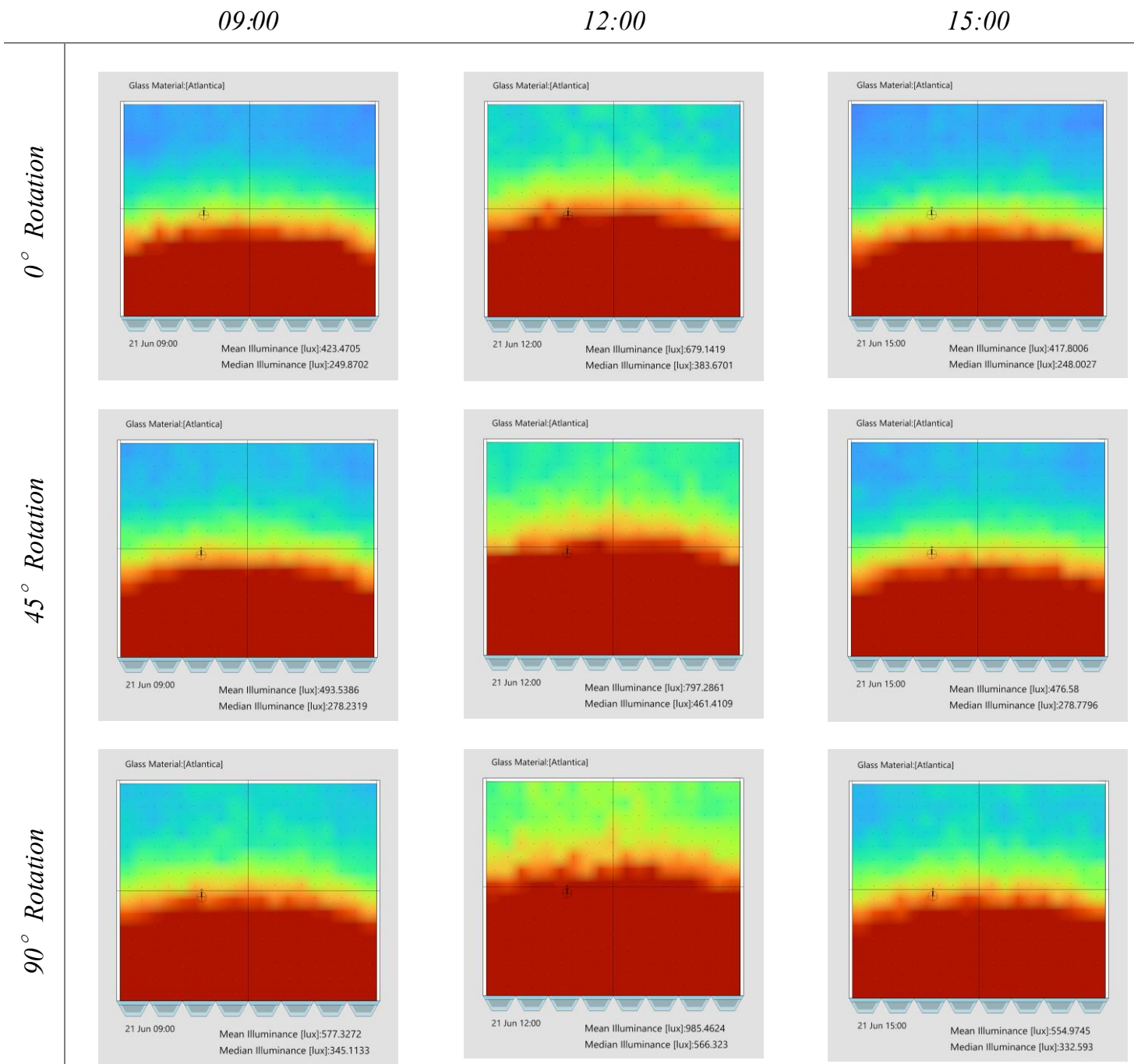
Table 10– Illuminance distribution for test number 2 under different rotation of blinds in Summer Solstice

Rotation/Time	09:00	12:00	15:00
0°	423	679	418
45°	494	797	467
90°	577	985	555

Table 11– Mean values of Illuminance for the Summer Solstice (Test 2) *all values are in LUX
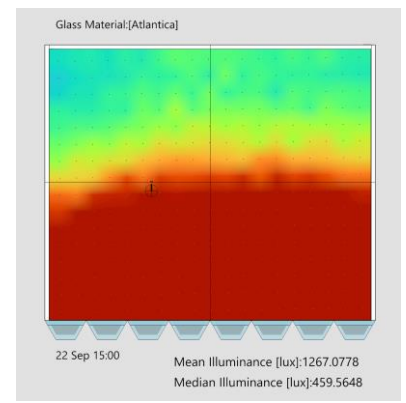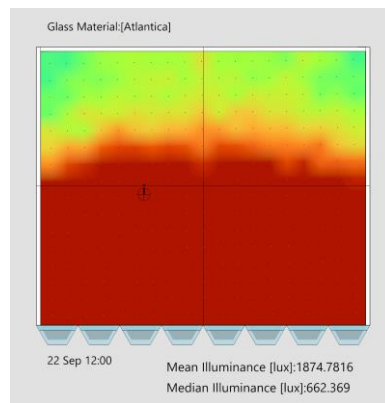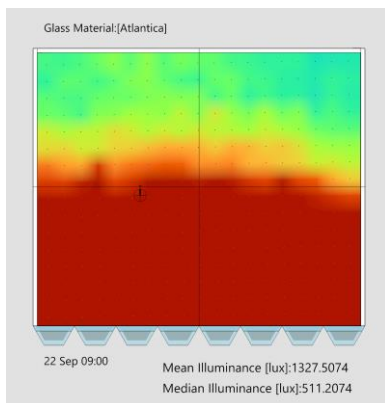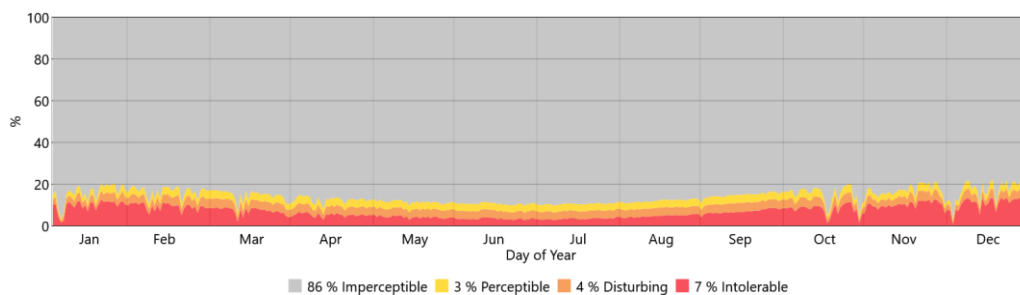
2-1-b (Autumnal Equinox)
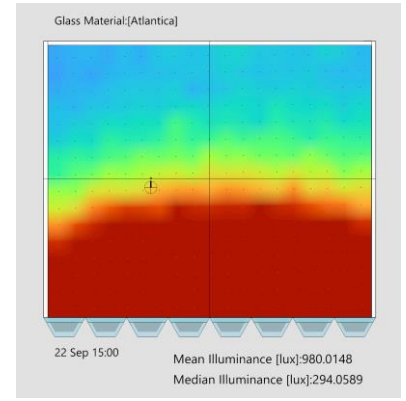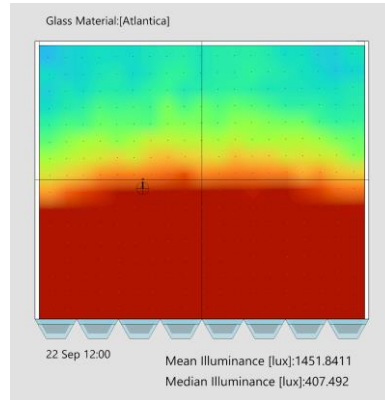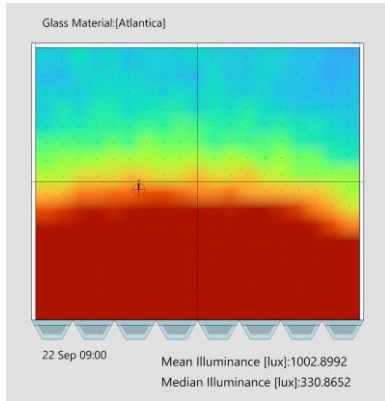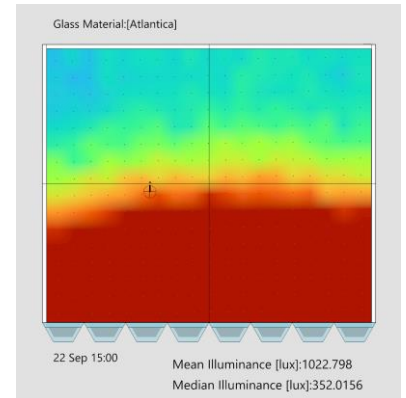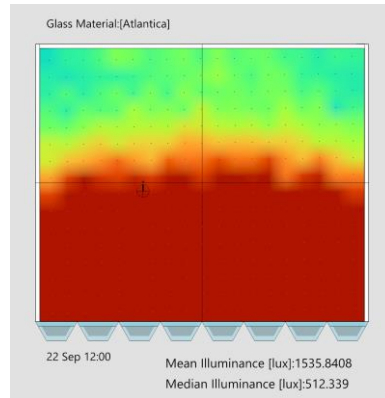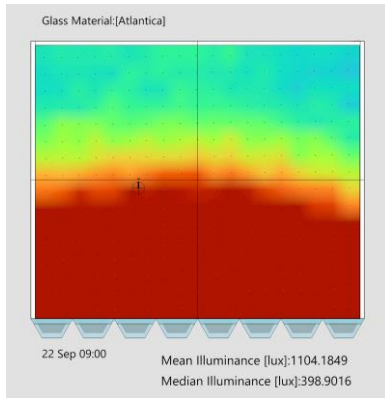
	09:00	*12:00*	*15:00*

Table 12– Illuminance distribution for test number 2 under different rotation of blinds in Autumnal Equinox

Rotation/Time	*09:00*	*12:00*	*15:00*
0°	1003	1451	980
45°	1104	1536	1023
90°	1327	1875	1267

Table 13 – Mean values of Illuminance for the Autumnal Equinox (Test 2) *all values are in LUX

Test 2-2: (Glare)

For the glare the following annual values were as follows in <u>Fig 48,49 and 50</u>, there was a decrease for the percentage of the intolerable glare that ranges between 10% to 14% from the previous threshold of 17%.

Closed system (0° Rotation):
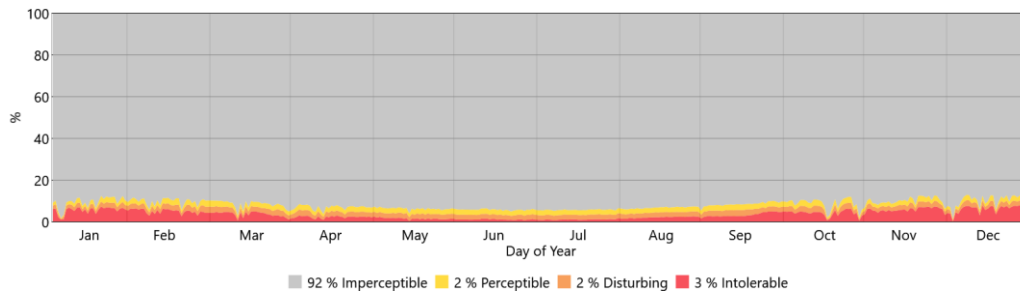
Fig 48– Annual glare values at 0° rotation of blinds (Test 2)

Semi-closed system (45° Rotation):
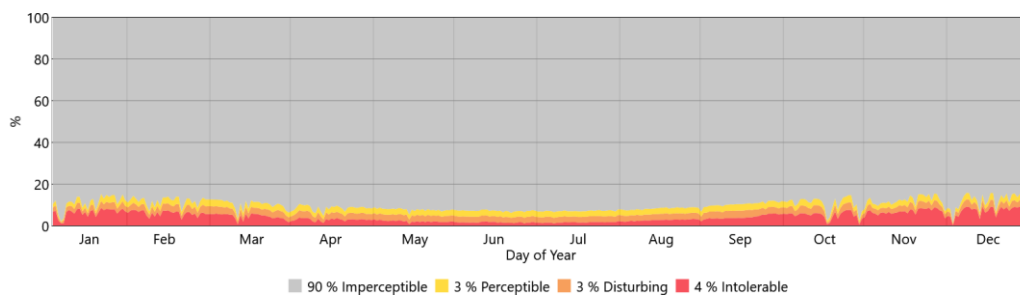
Fig 49– Annual glare values at 45° rotation of blinds (Test 2)

Open System (90° Rotation):

Fig 50– Annual glare values at 90° rotation of blinds (Test 2)

Test 3:

For the third test, a change was made for the glass material in the lower surface of the SAWH element highlighted in <u>Fig 51</u>. The glass material which had 66% transparency, would be replaced with Aluminium Cladding.

Fig 51– SAWH element with changing in the material from the original one at the highlighted surface
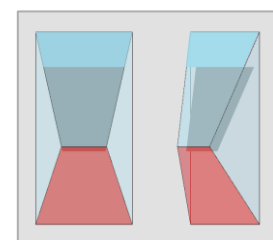
Test 3-1: (Illuminance)

3-1-a (Summer Solstice)
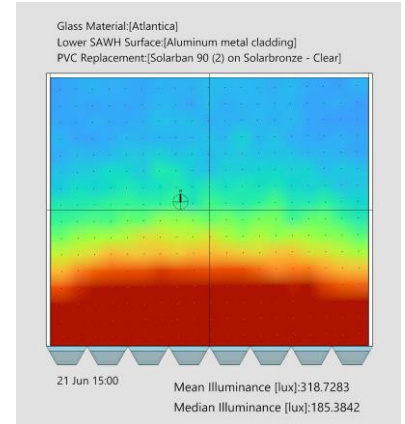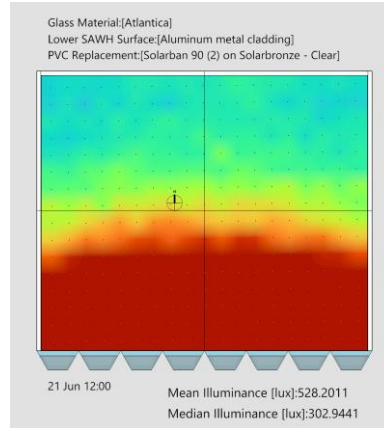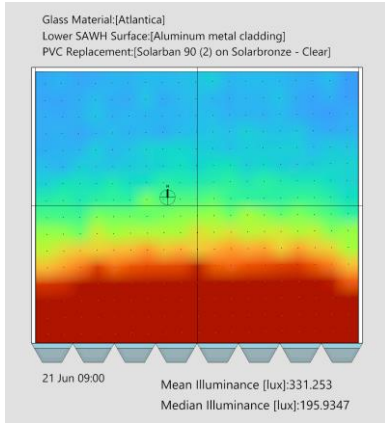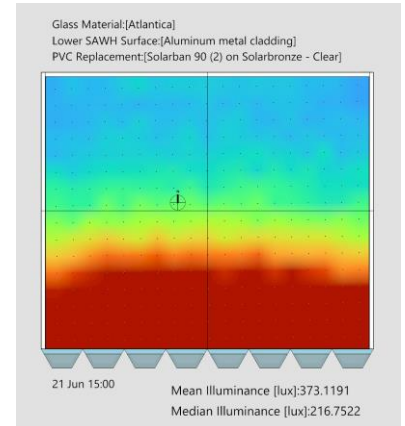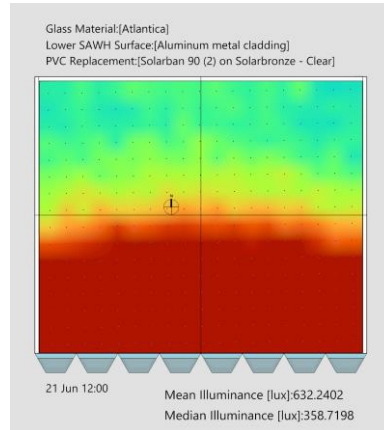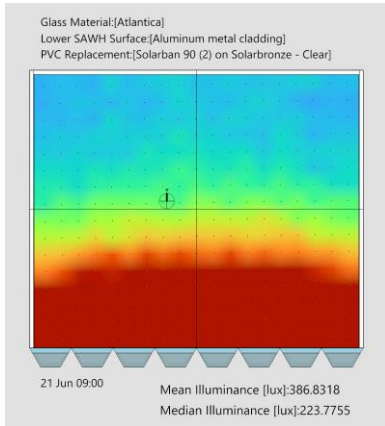
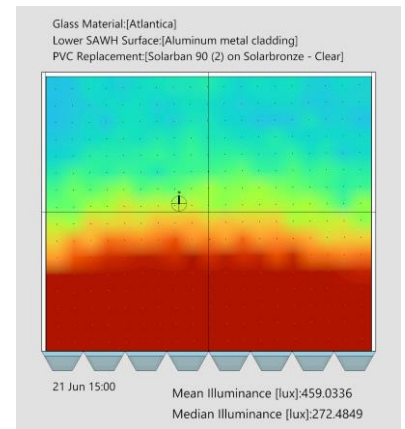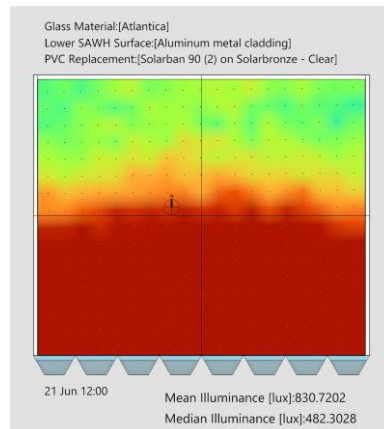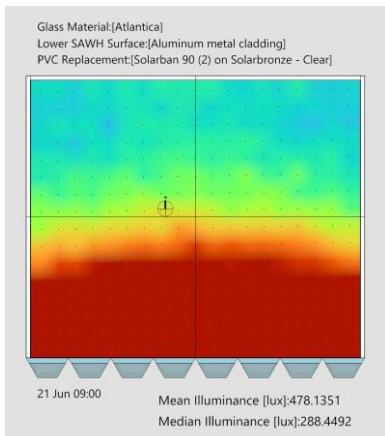|	*09:00*	*12:00*	*15:00*
0° Rotation			
45° Rotation			
90° Rotation			

Table 14– Illuminance distribution for test number 3 under different rotation of blinds in Summer Solstice

Rotation/Time	*09:00*	*12:00*	*15:00*
0°	331	528	318
45°	386	632	373
90°	478	830	459

Table 15 – Mean values of Illuminance for the Summer Solstice (Test 3) *all values are in LUX
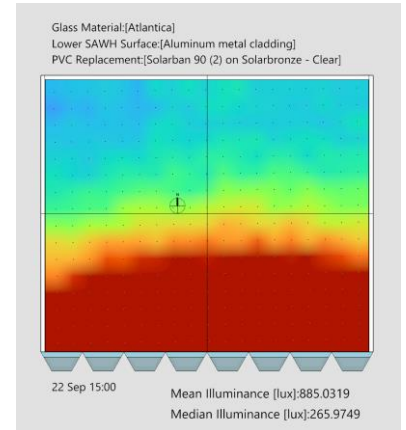
3-1-b (Autumnal Equinox)
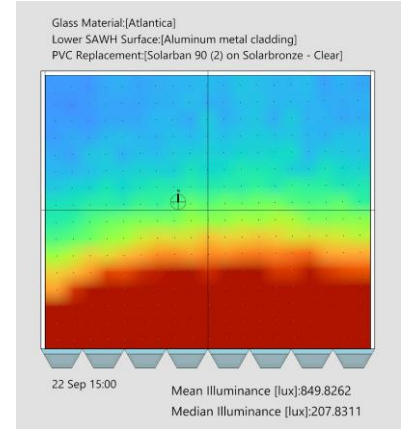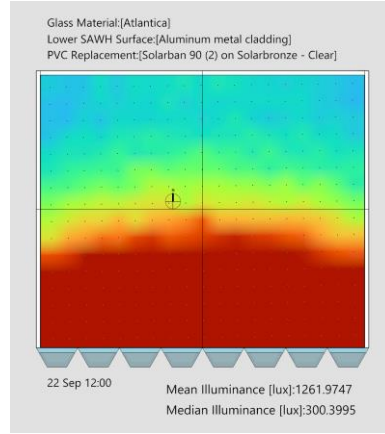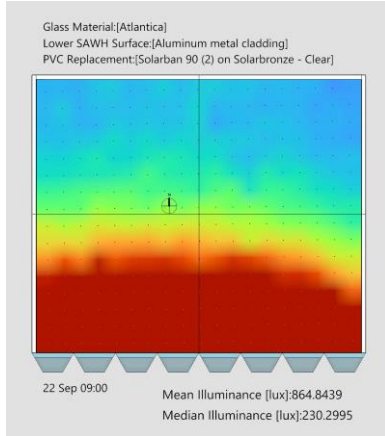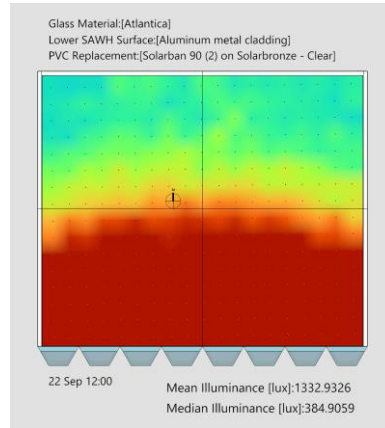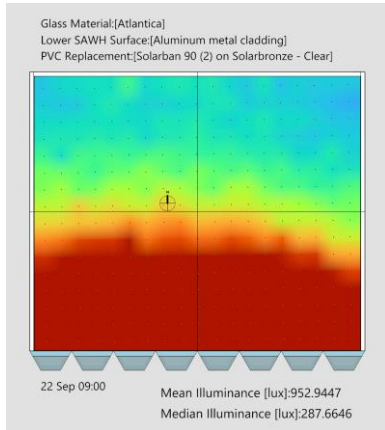
	09:00	*12:00*	*15:00*

Table 16– Illuminance distribution for test number 3 under different rotation of blinds in Autumnal Equinox

Rotation/Time	09:00	12:00	15:00
0°	864	1261	850
45°	952	1332	885
90°	1183	1686	1140

Table 17 – Mean values of Illuminance for the Autumnal Equinox (Test 3) *all values are in LUX
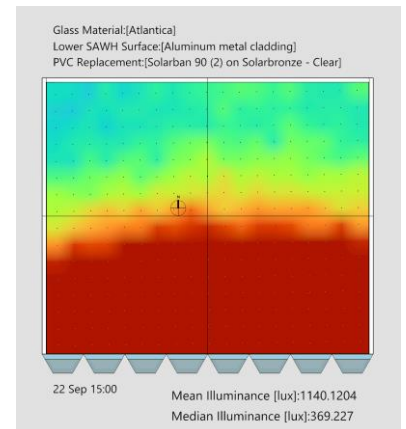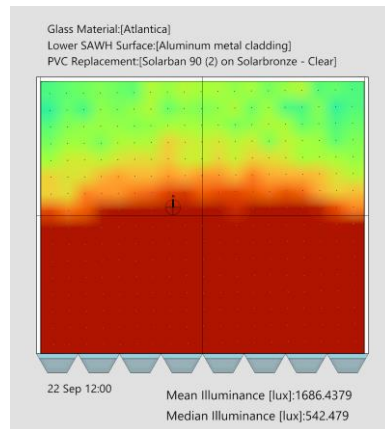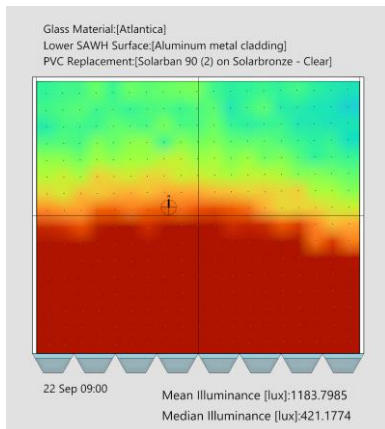
Test 3-2: (Glare)

For the glare the following annual values were as follows in <u>Fig 52,53 and 54</u>, there was a dramatic decrease for the percentage of the intolerable glare that ranges between 12% to 14% from the previous threshold of 17%.
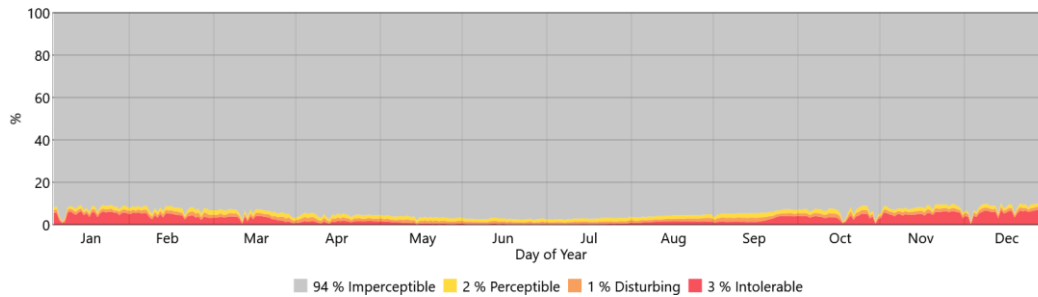
Closed system (0° Rotation):

94 % Imperceptible 2 % Perceptible 1 % Disturbing 3 % Intolerable

<u>Fig 52</u>– Annual glare values at 0° rotation of blinds (Test 3)

Semi-closed system (45° Rotation):

93 % Imperceptible 2 % Perceptible 2 % Disturbing 3 % Intolerable
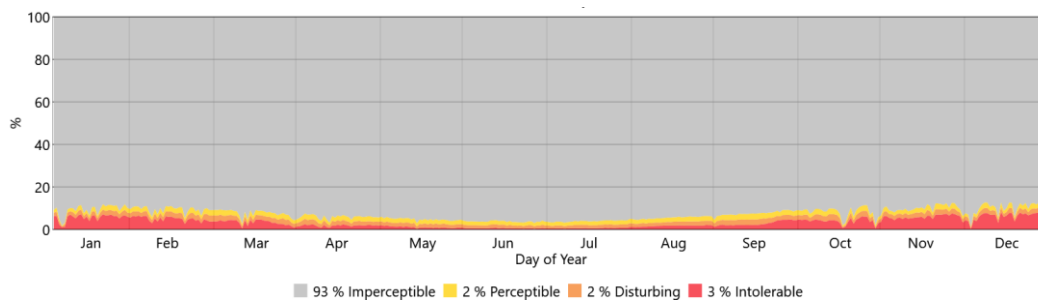
<u>Fig 53</u>– Annual glare values at 45° rotation of blinds (Test 3)

Open system (90° Rotation):

89 % Imperceptible 3 % Perceptible 3 % Disturbing 5 % Intolerable

<u>Fig 54</u>– Annual glare values at 90° rotation of blinds (Test 3)

Test 4:

For the fourth test, the glass material of the openable shutters on the sides of the SAWH element highlighted in red in <u>Fig 55</u>. were instead of changed into Aluminium Cladding and the lower surface was again returned to a glass material.
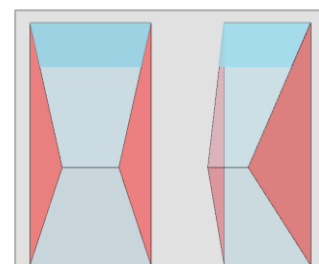
<u>Fig 55</u> – SAWH element with changing in the material from the original one at the highlighted surface

Test 4-1: (Illuminance)

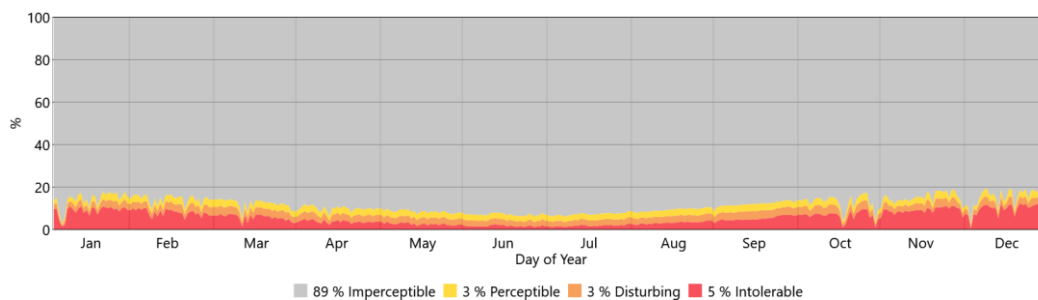**4-1-a (Summer Solstice)**
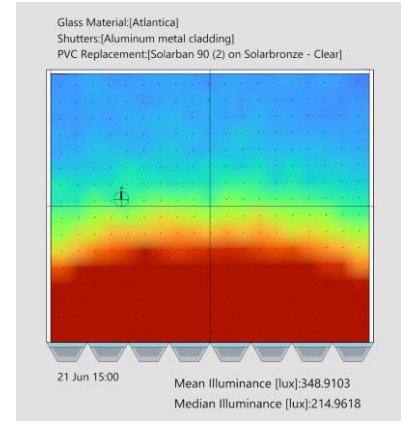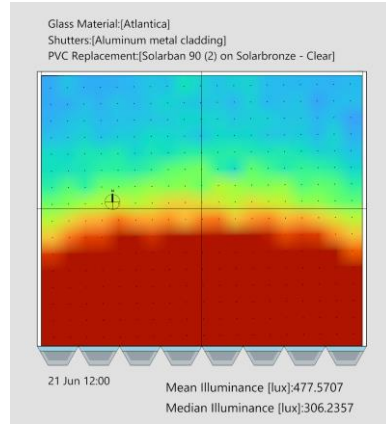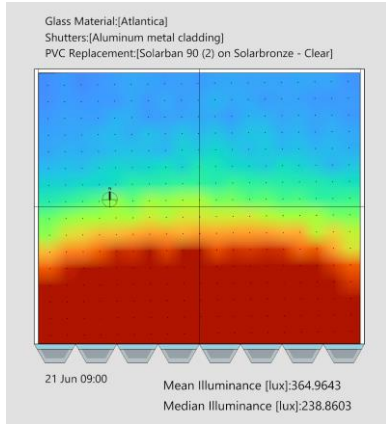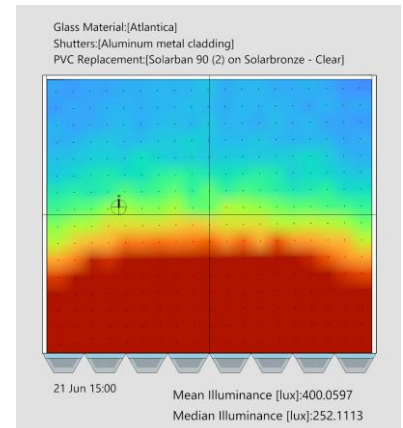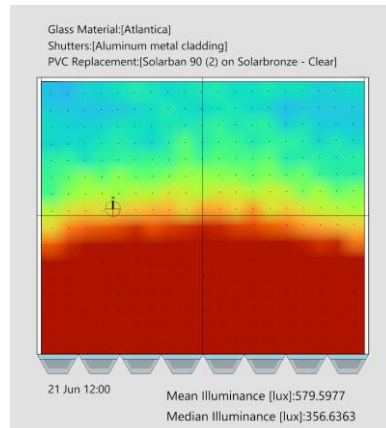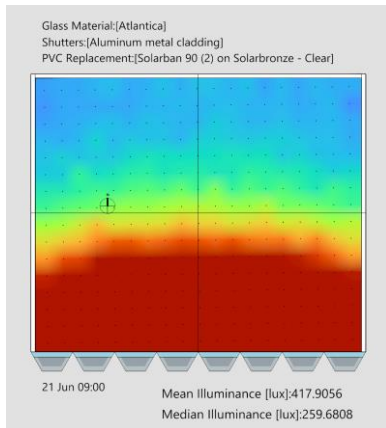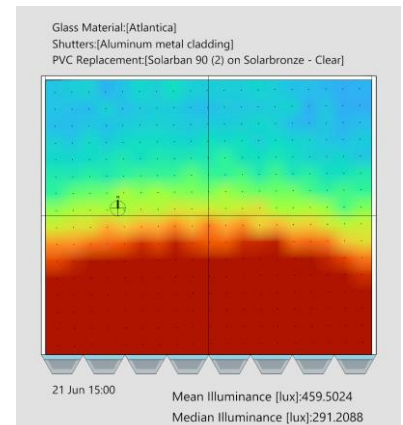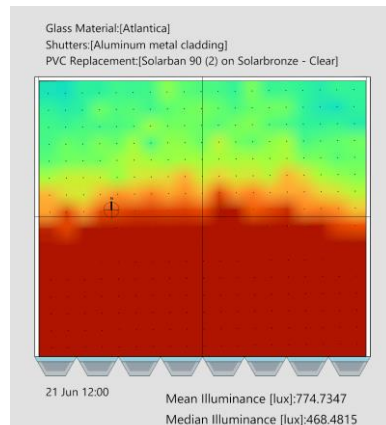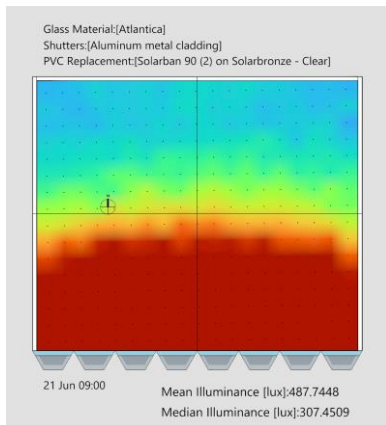
	09:00	*12:00*	*15:00*

Table 18– Illuminance distribution for test number 4 under different rotation of blinds in Summer Solstice

Rotation/Time	09:00	12:00	15:00
0°	364	477	348
45°	417	579	400
90°	489	774	459

Table 19 – Mean values of Illuminance for the Summer Solstice (Test 4) *all values are in LUX

4-1-b (Autumnal Equinox)
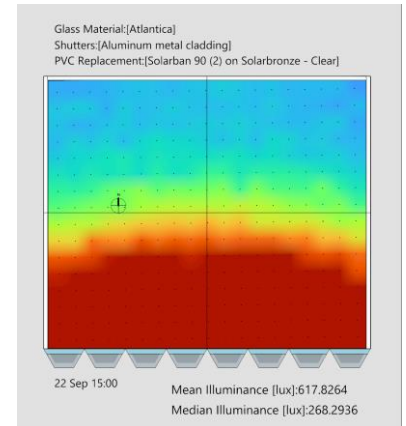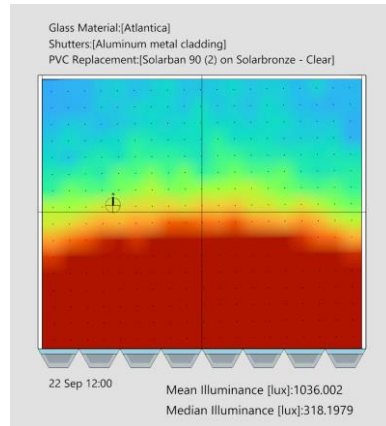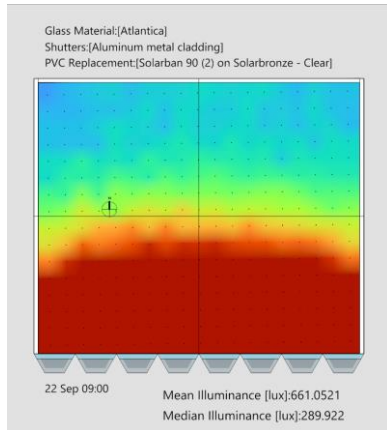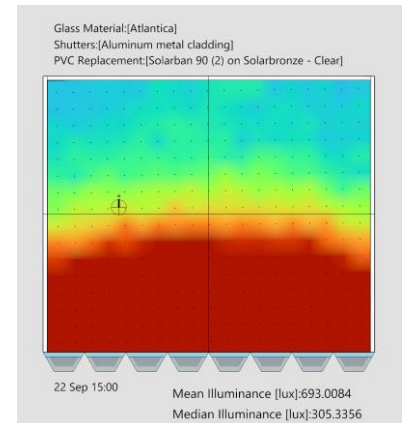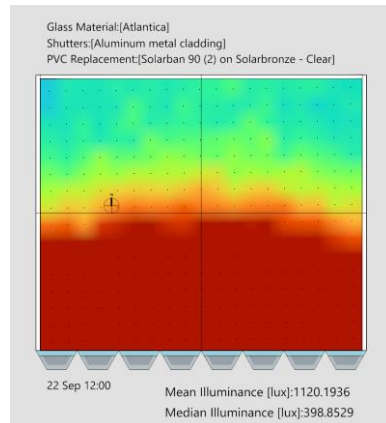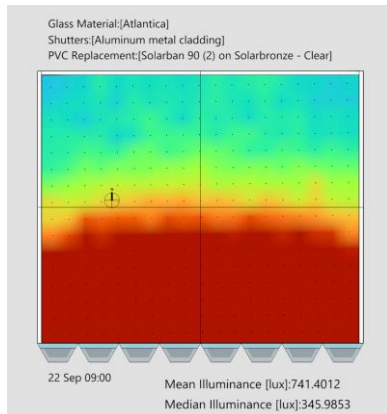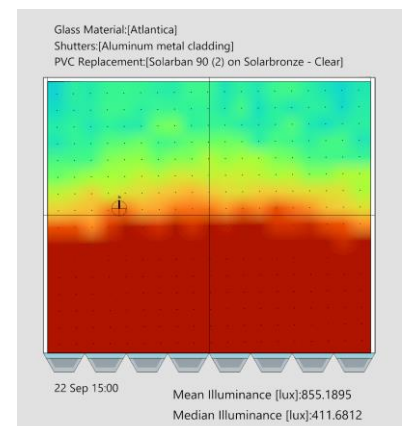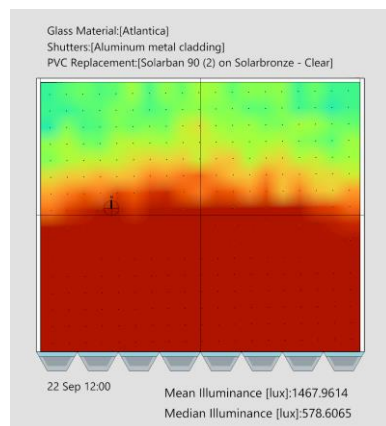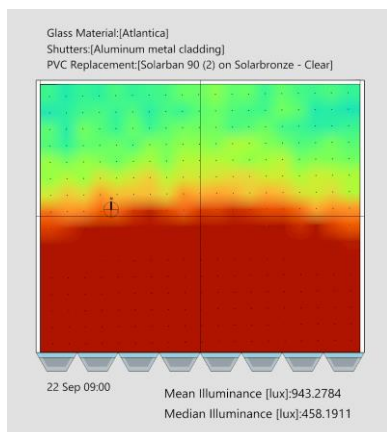
	09:00	*12:00*	*15:00*

Table 20– Illuminance distribution for test number 4 under different rotation of blinds in Autumnal Equinox

Rotation/Time	09:00	12:00	15:00
0°	661	1036	617
45°	741	1120	693
90°	943	1467	885

Table 21 – Mean values of Illuminance for the Autumnal Equinox (Test 4) *all values are in LUX

Test 4-2: (Glare)

For the glare the following annual values were as follows in <u>Fig 56,57 and 58</u>, there was a dramatic decrease for the percentage of the intolerable glare that ranges between 14% to 16% from the previous threshold of 17%.

Closed system (0° Rotation):

■ 98 % Imperceptible ■ 1 % Perceptible ■ 0 % Disturbing ■ 1 % Intolerable
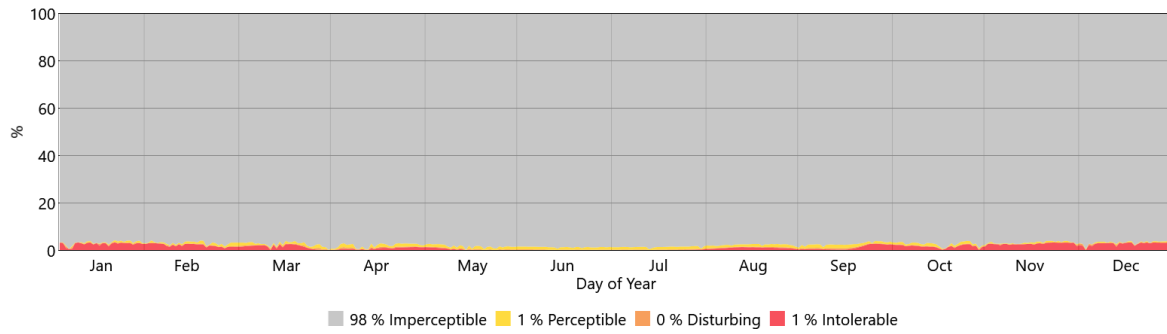
<u>Fig 56</u>– Annual glare values at 0° rotation of blinds (Test 4)

Semi-closed system (45° Rotation):

■ 96 % Imperceptible ■ 1 % Perceptible ■ 1 % Disturbing ■ 1 % Intolerable
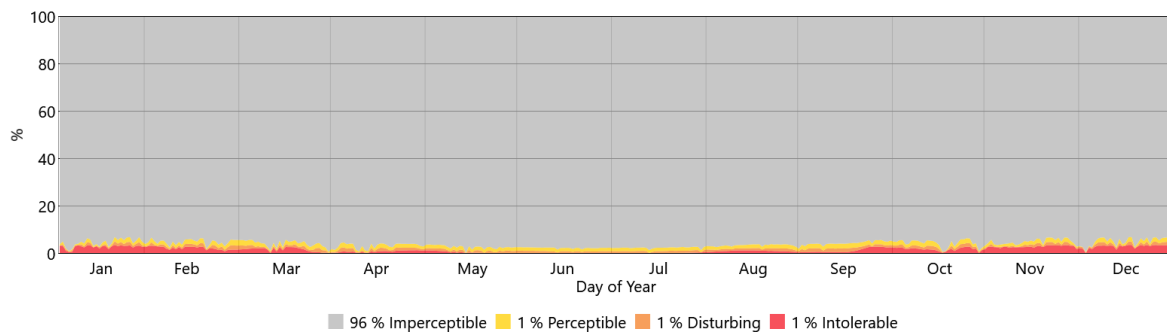
<u>Fig 57</u>– Annual glare values at 45° rotation of blinds (Test 4)

Open system (90° Rotation):

■ 92 % Imperceptible ■ 3 % Perceptible ■ 2 % Disturbing ■ 3 % Intolerable
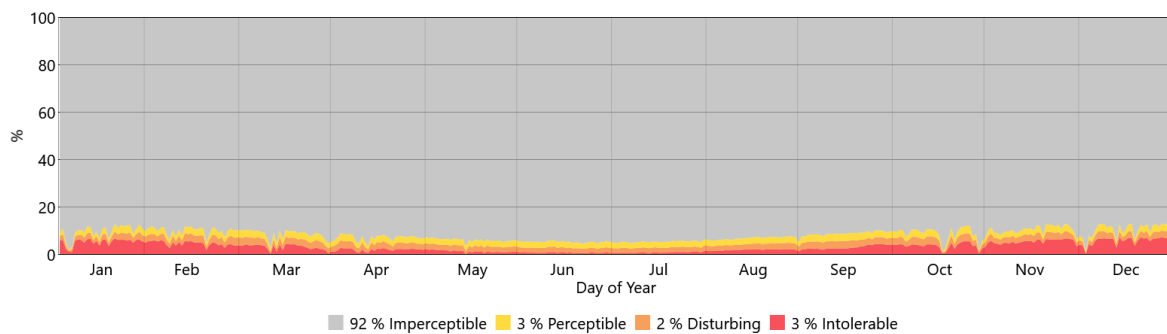
<u>Fig 58</u>– Annual glare values at 90° rotation of blinds (Test 4)

3-1-vi Parametric approach to the SAWH morphology due to Incident Radiation (Building Façade)

For this section, tests were made on the façade level using parametric design tools (Grasshopper in Rhino) regarding the Incident Radiation, and how would the system of SAWH adapt its parameters shown in Fig 59 with different surroundings, to decrease the value of the radiation falling on areas that have no shading highlighted in Fig 60, while increasing it on the areas that contain the SAWH highlighted in Fig 61 to increase the evaporation of the absorbed humidity thus increase the water production values.

(Front View)   (Side View)
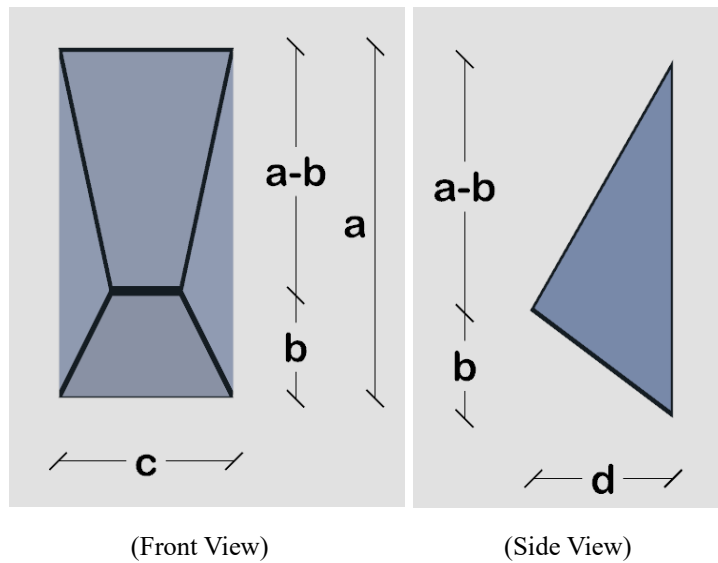
Fig 59 - SAWH element parameters
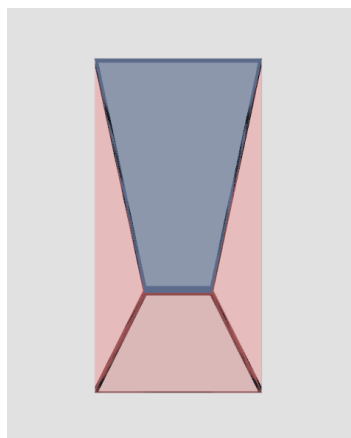
Fig 60 – Highlighted SAWH element Faces that should gain minimum radiation
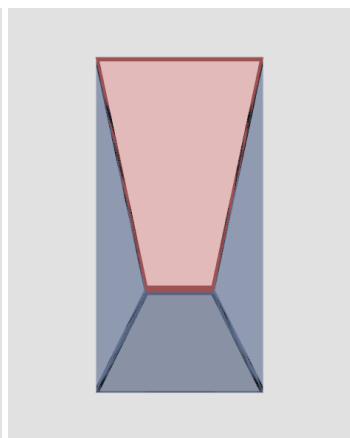
Fig 61– Highlighted SAWH element Faces that should gain maximum radiation

Tests of incident radiation were made on 3 façade systems with different curvature ranges shown in Fig 62 (Cylinder, ellipse and freeform) to see how the system would adapt to different façade orientations.
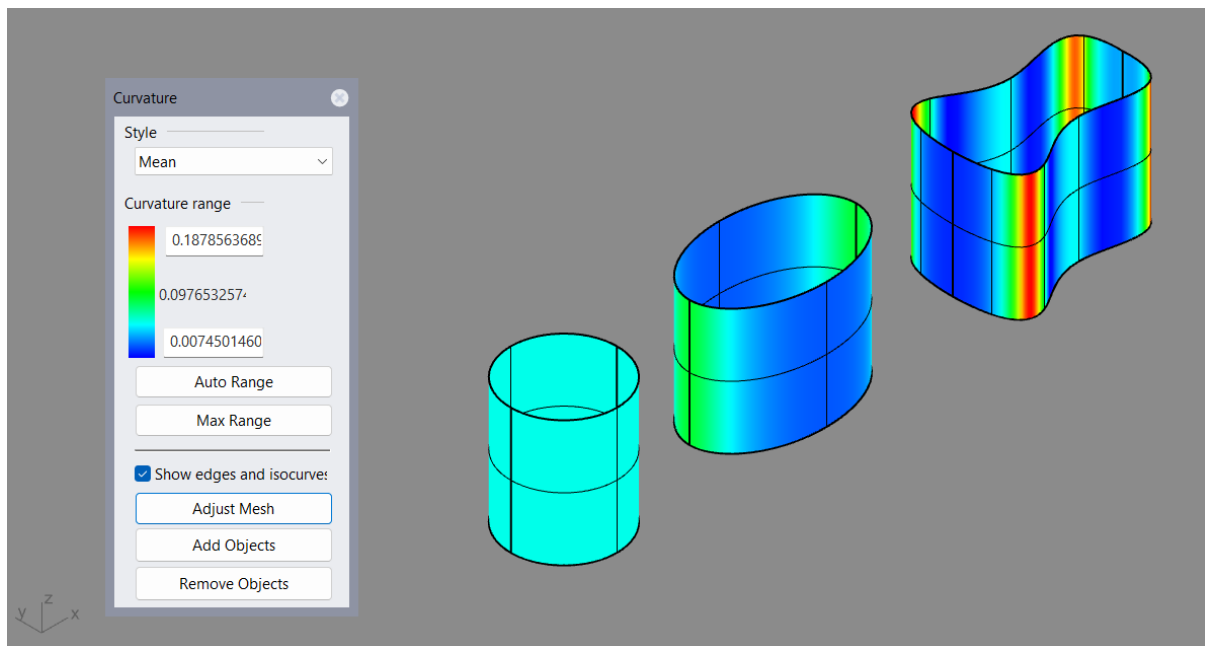
Fig 62 – Facades with different curvatures on which incident radiation tests would be performed

Test Dates

The next step was to use the dates of maximum temperature values to find the corresponding sun altitudes to control parameter "b" as mentioned before. The maximum temperatures were found on an online platform (Weatherspark) [24] shown in Fig 63 for the city of Cairo, Egypt.
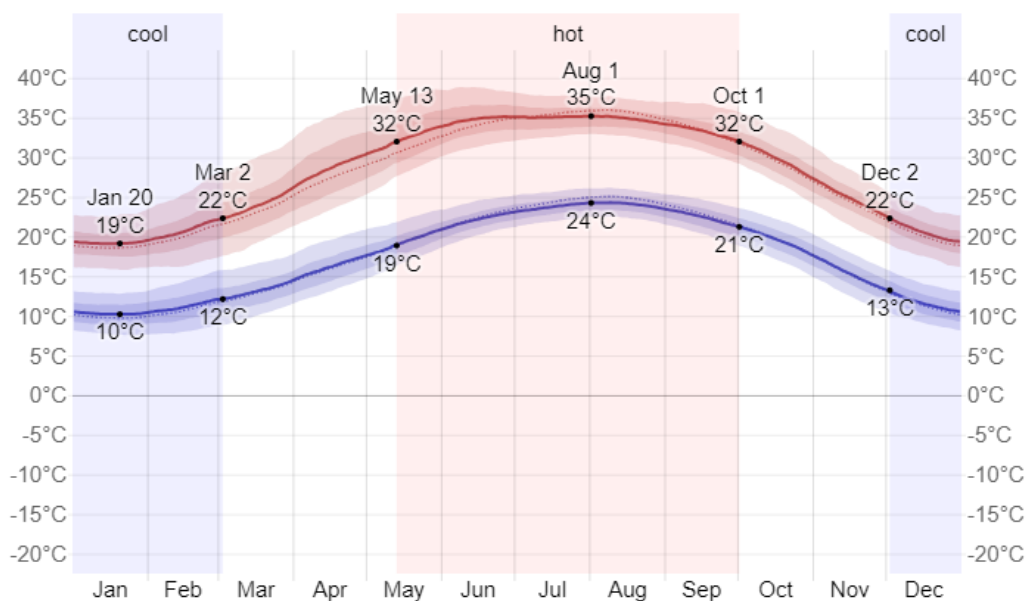
Fig 63 – Temperature graph Cairo-Egypt

Sun Altitudes

According to the previous graph, the hottest period is between the month of May and October and their corresponding sun altitudes were as follows:

Month	*9:00*	*12:00*	*15:00*
May	50°	80°	46°
June	50°	83°	49°
July	48°	80°	49°
August	45°	72°	44°
September	41°	60°	36°
October	34°	49°	27°

Table 22 – Sun altitudes during the hot period of the year in Cairo-Egypt

The average altitudes for the whole 6 months at 9:00am, 12:00pm and 15:00pm were 45°, 70° and 42° respectively. Since the values at 9am and 15pm are close, a common value can be taken as 45°, and since the top surface needs and inclination to allow the water to drop due do gravity 60° will be taken instead of 70° (70° will create a horizontal surface not allowing the water collected on the surface to flow to the collector). These values will later become the range in which parameter "b" moves as shown in Fig 64.
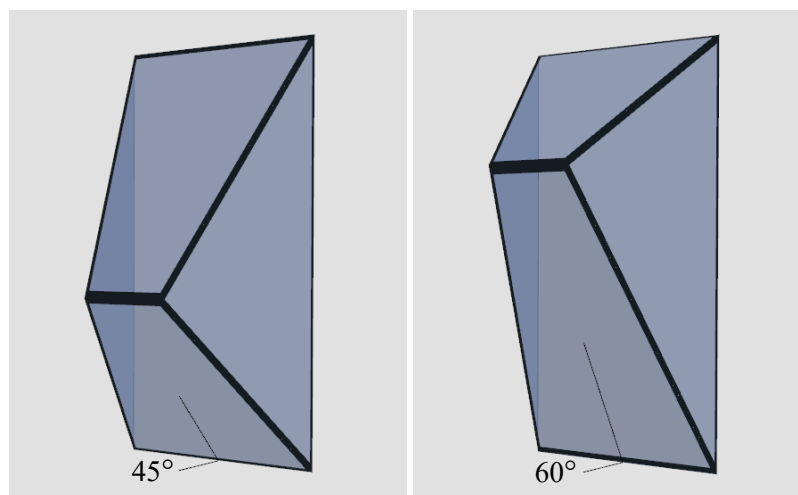
Fig 64 – Different SAWH element inclination depending on sun altitude

To understand the effect of these changes across the façades and how it affects the values of incident radiation, the base maximum and minimum incident radiation values were calculated throughout the months May to October at 9:00, 12:00 and 15:00 on the 1st day of the month. Since the minimum values for a certain hour tended to zero, the incident radiation for a 12-hour period was calculated from 6 am to 6pm.

Façade Configuration

To Relate dimension "b" previously shown in <u>Fig 59</u> to the sun altitudes, each façade was divided into a number of panels and each panel had an individual SAWH element. The angle between the sun vector and each of the panel normal vectors was calculated at 12pm and then dimension "b" was inversely proportional to the magnitude of that angle, so that the element has an inclination ranging between 45° and 60° as mentioned before, resulting in the following configurations:

Façade 1:
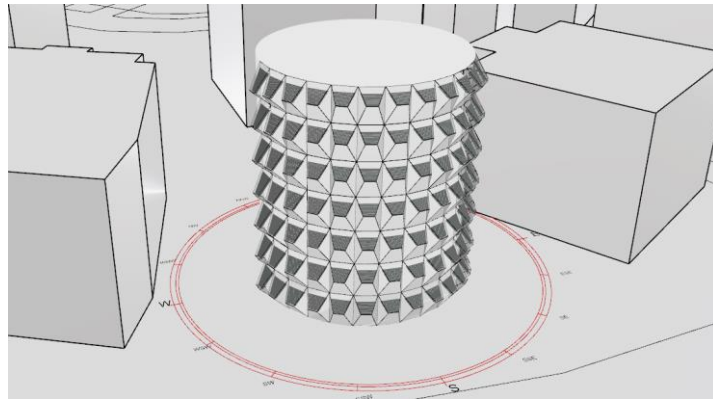
<u>Fig 65</u> – SAWH system configuration on façade 1

Façade 2:
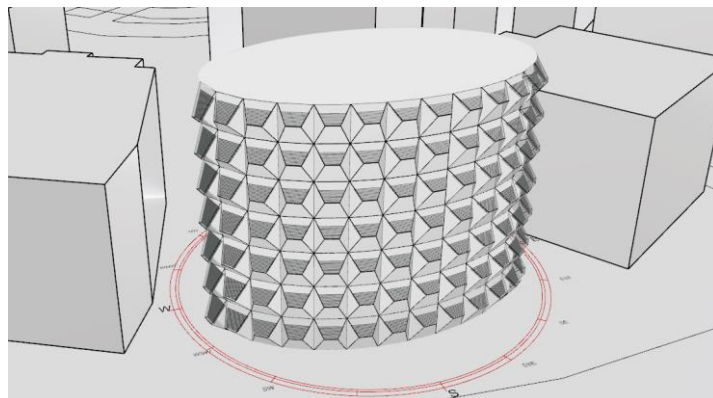
<u>Fig 66</u>– SAWH system configuration on façade 2

Façade 3:
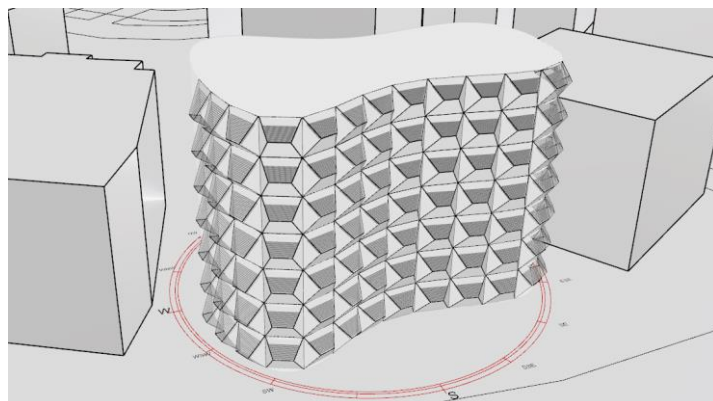
<u>Fig 67</u> - SAWH system configuration on façade 2

Incident Radiation Distribution

To get an idea about the incident radiation distribution before and after the installation of the SAWH the following tests were made on the 1st of August (Maximum radiation values):

Façade 1

Without SAWH
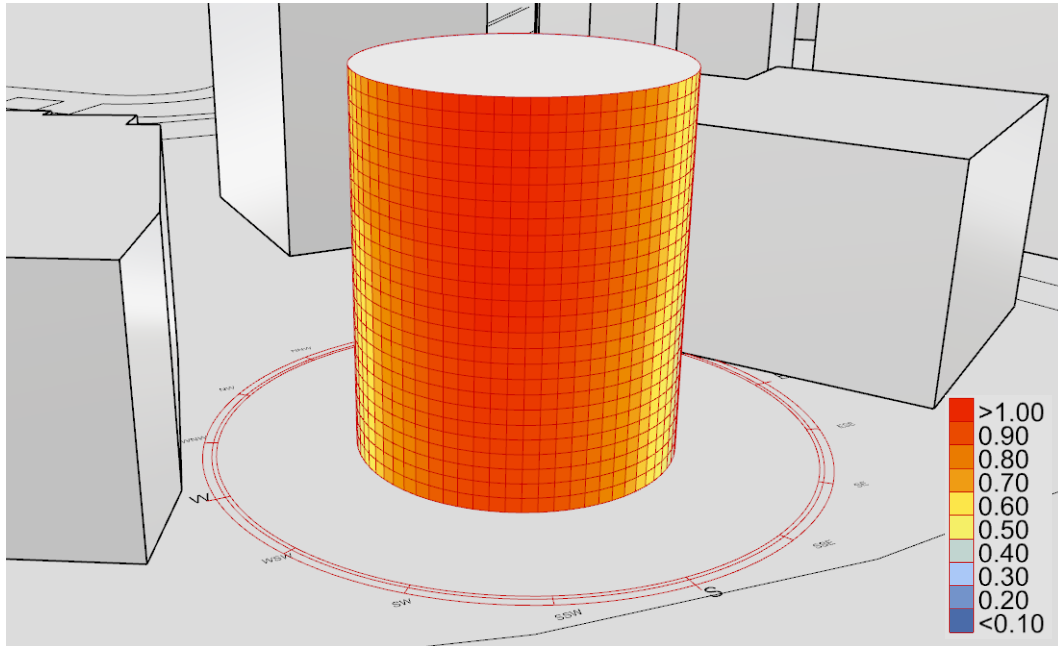
Fig 68– Incident radiation distribution on façade 1 (All Units are in kWh/m2)
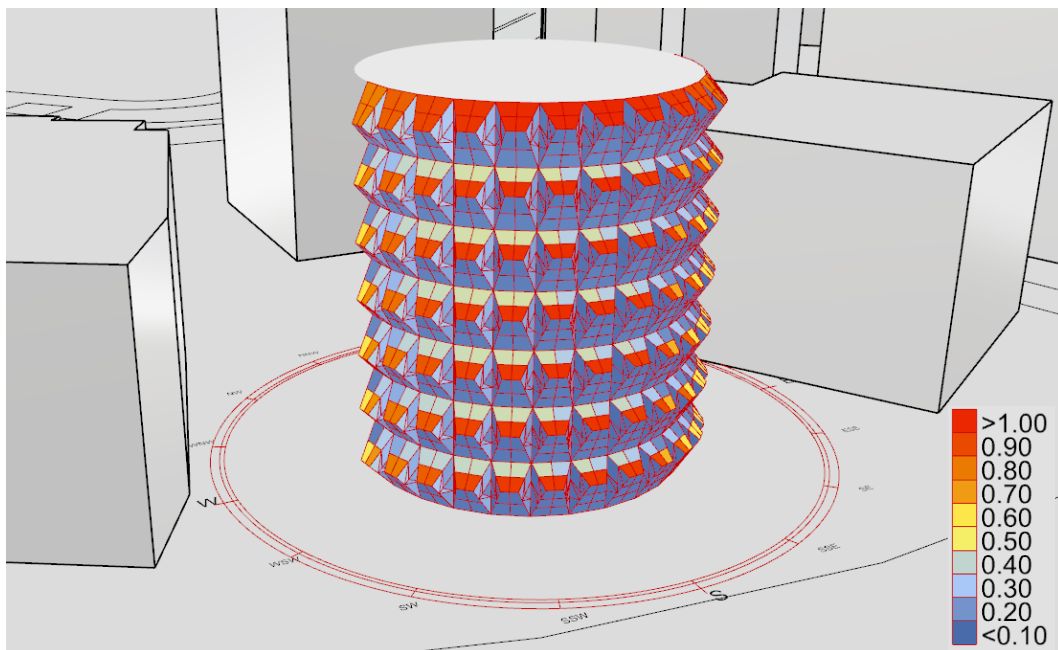
With SAWH

Fig 69– Incident radiation distribution on SAWH elements on façade 1 (All Units are in kWh/m2)

Façade 2

Without SAWH
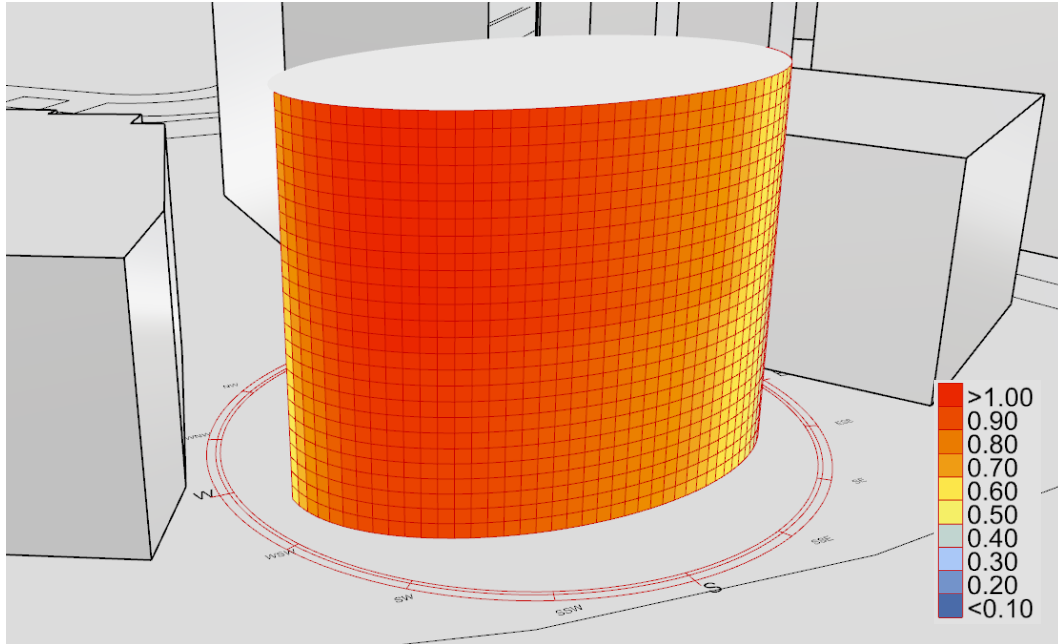
Fig 70 – Incident radiation distribution on façade 2 (All Units are in kWh/m2)
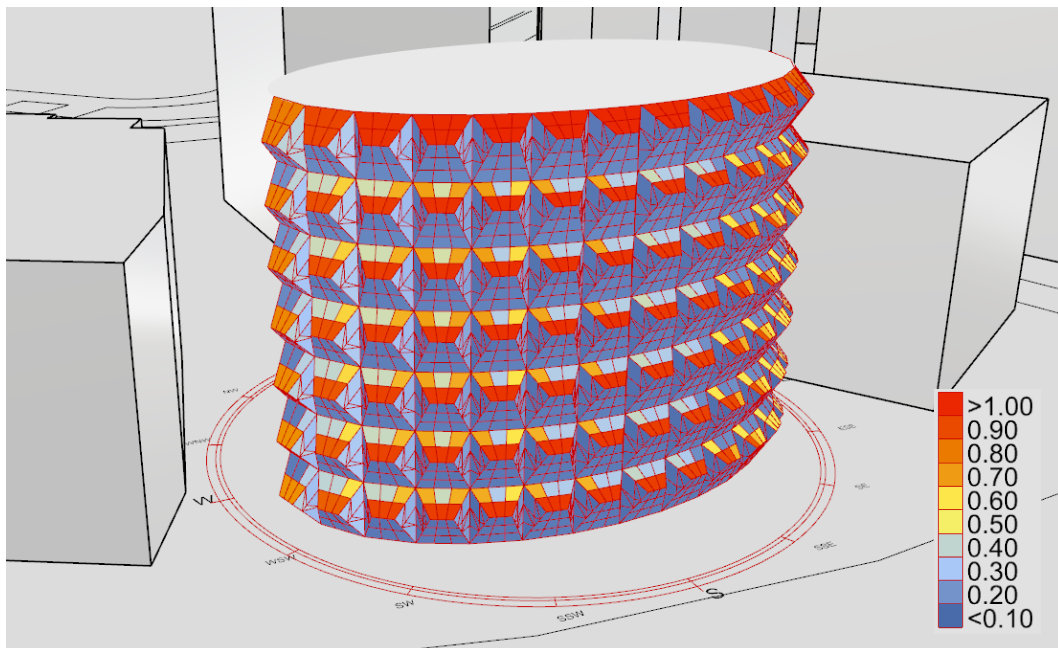
With SAWH

Fig 71– Incident radiation distribution on SAWH elements on façade 2 (All Units are in kWh/m2)

Façade 3

Without SAWH
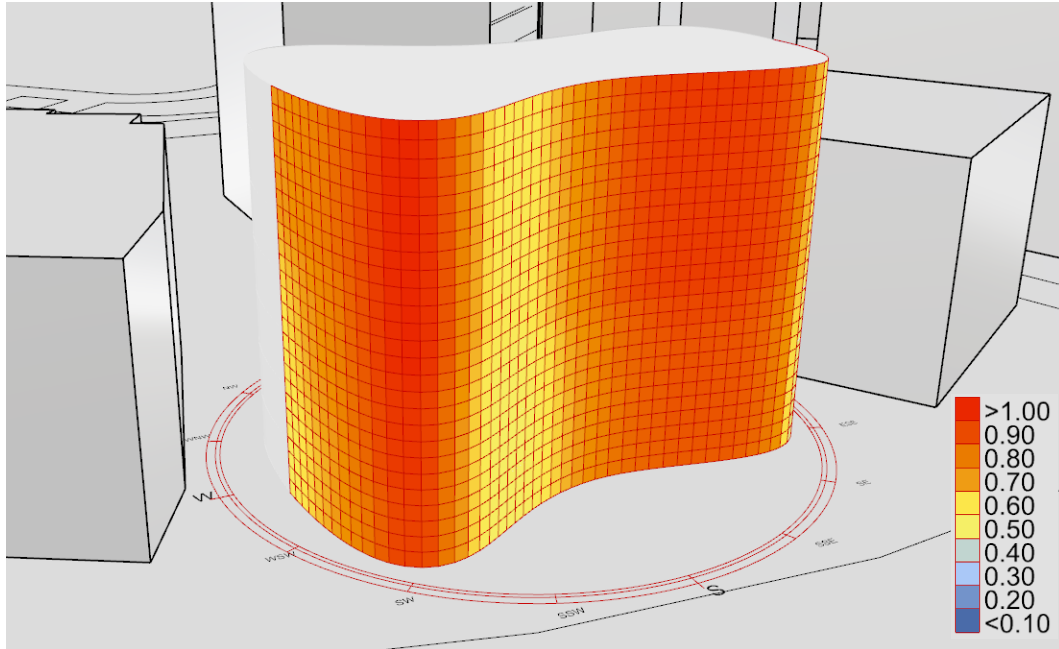
Fig 72– Incident radiation distribution on façade 3 (All Units are in kWh/m2)

With SAWH
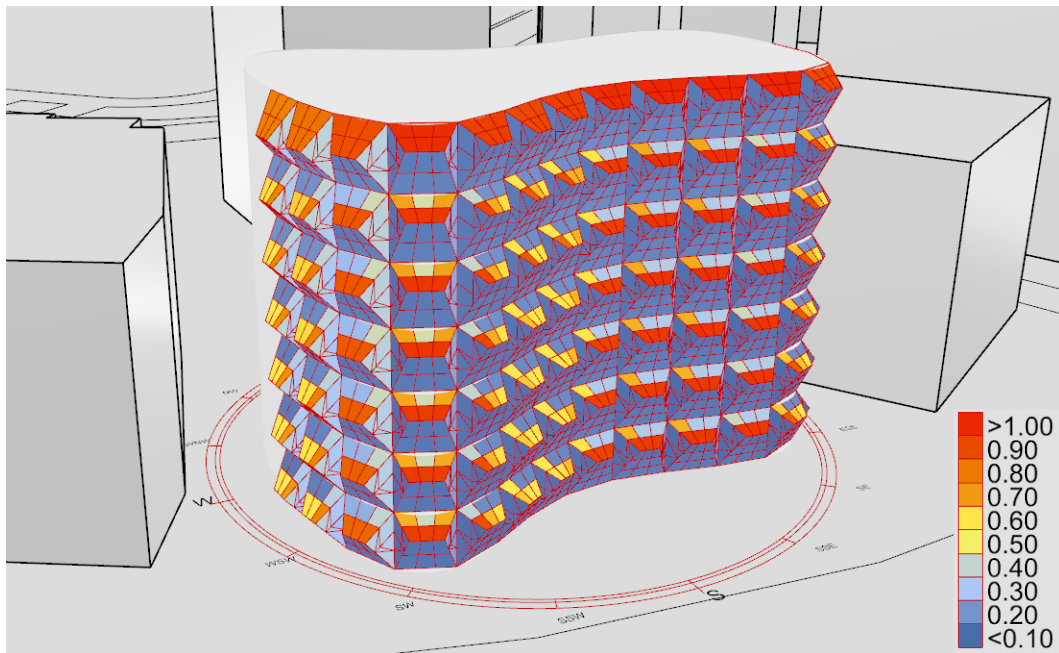
Fig 73 – Incident radiation distribution on SAWH elements on façade 3 (All Units are in kWh/m2)

4 Results

Summing up the tests done one the system, the first tests were made regarding the materials used for the surfaces containing the SAWH element and how would it effect the illuminance and the glare inside the test room and the second tests were on a façade level and the effect of changing the parameters of system on the amount of the incident radiation falling on the surface.

A-Test Room

The test room had dimensions of 12m x 10m x 3.4m. There were 4 tests each with a different composition of materials regarding the different surfaces. To be able to know the effect of the system on the Illuminance and Glare, base values were calculated with putting only a glass surface without shades or blinds.

A-1-Base Values

Maximum Illuminance: 1690 lux (Summer Solstice) and 6771 lux (Autumnal Equinox)

Minimum Illuminance: 984 lux (Summer Solstice) and 3553 lux (Autumnal Equinox)

Glare: 17% (Intolerable) , Disturbing 6% (Disturbing)

The 4 tests material configuration can be summed up in the following tables:

TESTS/ SURFACES	SURFACE A	SURFACE B	SURFACE C	SURFACE D	SURFACE E
TEST 1	Atlantica	Atlantica	Atlantica	Atlantica	Atlantica
TEST 2	Atlantica	Atlantica	Atlantica	Atlantica	PVC Panel
TEST 3	Atlantica	Aluminum Cladding	Atlantica	Atlantica	PVC Panel
TEST 4	Atlantica	Atlantica	Aluminum Cladding	Aluminum Cladding	PVC Panel

Table 23 - The tests' material configuration

MATERIAL/ CHARACTARESTICS	TRANSPARENCY	REFLECTANCE
ATLANTICA	66.3%	6.4%
PVC PANEL	30%	7%
ALUMINUM CLADDING	0%	65%

Table 24 – The materials' characteristics
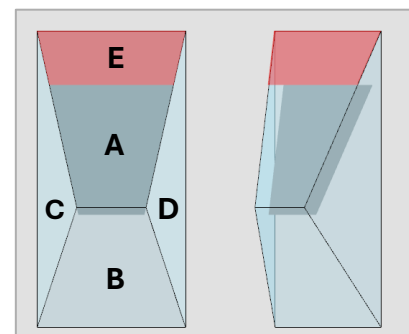
A-2-Illuminance Tests

Moreover, the tests regarded the rotation angle of the blinds between 0°, 45° and 90° and the values of the corresponding illuminance of each case during Summer Solstice and Autumnal Equinox. Values of each test can be summarized in the following tables:

<u>**Maximum Values:**</u>

Summer Solstice

TESTS/ DEGREE OF ROTATION	0	45°	90°
TEST 1	775	896	1119
TEST 2	679	797	985
TEST 3	528	632	830
TEST 4	477	579	774

Table 25-Maximum Illuminance values after applying the SAWH element -Summer Solstice (all units are in LUX)

Autumnal Equinox

TESTS/ DEGREE OF ROTATION	0	45°	90°
1TEST 1	2130	2124	2534
TEST 2	1451	1536	1875
TEST 3	1261	1332	1686
TEST 4	1036	1120	1467

Table 26 -Maximum Illuminance values after applying the SAWH element -Autumnal Equinox (all units are in LUX)

<u>**Minimum Values:**</u>

Summer Solstice

TESTS/ DEGREE OF ROTATION	0	45°	90°
TEST 1	461	521	614
TEST 2	418	467	555
TEST 3	318	373	459
TEST 4	348	400	455

Table 27 -Minimum Illuminance values after applying the SAWH element -Summer Solstice (all units are in LUX)

Autumnal Equinox

TESTS/ DEGREE OF ROTATION	0	45°	90°
TEST 1	1286	1312	1560
TEST 2	980	1023	1267
TEST 3	850	885	1140
TEST 4	647	693	885

Table 28 -Minimum Illuminance values after applying the SAWH element -Autumnal Equinox (all units are in LUX)

A-3-Glare Tests

The annual glare tests' results regarding the blinds rotation angle can be summed up in the following table:

<u>Intolerable glare percentage:</u>

TESTS/ DEGREE OF ROTATION	0	45°	90°
TEST 1	4%	5%	3%
TEST 2	3%	4%	7%
TEST 3	3%	3%	5%
TEST 4	1%	1%	3%

<u>Table 29</u> – Intolerable glare percentages across the 4 tests

<u>Disturbing glare percentage:</u>

TESTS/ DEGREE OF ROTATION	0	45°	90°
TEST 1	3%	3%	4%
TEST 2	2%	3%	4%
TEST 3	1%	2%	5%
TEST 4	0%	1%	2%

<u>Table 30</u> - Disturbing glare percentages across the 4 tests

B Parametric Design Tests

These tests were carried out on 3 facades with 3 different curvatures (cylinder, ellipse and freeform), they were put in a context geometry resembling a city in Cairo, Egypt.

B-1-Incident Radiation Base Values

Incident radiation values were calculated on the facade without adding the SAWH element to get the base values and it can be summarized as follows:

Maximum Values

MONTH/TIME	9:00	12:00	15:00
MAY	0.54	0.35	0.63
JUNE	0.57	0.27	0.67
JULY	0.49	0.22	0.65
AUGUST	0.58	0.32	0.65
SEPTEMBER	0.54	0.44	0.63
OCTOBER	0.49	0.5	0.61

Table 31- Base maximum values of incident radiation on façade without SAWH element (All units are in kWh/m2)

"These values were acquired putting the building in the in a context geometry resembling an urban fabric of a city in Cairo."

Minimum Values

MONTH/TIME	6:00-18:00
MAY	1.04
JUNE	1.09
JULY	0.98
AUGUST	1.16
SEPTEMBER	1.08
OCTOBER	1.17

Table 32 – Base minimum values of incident radiation on façade without SAWH element (All units are in kWh/m2)

*The minimum values for a certain hour tended to zero so the incident radiation for a 12-hour period was calculated
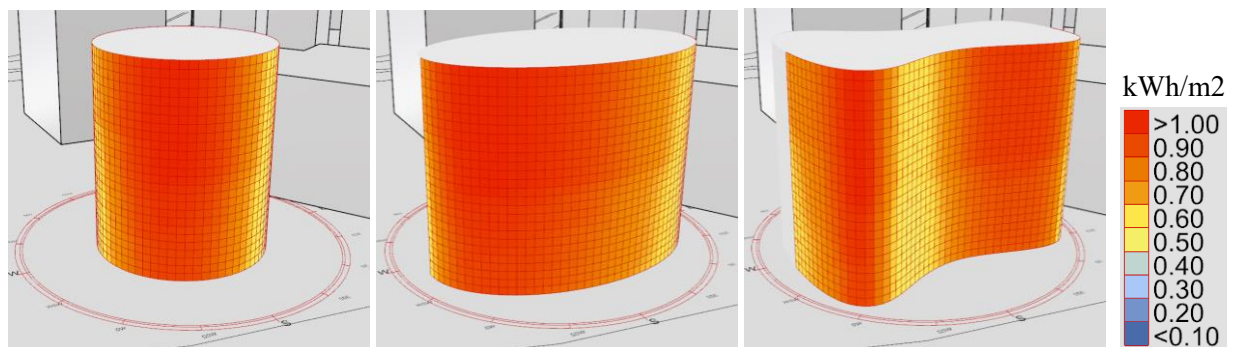
*The distribution of Incident radiation on the 3 facades

Incident Radiation With SAWH

The maximum incident radiation values after applying the SAWH element were as follows for the upper surface of the element (previously mentioned in Fig 56):

Maximum Values

MONTH/TIME	9:00	12:00	15:00
MAY	0.9	0.84	0.78
JUNE	0.98	0.92	0.86
JULY	0.82	0.88	0.86
AUGUST	0.94	0.93	0.84
SEPTEMBER	0.81	0.97	0.75
OCTOBER	0.68	0.82	0.62

Table 33- Maximum values of incident radiation on façade with SAWH element (All units are in kWh/m2)

The minimum incident radiation values after applying the SAWH element were as follows for the lower and side surfaces of the element (previously mentioned in Fig 55):

Minimum Values

MONTH/TIME	6:00-18:00
MAY	0.04
JUNE	0.1
JULY	0.13
AUGUST	0.07
SEPTEMBER	0.02
OCTOBER	0.01

Table 34- Minimum values of incident radiation on façade with SAWH element (All units are in kWh/m2)

*The minimum values for a certain hour tended to zero so the incident radiation for a 12-hour period was calculated
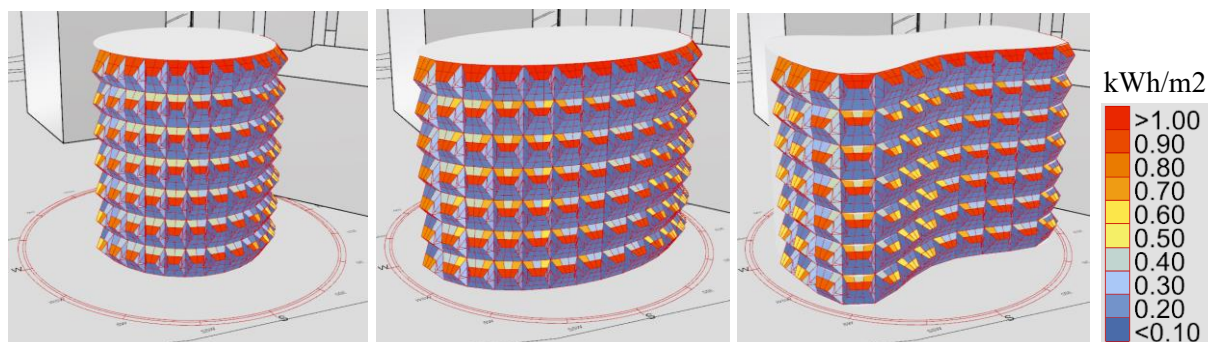
*The distribution of Incident radiation on the 3 facades

5 Discussion

The two types of testes done to a test the workability and effect of adding a basic SAWH element on an outer envelope on illuminance, glare and incident radiation, were at a room level and on a façade level. At the room level, illuminance and glare were compared. Illuminance values can be compared between the 4 tests and the base value, with 3 different rotations of blinds in the following figures:

0° Rotation:
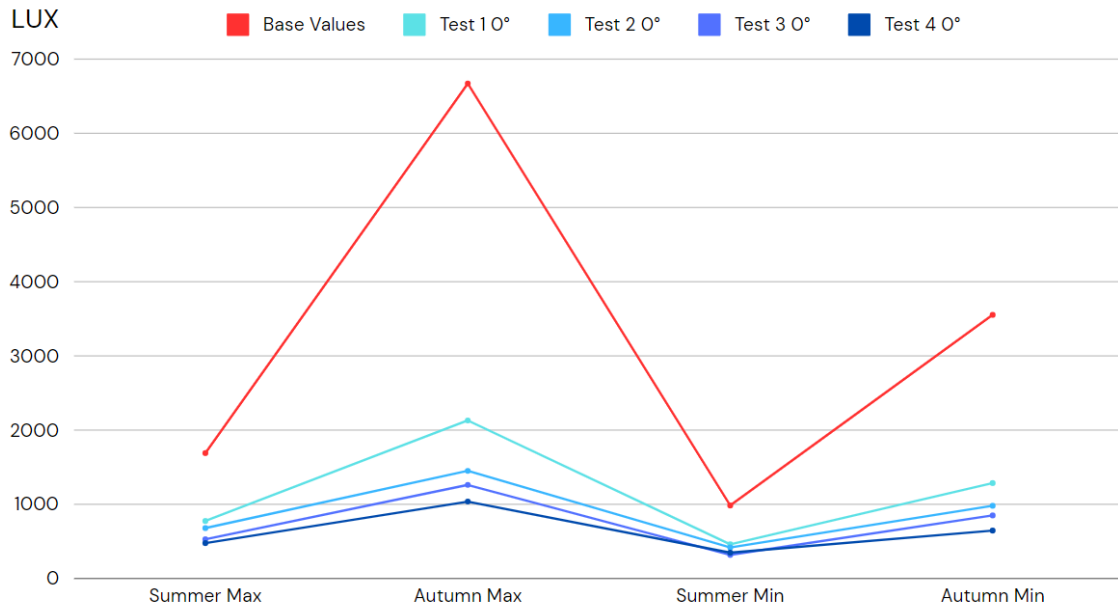
Fig 74 – Illuminance values for the 4 tests and base value of the test room at 0° rotation

45° Rotation:
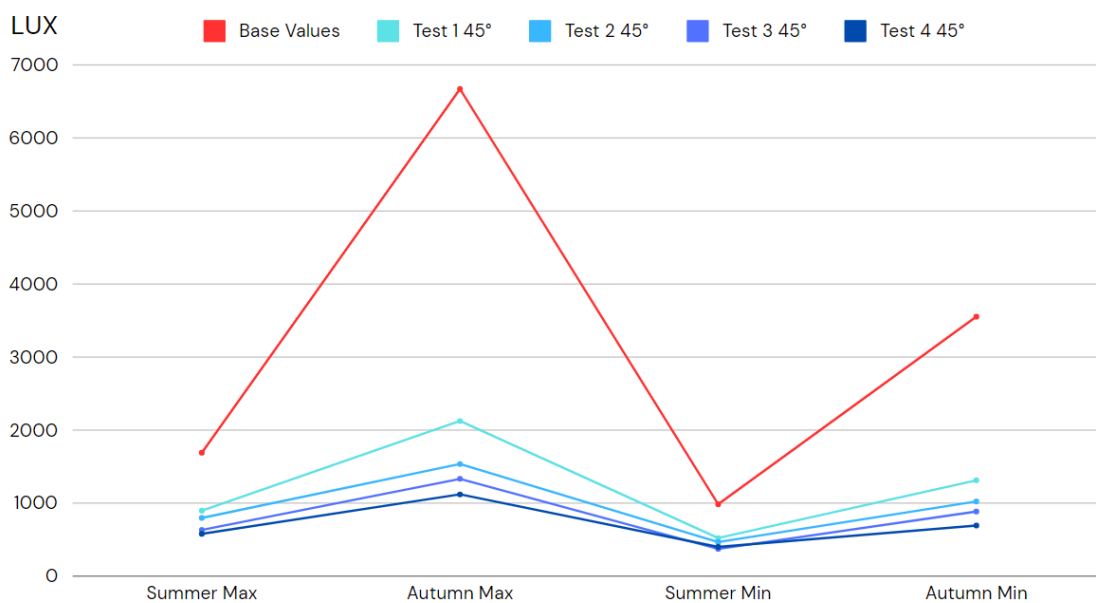
Fig 75 -Illuminance values for the 4 tests and base value of the test room at 45° rotation

90° Rotation:
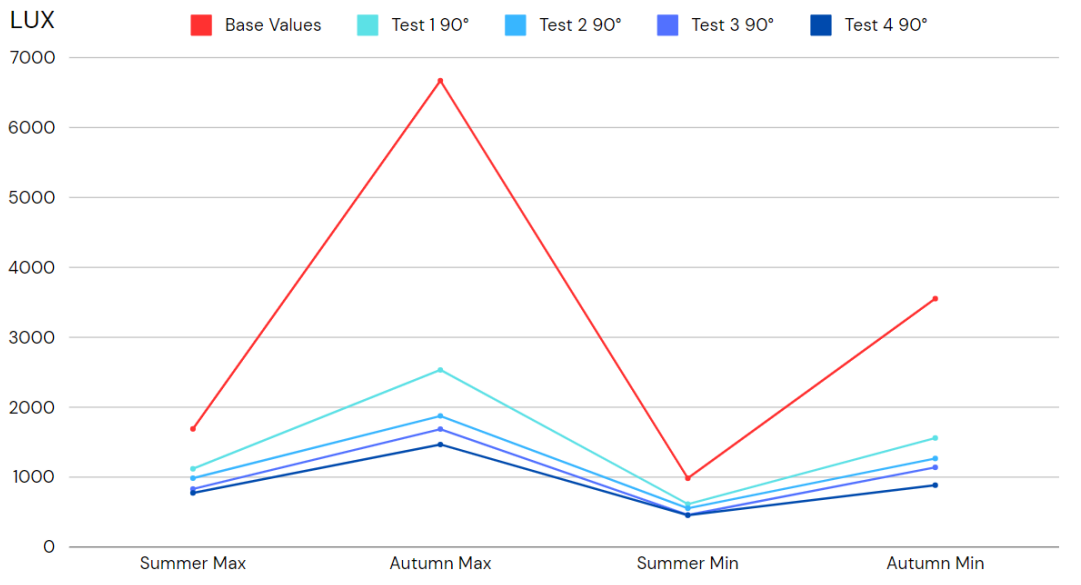
Fig 76 - Illuminance values for the 4 tests and base value of the test room at 90° rotation

From the previous results we get that the illuminance decreased from the base value in a remarkable way throughout the 4 tests during the Autumnal Equinox with a maximum value decreased from 6771 LUX to 2534 LUX and a minimum value that decreased from 3553 LUX to 1560 LUX. The least illuminance was at test number 4 which had the following distribution of the materials on its surfaces as follows:

SURFACES	TEST 4 MATERIALS
SURFACE A	Atlantica (Glass)
SURFACE B	Atlantica (Glass)
SURFACE C	Aluminum Cladding
SURFACE D	Aluminum Cladding
SURFACE E	PVC Panel
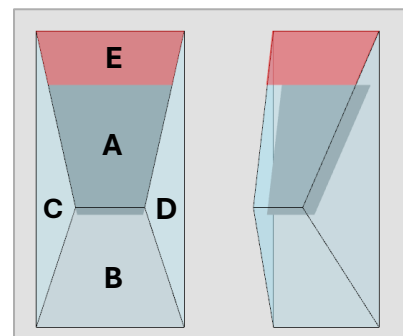
Table 35 – Test 4 Material Configuration

At test number 4 the maximum values of illuminance decreased from 6771 LUX to 1467 LUX and the minimum values decreased from 3553 LUX to 885 LUX.

As for glare the values calculated in the 4 tests with different rotation angles resulted in the results of intolerable and disturbing glare values put in a staggered way as they happen during the same period of time shown in the following graphs:

0° Rotation:
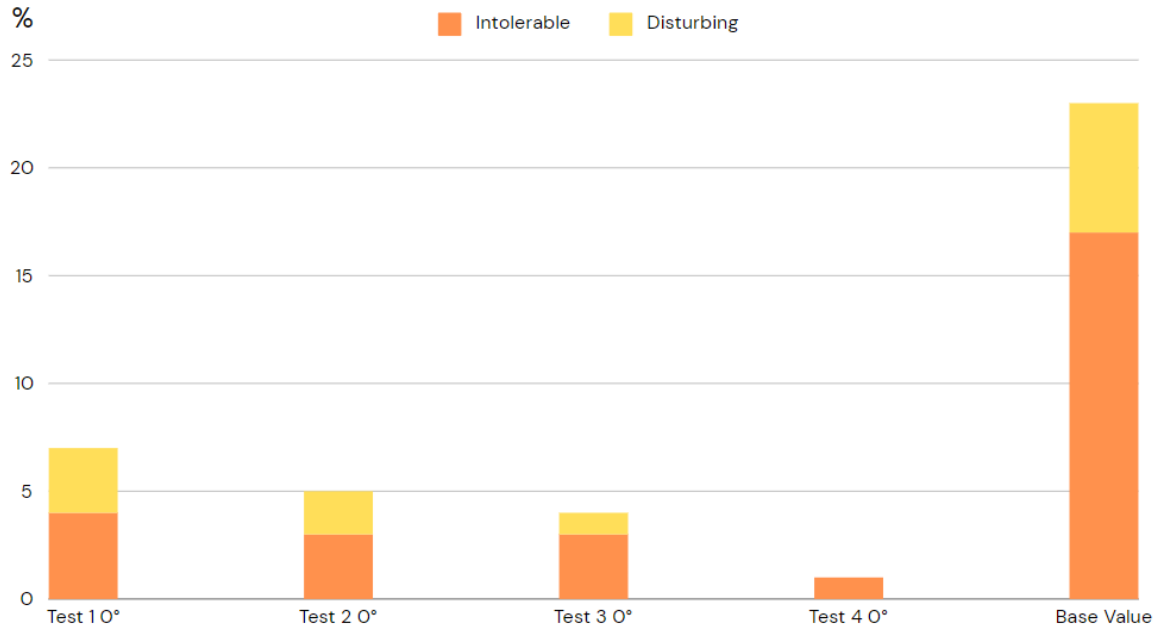
Fig 77 – Annual glare at 0° rotation of the blinds

45° Rotation:
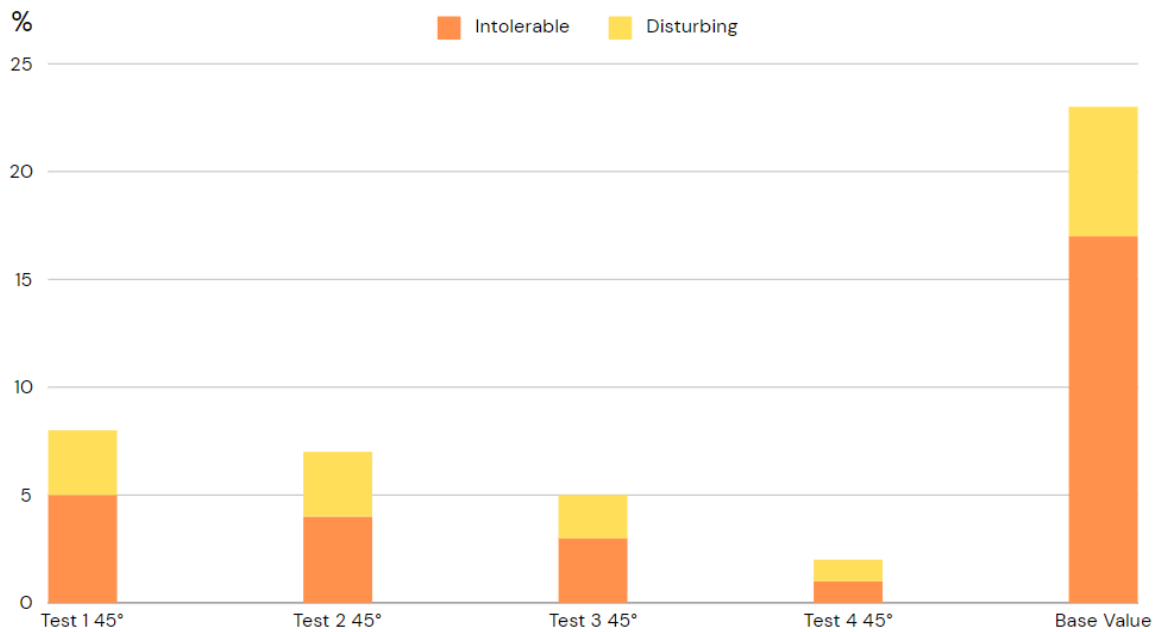
Fig 78 - Annual glare at 45° rotation of the blinds

90° Rotation:
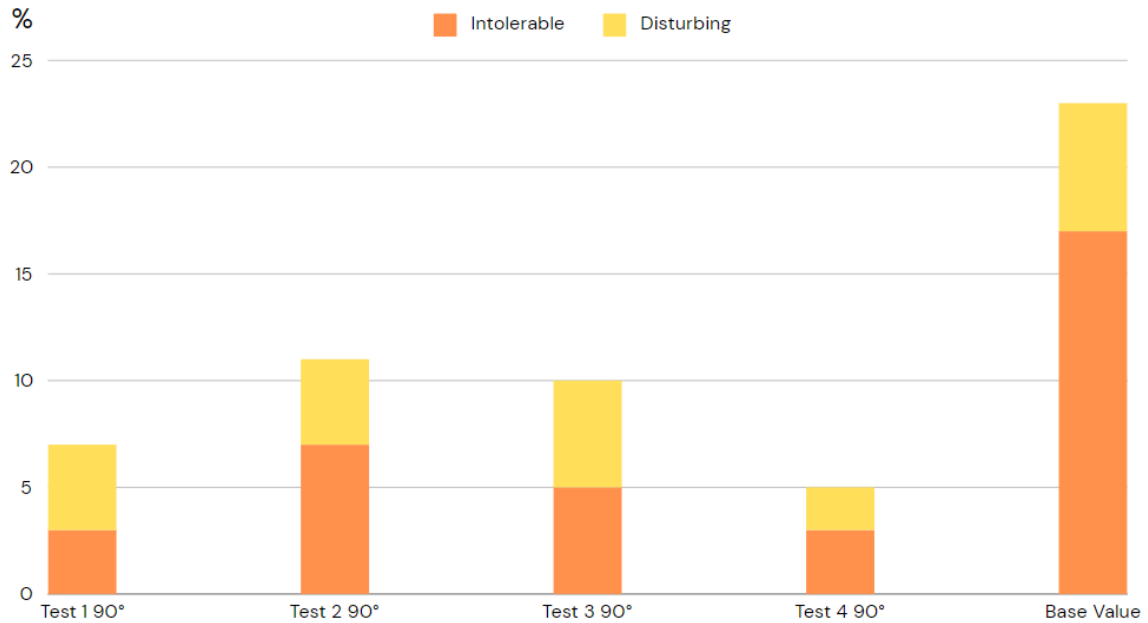
Fig 79– Annual glare at 90° rotation of the blinds

From the previous results we get that the SAWH element decreased the percentage of annual intolerable and disturbing glares significantly in the 4 tests. The minimum values of glare were at test number 4 with a decrease of annual intolerable glare from 17% to 3%,1% or 1% for a rotation angle of the blinds 0°, 45° and 90° respectively, and a decrease of intolerable glare from 6% to 2%,1% or 0% ° for a rotation angle of the blinds 0°, 45° and 90° respectively.

As for the tests regarding the façade level, the incident radiation values were calculated on the façade and then once again on the SAWH element, the idea was to get the maximum radiation on the part of the SAWH element that has the desiccant beds and therefor the blinds and to get the minimum values of radiation on the area that has no shading, so that it would prevent the highest percentage of radiation throughout the hot period of the year.

The maximum radiation values that were on the upper surface of the SAWH element "Surface A" in the hours of 9am, 12pm and 15pm can be compared in the following graphs:

9:00 AM

10^−2 kWh/m2

■ Base Values   ■ SAWH Maximum Values
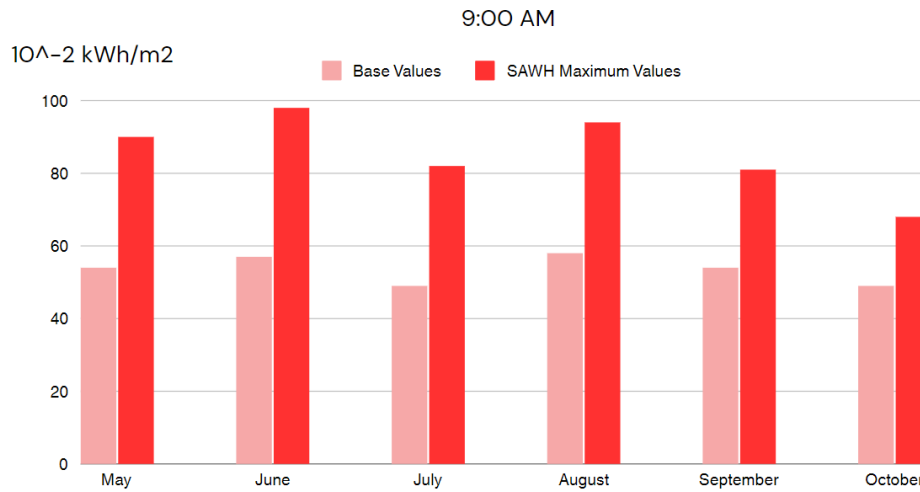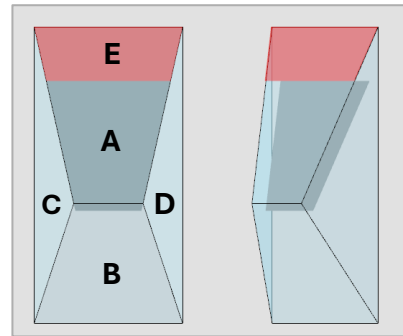
Fig 80 - Maximum incident radiation values after applying SAWH element on façade at 09:00

12:00 PM

10^−2 kWh/m2

■ Base Values   ■ SAWH MaximumVAlues
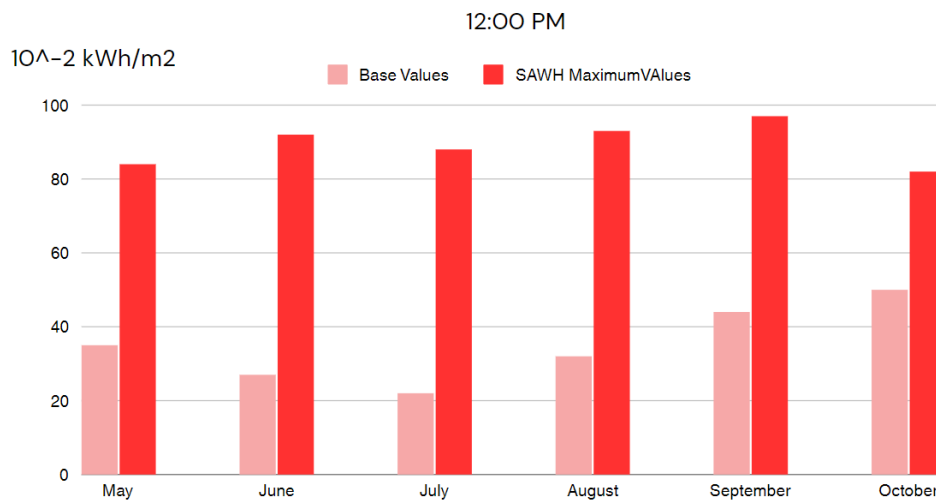
Fig 81-Maximum incident radiation values after applying SAWH element on façade at 12:00
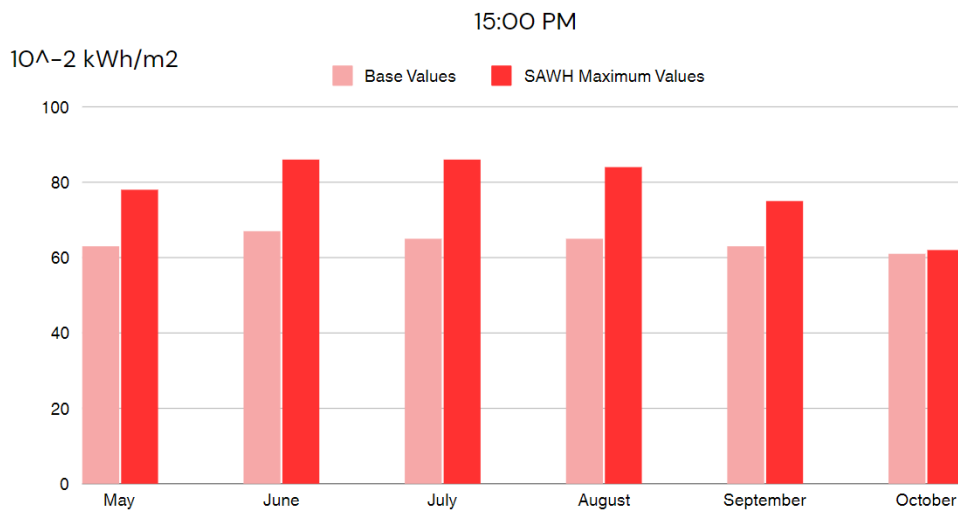
Fig 82 -Maximum incident radiation values after applying SAWH element on façade at 15:00

The previous graphs tell us that generally the incident radiation at 12pm is the lowest on the base façade and that the SAWH element increased that radiation significantly in that period. There is also an increase in incident radiation at 9am and 15pm but not as significant as the previous one.

The minimum values of incident radiation can be seen in the following graphs:

Fig 83 – Minimum incident radiation values after applying SAWH element on facade

Noting that the values are across 12 hours period as it would be insignificant during at a certain hour tending to zero. There is a significant decrease in the minimum incident radiation on the SAWH element that can reach 90%.

6 Conclusions

This research dealt atmospheric water harvesting technologies as a solution that would be given to areas with low rainwater levels as well as low humidity levels which were the primary method of wate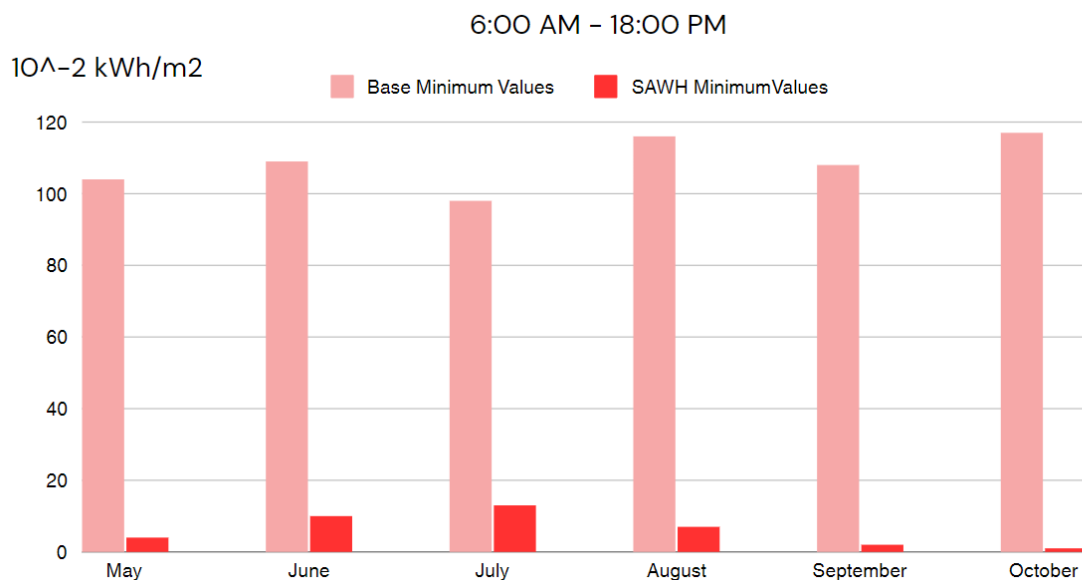r collection. One of these methods to collect water from the atmosphere is sorption based atmospheric water harvesting which can produce water under a relatively low humidity levels as well as high temperatures, which made it perfect for hot-arid climates like Egypt. This method of atmospheric water harvesting was found to be productive in experiments conducted primarily in university research labs but yet it needs further investigations to be able to enter to the market as a product that can be user friendly, saving energy and money and unrenewable water resources. This research takes the concept and primary design of the experiments found and tries to implement it on an architectural level, specifically on building envelopes while considering visual and thermal comforts for occupants in the building. The materials used in such technologies vary according to its type and therefor the water production values, and choosing a material for this research depended on whether or not that material was economic, easy to maintain and if it had a good water production value. The material chosen for this project was Calcium Chloride solution on a piece of cloth, a simple yet effective material as described by researchers, H.E. Gad, A.M. Hamed, I.I. El-Sharkawy [14], who dealt and did experiments of that kind. The method to reach a design that can be implemented on such scale was to understand the geometry of apparatuses that were used to harvest water using this technology by researchers and modify it without removing any components that would affect the water production values. The morphology then got adapted to allow the element to work properly in its 2 phase giving space for kinetic shutters to open during the night for the desiccant beds to catch the humidity and close during the morning for the water to be evaporated and then collected on the glass surface, falling under the effect of gravity into the water collection tubes. The morphology also depended on environmental conditions such as sun altitudes during hot periods. To test the element that would be that put on the façade experiments were done on two scales, the first is a test room scale with dimensions of 12m x 10m x 3.4m and the second on a façade level of buildings with more than one floor and with a curvature to test the element adaptability to different orientations.

The first test considered the illuminance and the annual glare. First the illuminance was tested throughout the Summer and Winter solstices and the Autumnal and Vernal Equinoxes resulting in a maximum and similar illuminance values during the Autumnal and Vernal Equinoxes (The winter illuminance was disregarded for its corresponding low temperature). The values of these tests were then taken as a benchmark to compare the results after installing the SAWH element on the façade. Second, 4 different material configurations considering the SAWH element were tested and resulted in a significant drop in both the illuminance and the annual glare, proving the design to be effective in that area. In further research, more materials should be tested and especially glass materials, to try to reach a more optimum solution.

The second test using parametric design tools was done to see the influence of façade orientation on the configuration of the SAWH element. This configuration was tested by testing the amount of incident radiation on the façade and how would these values and their distribution change after installing the SAWH element. In the attempt to increase the values of incident radiation on the areas corresponding to the desiccant bed for higher water production values, and to decrease the amount of incident radiation corresponding to areas with no shading, the design proved to work properly.

In further research some points need to be taken into consideration. First, on a façade level, an importance should be given to the phase of water collection, adding collection pipes into the design with a proper dimension and connections to the whole system. Second, the mechanism of opening and closing of the shutters should be put into consideration as it can highly affect the design considering the electrical connections as well as its connections to the PVC panels. Water production values should be tested using the outcome configuration as it is a relatively new design that was not tested in labs.

References

[1] "façade, n.". Oxford English dictionary (Second, online ed.). Oxford University Press. December 2011 [1989]. (subscription required)

[2] Loonen RCGM, Rico-Martinez JM, Favoino F, Brzezicki M, Menezo C, La Ferla G, et al. Design for façade adaptability – Towards a unified and systematic characterization. Proc. 10th Energy Forum - Adv. Build. Ski., Bern, Switzerland: 2015, p. 1274–84.

[3] Michael F, Miles K (2009) Interactive Architecture. Princeton Architectural Press, New York, USA.

[4] - Res. Assist. E. Kızılörenli , Assist. Prof. Dr. F. Maden (2021) A Comparative Study on Responsive Façade Systems

[5] M. M. Mekonnen, A. Y. Hoekstra, Sci. Adv. 2016, 2, e1500323;b) R. Connor, The United Nations World Water Development Report 2015: Water for a Sustainable World, Vol. 1, UNESCO Publishing, Paris, France 2015.

[6] Awareness of Atmospheric Water Harvesting Technology in a Community: Case Study of Pretoria North in South Africa. Palesa Mkabane, Frans Boudewijn Waanders, Elvis Fosso-Kankeu, Ali Al Alili, and Hemant Mittal

[7] The world's road to water scarcity: shortage and stress in the 20th century and pathways towards sustainability M. Kummu, J. H. A. Guillaume, H. de Moel, S. Eisner, M. Flörke, M. Porkka, S. Siebert, T. I. E. Veldkamp & P. J. Ward

[8] Water scarcity -Addressing the growing lack of available water to meet children's needs. https://www.unicef.org/wash/water-scarcity

[9] "Atmospheric Water Generator Technologies" Irfan Majeed Bhat, Ruheena Tabasum, Ghulam Mohd, Kowsar Majid, and Saifullah Lone[10] Progress and Expectation of Atmospheric Water Harvesting Yaodong Tu,1 Ruzhu Wang,1, * Yannan Zhang,1 and Jiayun Wang1

[10] Progress and Expectation of Atmospheric Water Harvesting Yaodong Tu,1 Ruzhu Wang,1, * Yannan Zhang,1 and Jiayun Wang1

[11] Review of sustainable methods for atmospheric water harvesting Hasila Jarimi1,2,*, Richard Powell1 and Saffa Riffat1

[12] Sorption-Based Atmospheric Water Harvesting: Materials,Components, Systems, and Applications Akram Entezari, Oladapo Christopher Esan, Xiaohui Yan, Ruzhu Wang,* and Liang An*

[13] Performance Evaluation of Solar-Powered Atmospheric Water Harvesting Using Different Glazing Materials in the Tropical Built Environment: An Experimental Study Husam S. Al-Duais 1, Muhammad Azzam Ismail 1,* , Zakaria Alcheikh Mahmoud Awad 2 and Karam M. Al-Obaidi 3,* a) Kumar, M.; Yadav, A. Experimental investigation of solar powered water production from atmospheric air by using composite desiccant material "CaCl2/saw wood". Desalination 2015, 367, 216–222.b) William, G.E.; Mohamed, M.H.; Fatouh, M. Desiccant system for water production from humid air using solar energy. Energy 2015, 90, 1707– 1720. c) Talaat, M.A.; Awad, M.M.; Zeidan, E.B.; Hamed, A.M. Solar-powered portable apparatus for extracting water from air using desiccant solution. Renew. Energy 2018, 119, 662–674.d) Khechekhouche, A.; Benhaoua, B.; Manokar, A.M.; Kabeel, A.E.; Sathyamurthy, R. Exploitation of an insulated air chamber as a glazed cover of a conventional solar still. Heat Transf. Asian Res. 2019, 48, 1563–1574.

[14] Application of a solar desiccant/collector system for water recovery from atmospheric air. H.E. Gad, A.M. Hamed*, I.I. El-Sharkawy

[15] https://www.infobuildenergia.it/progetti/al-bahar-towers-le-torri-di-abu-dhabi-con-facciata-solare-intelligente/

[16] A Comparative Study on Responsive Façade Systems *Res. Assist. Ecenur Kızılörenli , Assist. Prof. Dr. Feray Maden.

[17] Composite desiccant material "CaCl2/Vermiculite/Saw wood":a new material for freshwater production from atmospheric air. Manoj Kumal• Avadhesh Yadav

[18] Desiccant system for water production from humid air using solar energy. G.E. William, M.H. Mohamed, M. Fatouh

[19] Outdoor Testing of Double Slope Condensation Surface for Extraction of WaterfromAi. Karim H. Awad, Mohamed M. Awad, and Ahmed M. Hamed

[20] 9tps://media.warema.com/dokumente/marketing/514644/warema_2035576_tu_external-venetian-blinds_20240401_low_en-int.pdf page:29

[21] EUROPEAN STANDARD EN 12464-1 : Light and lighting - Lighting of work places - Part 1: Indoor work Places. Page:23

[22]ISO 8995-1:2002 Lighting of work place, Part One: Indoor

[23] https://onyxsolar.com/ - a- https://onyxsolar.com/product-services/technical-specifications

[24] https://weatherspark.com/y/96939/Average-Weather-in-Cairo-Egypt-Year-Round#Sections-Temperature

[25] https://www.solemma.com/climatestudio